



University  
of Glasgow

<https://theses.gla.ac.uk/>

Theses Digitisation:

<https://www.gla.ac.uk/myglasgow/research/enlighten/theses/digitisation/>

This is a digitised version of the original print thesis.

Copyright and moral rights for this work are retained by the author

A copy can be downloaded for personal non-commercial research or study, without prior permission or charge

This work cannot be reproduced or quoted extensively from without first obtaining permission in writing from the author

The content must not be changed in any way or sold commercially in any format or medium without the formal permission of the author

When referring to this work, full bibliographic details including the author, title, awarding institution and date of the thesis must be given

Enlighten: Theses

<https://theses.gla.ac.uk/>  
[research-enlighten@glasgow.ac.uk](mailto:research-enlighten@glasgow.ac.uk)

# **TOPOLOGICAL PROPERTIES OF GAUGE FIELDS ON A LATTICE**

*Sarantos J Psycharis*

**Thesis**

**Presented for the Degree of Ph.D**

**University of Glasgow**

*December 1988*

© *Sarantos J Psycharis 1988*

ProQuest Number: 10999230

All rights reserved

INFORMATION TO ALL USERS

The quality of this reproduction is dependent upon the quality of the copy submitted.

In the unlikely event that the author did not send a complete manuscript and there are missing pages, these will be noted. Also, if material had to be removed, a note will indicate the deletion.



ProQuest 10999230

Published by ProQuest LLC (2018). Copyright of the Dissertation is held by the Author.

All rights reserved.

This work is protected against unauthorized copying under Title 17, United States Code  
Microform Edition © ProQuest LLC.

ProQuest LLC.  
789 East Eisenhower Parkway  
P.O. Box 1346  
Ann Arbor, MI 48106 – 1346

*To my wife, Mary  
my mother, Anastasia  
and my father, Ioannis*

## **Acknowledgements**

I would like, first of all, to thank the University of Glasgow for the Graduate Scholarship which allowed me to do this work and Professor I S Hughes, Head of the Department of Physics and Astronomy, for research facilities. I thank most sincerely my supervisor, Dr I M Barbour, to whom I am indebted not only for his scientific but moral support, and Professor R G Moorhouse, Head of the Theory Division for his kindness and help. My special thanks are due to Dr D G Sutherland for many hours of discussion on this work and for persuading me of the benefit of a little of his own thorough and critical assessment of results and particularly my own! I thank also Dr C Davies for time spent explaining most of the "difficult" points of the Lattice Gauge Theories, and Dr A Davies and Dr C D Froggatt for many helpful discussions. I am also most grateful to Malika Mimi for her help with the preparation of the graphs and Dr R L Crawford and Dr T Blackwell for their help with the final presentation of this thesis.

I would like to thank the staff of the Department of Physics and Astronomy who have helped me in many ways during my stay in Glasgow and especially Mr Brian Swann for much kindness and help.

My special thanks to Rahim Setoodeh for his friendship and to my colleagues, Zoheir Sabeur and Leila Ayat for many interesting discussions not only on physics!

Nikos Mavromatos, although not in Glasgow, offered me real friendship during my stay in this country and I thank him most sincerely for many discussions on physics and also for entertainment!

In all research we have moments of doubt and despair and my wife, Mary, and daughter Nastazia, helped me through the bad days and gave me the strength and determination to finish this work.

Mary, you are the best!



## Contents

	<i>Page</i>
<b><i>Abstract</i></b>	<b>5</b>
<b>Chapter 1</b>	
<b><i>Introduction</i></b>	<b>7</b>
<b>1. 1 Generalities on Lattice Gauge Theories</b>	<b>7</b>
<b>1. 2 Path Integrals on the Lattice</b>	<b>9</b>
<b>1. 3 One Dimensional Ising Model</b>	<b>11</b>
<b>1. 4 Gauge Action on the Lattice</b>	<b>14</b>
<b>1. 5 Strong Coupling Expansion and the Confinement of Heavy Quarks</b>	<b>17</b>
<b>1. 6 Renormalizability and Scaling</b>	<b>18</b>
<b>1. 7 Monte Carlo Theory</b>	<b>20</b>
<b>1. 8a Lattice Fermion Schemes</b>	<b>22</b>
<b>1. 8b Wilson Fermions</b>	<b>24</b>
<b>1. 8c Kogut-Susskind Fermions</b>	<b>25</b>
<b>1. 9 Fermion Calculations</b>	<b>25</b>
<b>1.10 Chiral Symmetry</b>	<b>26</b>

## Chapter 2

<b><i>General Topological Aspects</i></b>	<b>2 8</b>
<b>2.1 An Introduction to Continuum Topology</b>	<b>2 8</b>
<b>2.2 Introduction to Twisted Boundary Conditions (TBC)</b>	<b>3 4</b>

## Chapter 3

<b><i>Topology and Lattice</i></b>	<b>4 6</b>
<b>3.1 Dependence of the Topological Charge on the Twist Transition Functions</b>	<b>4 6</b>
<b>3.2 Topological Properties of the Pure Gauge Field on the Lattice</b>	<b>5 7</b>
<b>3.3 Numerical results</b>	<b>6 1</b>

## Chapter 4

<b><i>The Index Theorem</i></b>	<b>7 1</b>
<b>4.1 Generalities on the Index Theorem</b>	<b>7 1</b>
<b>4.2 The Index Theorem on a Lattice</b>	<b>7 4</b>
<b>4.3 Numerical Results</b>	<b>8 3</b>

<b><i>Appendix A</i></b>	<b>8 8</b>
--------------------------	------------

Spin Diagonalisation	8 8
----------------------	-----

<b><i>Appendix B</i></b>	<b>9 3</b>
--------------------------	------------

The Lanczos Algorithm	9 3
-----------------------	-----



<b>Appendix C</b>	94
The Eigenvalue Problem for Specific Configurations	94
<b>Conclusions</b>	98
<b>References</b>	100

## Abstract

Euclidean solutions to the classical Yang-Mills equations (instantons, merons, e.t.c.) are important for the non-perturbative description of gauge theories. It is believed that these (topological in nature) solutions should provide a hint of confinement, chiral symmetry breaking e.t.c.

It was realised by 't-Hooft that there are several types of boundary conditions (Twisted Boundary Conditions) for the gauge field which preserve the periodicity of non-local gauge invariant quantities.

In this work we present numerical evidence that on a lattice and using Twisted Boundary Conditions we can have topological objects with non-integer topological charge (second Chern class).

The theory of fibre bundles (Chapter 2) is discussed and emphasis is given on its connection with the topological properties of the Gauge Theories. We introduce the gauge invariants twists  $\eta_{\mu\nu}$  and we define non-Abelian fluxes.

Since the  $Z(N)$  Group does not act identically on the matter field we have to introduce the flavor twist in addition to the color twist on the  $\Psi$ -field.

We express (Chapter 3) the winding number in terms of the twist transition functions in a finite Euclidean box in the continuum and its implications on the lower bounds of the action are discussed. Various combinations of the  $\eta_{\mu\nu}$ 's were constructed and applied on the lattice. The only assumption for the incorporation of the twist on the lattice is the periodicity of the plaquette.

We evaluated (Chapter 4) the eigenvalues of  $\Gamma_5 M$  ( $M$  is the Fermion Matrix) both for Wilson and Kogut-Susskind Fermions. The spectrum of the eigenvalues showed that under the introduction of color and flavor twist for the fermion field there is evidence for the restoration of a "form" of the Index Theorem on a Lattice.

The eigenvalue problem for specific twisted configurations was



## CHAPTER ONE

### 1. Introduction

#### 1.1 Generalities on Lattice Gauge Theories

It is now believed that the strong nuclear force is a reflection of the color force between quarks and gluons via the gauge theory of Quantum Chromodynamics(QCD). Since the peculiar characteristic of the force due to the color number of quarks is that it is weak at short distances, "high momentum transfers"  $Q^2$ , (asymptotic freedom), and becomes strong at large scales (confinement, bound colourless states), we should find a way to approach QCD at low energies beyond the regime of perturbation theory. This could enable us to study non-perturbative phenomena, such as long-range topological objects, confinement, chiral symmetry breaking, and to calculate the mass spectrum of hadrons.

There is no full explanation of how the quark confinement works. The most popular scenario to explain the confinement problem is based on the application of the ideas of superconductivity to particle physics. A linear potential between the quarks leads to electric flux lines "squeezed" into flux tubes which bind the quarks.

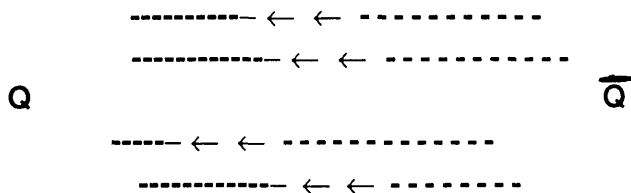


**Fig.1.1**     *Colour Electric Flux Lines between  $Q$ ,  $\bar{Q}$  Quarks*

The analogy with the superconductor comes from the fact that there we have confinement of magnetic flux lines since  $\Phi_B = 0$ . Using duality arguments between the electric and magnetic color fields, we should, in principle, find a way to rigorously describe the electric confinement of quarks.

In the perturbative field theory, the main idea is to use a perturbative expansion in terms of the coupling constant and to use a renormalisation technique by redefining the mass and the coupling constant to regulate the ultra-violet divergences. In the case of the QCD, the coupling at small distances gets greater than one and the perturbation expansion fails.

Using the lattice automatically, we have a minimum distance "a" between neighbouring points, and so a maximum momenta  $\Lambda \sim 1/a$  which leads to an ultra-violet finite theory. K.Wilson[1] introduced the lattice method of regularisation of gauge theories on a discretised Euclidean space and proved confinement at the strong coupling limit. At the same time in the lattice regularisation scheme, we have a finite number of degrees of freedom and so we can use computer tricks. Another advantage of the lattice is the close analogy between a Quantum Field Theory formulated on the lattice, and a Statistical Mechanical System.

Once the equivalence of a model field theory to a Statistical Spin System in equilibrium was established, we could exploit all the existing techniques for studying spin systems in order to solve the model field theory.

In the limit  $a \rightarrow 0, (V \rightarrow \infty)$  (continuum limit) the physics should not depend on the lattice regulator and the correlation length  $\xi$  should be  $\xi \gg a$  ( $\xi \rightarrow \infty$ ). This corresponds to a second order phase transition. The analogy between various quantities in Field Theory (F T) and a Statistical Mechanical system (SM) follows:

FT	SM
<i>Propagator G</i>	<i>Correlation Function G</i>
$G = \langle \Phi \Phi \rangle$	$G = \langle SS \rangle$
$G \sim e^{-(E_1 - E_0)a}$	$G \sim e^{-r/\xi}$
$\xi = [1/(E_1 - E_0)a] = 1/m_r a$	

So, at the continuum limit,  $a \rightarrow 0, m_R = \text{fixed} \Rightarrow \xi \rightarrow \infty \Leftrightarrow$  2nd order phase transition.

## 1.2 Path Integrals on the Lattice

In the path integral formalism[2] the expectation value of an observable is expressed by averaging over classical field configurations "weighted" by the factor  $e^{i/\hbar S}$  where  $S$  is the action of the configuration and  $\hbar$  is the Planck's constant. For a scalar theory with a  $\phi^4$  interaction, the action is

$$S(\phi, \partial_\mu \phi) = \int d^4x \frac{1}{2} \{ (\partial_\mu \phi)^2 + m^2 \phi^2 + g^2 \phi^4 \} \quad (1.2.1)$$

The propagator (2-point Green's function) is given by :

$$G[x, y] = \langle 0 | \Phi(x) \Phi(y) | 0 \rangle = -\delta^2 Z(j) / \delta \Phi(x) \delta \Phi(y) |_{j=0} \quad (1.2.2)$$

$$= (1/Z) \int d\Phi(x) \Phi(x) \Phi(y) e^{i/\hbar S(\phi, \partial_\mu \phi)}, \text{ where}$$

$$Z = \int d\Phi(x) e^{i/\hbar S(\phi, \partial_\mu \phi)}. \quad (1.2.3)$$

For the free case ( $g = 0$ ), it is easy to find all the  $n$ -point Green functions, but for the case where  $g \neq 0$  we have to expand the interacting part of the action to find  $G(x, y)$ . In this case the resulting integrals are divergent but with a renormalisation of the mass and the coupling the various observables are finite.

In order to improve the situation we use the lattice approximation by approaching the space-time by a finite hypercubic lattice of  $N_L$  sites in every direction separated by the lattice spacing  $a$ , and replacing the derivatives by finite differences, i.e.,

$$\partial_\mu \Phi = \Delta_\mu \Phi(n) = (1/a_\mu) [\Phi(n+a_\mu) - \Phi(n)], \quad (1.2.4)$$

$\mu$  = unit vector in the  $\mu$  direction and the action (1.2.1) becomes

$$S = (1/2) a^2 \sum_{n, \mu} [\Delta_\mu \Phi(n)]^2 + (1/2) a^4 \sum_n [m^2 \Phi(n)^2 + g^2 \Phi^4(n)]. \quad (1.2.5)$$

The continuum limit is recovered by taking the limits  $N_L \rightarrow \infty$ ,  $a \rightarrow 0$  with  $N = aN_L$  fixed.

We now apply the lattice approximation to the free scalar field theory[3]

$$S = \int d^4x [(1/2) \partial_\mu \Phi \partial^\mu \Phi^* + (1/2) m^2 \Phi^2]. \quad (1.2.6)$$

Using  $\int d^4x \rightarrow a^4 \sum_n$  (where on the Lattice  $n = (n_1, n_2, n_3, n_4)$  and  $\Phi(x) \rightarrow \Phi(n)$ ) we get:

$$S = a^4 \sum_{n, \mu} \{ (1/2a^2) [\Phi(n+a\mu) - \Phi(n)]^2 + (1/2) m^2 \Phi^2(n) \} \quad (1.2.7)$$

The Z-functional:

$Z = \int d\Phi(x) e^{-S(\phi, \partial_\mu \phi)}$  is now given by:

$$Z = \int \prod_n d\Phi_n e^{-S} = (\text{Det}(M/2\pi))^{-1/2} \quad (1.2.8)$$

where  $M$  is defined by

$$S = \phi_m M_{mn} \phi_n \quad (1.2.9)$$

To gain familiarity with the techniques used in solid state physics, we consider the Fourier transforms of any  $\phi_n$  to be:

$$\tilde{\phi}_k = \sum_n \phi_n e^{2i k_\mu \cdot n_\mu / N_L} \quad \phi_k = N_L^{-4} \sum_k \tilde{\phi}_k e^{-2i k_\mu \cdot n_\mu / N_L}$$

where  $N_L$  is the lattice size. Now the kinetic part of (1.2.7) can be written as

$$\begin{aligned}
(1/2)\partial_\mu \Phi \partial^\mu \Phi^* &= (1/2)a^2[\Phi_{n+\mu}^* \Phi_{n+\mu} + \Phi_n^* \Phi_n - \\
&\Phi_{n+\mu}^* \Phi_n - \Phi_n^* \Phi_{n+\mu}] = \\
\frac{a^2}{2N_L^4} \sum_{k,\mu} \{2-2\cos(2\pi k_\mu/N_L)\} |\tilde{\Phi}_k|^2
\end{aligned}
\tag{1.2.10}$$

and the total action becomes:

$$S = (a^2/(2N_L^4)) \sum_{k,\mu} [2-2\cos 2\pi k_\mu/N_L] |\tilde{\Phi}_k|^2 + (a^4/2N_L^4) m^2 |\tilde{\Phi}_k|^2.
\tag{1.2.11}$$

The scalar propagator is given by:

$$\langle \phi_m \phi_n \rangle = \int_{-\pi/a}^{\pi/a} \frac{d^4 x}{(2\pi)^4} \frac{e^{-iqx}}{M^2 + 2a^{-2} \sum_{\mu} (1 - \cos a q_{\mu})}
\tag{1.2.12}$$

with  $q_{\mu} = 2\pi k_{\mu}/aN_L$ . If we take the lattice spacing to zero, and expand the cosine we regain the continuum scalar free field propagator.

### 1.3 One-Dimensional Ising Model

We have a chain of N spins with periodic boundary conditions.

$$1 \rightarrow 2 \dots \dots \dots \dots \dots N-1 \rightarrow N \rightarrow 1$$

**Fig.1.3 Ising Model with Periodic Boundary Conditions**



The Hamiltonian is given by:

$$H = -J \sum_{i=1}^N S_i S_{i+1} - h/2 (S_i + S_{i+1}) \quad (1.3.1)$$

and the partition function

$$Z = \sum_{S_i=\pm 1} \prod_i (e^{-\beta H_{i,i+1}}) = \sum_{S_1=\pm 1} \langle S_1 | \hat{T} | S_2 \rangle \dots \langle S_N | \hat{T} | S_1 \rangle. \quad (1.3.2)$$

(where  $\hat{T}$  is the transfer matrix).  
Consider now a quantum mechanical system in a 2-dimensional Hilbert space with Hamiltonian  $H = -[\sigma_1 - \lambda \sigma_3]$ ,  $\sigma_1, \sigma_3$  the Pauli-matrices.

We can express the transition amplitude between states  $|a\rangle$  and  $|b\rangle$  in time  $T$  by  $\langle b | e^{-HT} | a \rangle$  and dividing  $T$  into  $N$  segments,  $T = N (\Delta T)$  we have

$$\begin{aligned} \langle b | e^{-HT} | a \rangle &= \langle b | e^{-HN\Delta T} | a \rangle = \\ &\sum_{S_1=\pm 1} \dots \sum_{S_{N-1}=\pm 1} \langle b | e^{-H\Delta T} | S_1 \rangle \langle S_1 | e^{-H\Delta T} | S_2 \rangle \dots \\ &\langle S_{N-1} | e^{-H\Delta T} | a \rangle. \end{aligned} \quad (1.3.3)$$

We then define the transition matrix by

$$\langle S | e^{-H\Delta T} | S' \rangle \equiv \langle S | \hat{T} | S' \rangle \equiv e^{-V(S,S')} \quad (1.3.4)$$

and from (1.3.3), (1.3.4) we get

$$\langle b | e^{-HT} | a \rangle = \sum_{S_1=\pm 1} \dots \sum_{S_{N-1}=\pm 1} e^{[V(b,S_1) + \dots + V(S_{N-1},a)]}.$$

If we consider it as a lattice  $b \rightarrow 1 \rightarrow 2 \dots N-1 \rightarrow a$  and make site  $a$

coincide with site  $b$  then it is clearly an Ising Model with a general coupling  $V(S_i, S_{i+1})$ .

For small  $\Delta T$ , equation (1.3.4) becomes

$$e^{-V(S,S')} = \langle S | \hat{T} | S' \rangle = \langle S | 1 + \Delta T (\sigma_1 - \lambda \sigma_3) | S' \rangle \quad (1.3.5)$$

Then

$$\langle S | \hat{T} | S' \rangle = \begin{bmatrix} 1 - \lambda \Delta T & \Delta T \\ \Delta T & 1 + \lambda \Delta T \end{bmatrix} = \begin{bmatrix} e^{-V(1,1)} & e^{-V(1,-1)} \\ e^{-V(-1,1)} & e^{-V(-1,-1)} \end{bmatrix}$$

and this means that the more general form of  $V$  is

$$V(S, S') = (K/2)(S-S')^2 + h/2(S+S') \quad (1.3.6)$$

with  $e^{-2K} = \Delta T$ ,  $e^h = 1 + \lambda \Delta T$ .

For the quantum mechanical system, the partition function is:

$$\begin{aligned} Z &= \text{Tr } e^{-HT} = \sum_a \langle a | e^{-HT} | a \rangle = \sum_{\{S_i = \pm 1\}} e^{-\sum_{i=1}^N V(S_i, S_{i+1})} \\ &= \sum_{\{S_i = \pm 1\}} \exp \left[ -\sum_{i=1}^N (K^2 + K S_i S_{i+1} + (h/2) S_i) \right] \quad (1.3.7) \end{aligned}$$

which is the partition function of the 1-dimensional Ising Model with general coupling  $K$ . So the analogy:

QFT path integral  $\equiv$  Statistical Mechanics partition function.

The Free Energy "Density" of the 1-dimensional Ising model is given by

$$F = \lim_{N \rightarrow \infty} \left[ -\frac{1}{N(\Delta T)} \ln Z \right] = \lim_{T \rightarrow \infty} \left[ -\frac{1}{T} \ln \text{Tr} e^{-HT} \right] = E_0$$

(1.3.8)

So in QFT ground state energy = Statistical Mechanics free energy.

#### 1.4 Gauge Action on the Lattice

The essential idea to put gauge theories on the lattice is to make the theory well defined as possible even losing Lorentz invariance but preserving the most important gauge invariance. In order to achieve this, Wilson[1] set up the whole theory from the scratch, i.e. by redefining the degrees of freedom of the theory.

In the continuum for every path joining  $x$  and  $x'$  we define the parallel transport from  $x$  to  $x'$  by

$$U_{xx'} = e^{ig \int A_\mu(y) dy^\mu} \quad (1.4.1)$$

where  $A_\mu = A_\mu^a T^a$  ( $T^a$  are the generators of the group under consideration) and  $U_{xx'}$  belongs to the group ( $a$  runs from 1 to the dimension of the group).

Under a gauge transformation  $U(x)$  on  $A_\mu(x)$  the parallel transport  $U_{xx'}$  undergoes the transformation:

$$U_{xx'} \rightarrow U(x) U_{xx'} U(x') \quad (1.4.2)$$

The rotation of the frame in the charge space along a path through the points  $i_1 \rightarrow i_2 \dots \dots \rightarrow i_N$  is

$$U_\gamma = U_{i_N i_{N-1}} U_{i_{N-1} i_{N-2}} \dots U_{i_2 i_1}$$

and under a gauge transformation it transforms as

$$U_\gamma \rightarrow U_{i_N} U_\gamma U_{i_1}^{-1}.$$

In particular, for a closed path  $U_\gamma \rightarrow U_{i_1} U_\gamma U_{i_1}^{-1}$  and this shows that the trace of  $U_\gamma$  is gauge invariant. On the lattice the parallel transport operator  $U_{xx'}$  is the basic dynamical variable which is defined on the link connecting the sites  $x$  and  $x'$ . So on the lattice, the dynamical variables  $U_{xx'}$  always represent finite group transformations since they correspond to the transport along a path with finite length. This means that on the lattice, we should have not only Lie groups, but we could have also discrete finite groups as gauge groups.

The pure gauge action (for  $SU(N)$  groups) in the continuum is

$$S_G = (2/g^2) \int \text{tr} F_{\mu\nu} F^{\mu\nu} \quad (1.4.3)$$

where  $F_{\mu\nu}$  is the covariant field strength. Denoting  $U_{xx'}$  by  $U_\mu(x)$  as the link joining the lattice sites  $x$  and  $x+a_\mu$ , we write the simplest possible gauge invariant action on the lattice (no fermions included):

$$S_G = (\beta/N) \text{Re} \left[ \sum_{x, \mu, \nu, \text{plaquettes}} \text{Tr} [U_\mu(x) U_\nu(x+a_\mu) U_\mu^\dagger(x+a_\nu) U_\nu^\dagger(x)] \right] \quad (1.4.4)$$

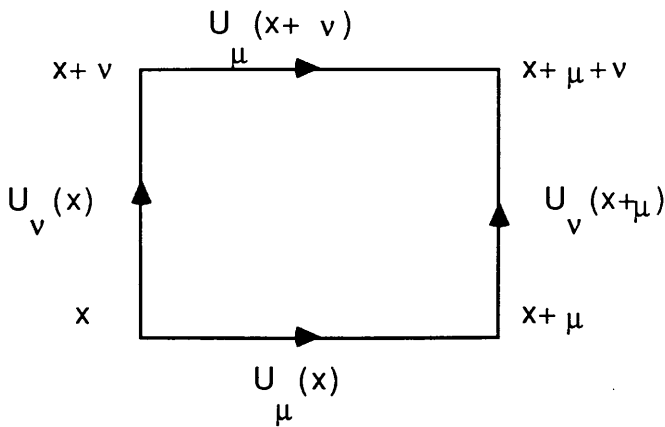


**Fig. 1.4.1 Elementary Plaquette on a Lattice**

Writing  $U_\mu(x) = e^{-ia g_0 A_\mu(x)}$  and using :

$$e^{ax} e^{ay} = e^{ax+ay+(1/2)a^2[x, y]} + O(a^3),$$

we get  $S_G = (\beta/2N) \sum_{x, \mu, \nu} \text{Tra}^4 F_{\mu\nu} F^{\mu\nu} + O(a^5)$

which is the continuum action if we identify  $\beta = 2N/g_0^2$ .

Some notable remarks follow:

(i) From the above we see that on the lattice, the dynamical variables are elements of the gauge group associated with every link of the lattice.

From  $U_\mu(n) = e^{ia g_0 A_\mu(n)}$  and the fact that  $ag_0 A_\mu(x)$  ranges from  $[-\pi, \pi]$  (in  $SU(N)$  groups (compact groups)), we have noticed that the values of  $A_\mu(n)$  are restricted to  $(-\pi/ag_0, \pi/ag_0)$ .

(ii) From (1.4.2) we see that  $U(x)$  lives on the lattice sites and is not a dynamical degree of freedom. These are used just to gauge transform the dynamical variables  $U_\mu(x)$ .

(iii) The generating functional

$$Z = \int \prod_{\text{links } l} dU_l e^{-\beta(U)}$$

(where  $dU_l$  is the gauge invariant Haar measure[4] and  $\beta = 2N/g_0^2$ ) is well defined as a multiple integral of a finite number of integrals and so we do not need to introduce gauge fixing à la Fadeev-Popov[4].

(iv) Even if it is not necessary, we can do a gauge fixing on the lattice eliminating a few degrees of freedom. This can be done by choosing the group elements  $U(x)$  and  $U(x+\mu)$  such that (1.4.2) becomes  $U_\mu(x) \rightarrow U'_\mu(x) = 1$ .

We can continue in this way for more links of the lattice up to a point where we have a maximal gauge fixing. Figure 4 shows two ways of gauge fixing in a 2-dimensional  $4^2$  lattice.

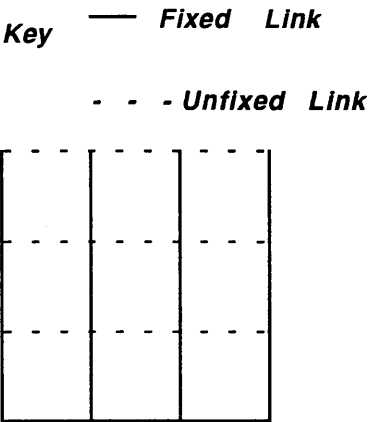


Fig. 1. 4. 2.      *Axial Gauge Fixing*

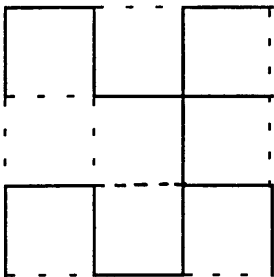


Fig. 1. 4. 3.      *Random Gauge Fixing*

The important point about gauge fixing on a periodic lattice is that since the boundary links "curve back" to the lattice edges, they cannot be fixed.

### 1.5 Strong Coupling Expansion and the Confinement of Heavy Quarks

In the statistical analogue the strong coupling expansion

corresponds to the high temperature limit. In the continuum theory the strong coupling is difficult to be treated but on the lattice this limit is easy since we exponentiate in the path integral

$$e^{\beta \sum_{\text{plaq's}} S_{\text{plaq}}} \quad \text{and} \quad \beta = 2N/g_0^2.$$

Consider the vacuum expectation value of the  $W_C = \text{Tr} \prod_{l \in C} U_l$ ,  $C$  is a closed contour on the lattice and  $b, l$  denote links of the lattice,

$$\langle W_C \rangle = (1/Z) \int \prod_b dU_b \text{Tr} \prod_{l \in C} U_l \prod_{\text{plaq}} e^{\beta S_p}. \quad (1.5.1)$$

We can expand the exponential when  $\beta \ll 1$  and since,

$$\int dU_{ij} = 1, \quad (1.5.2)$$

$$\int dU U_{ij} = 0 \quad (1.5.3)$$

and

$$\int dU U_{ij} U^{+}_{kl} = (1/N) \delta_{ij} \delta_{kl}, \quad (1.5.4)$$

where  $i, j$  are color indices, we get  $\langle W_C \rangle \sim e^{-\text{area}}$ . Writing  $\langle W \rangle = e^{-V(R)T}$  (since the quarks are static and are used as external sources only), we get  $V(R) \sim R$  where  $R$  is the spatial distance between the quarks and  $V(R)$  is the potential between the static quarks. (This is to leading order in strong coupling expansion and for large loops).

In general we expect:

$$V(x) = \sigma(g_0)x, \quad (1.5.5)$$

where  $\sigma$  = string tension. So we have a linearly confining potential at the strong coupling limit.

## 1.6 Renormalisability and Scaling

Physical quantities should be independent of the lattice cut-off  $a$ . This is the requirement of renormalisability which in mathematical form is written as:

$$a(d/da)m(a,g)=a(\partial/\partial a-\tilde{\beta}(g)\partial/\partial g)m(a,g)_{a \rightarrow 0}=0, \quad (1.6.1)$$

$m(a,g)$  = some physical mass.

The cut-off independence determines

$$\tilde{\beta}(g) = - \partial g / \partial a, \quad (1.6.2)$$

( $\tilde{\beta}$  = the Gell-Mann beta function) which is equivalent to:

$$\frac{a(g)}{a(g_0)} = \exp\left(- \int_{g_0}^g \frac{dg}{\beta(g)}\right) \quad (1.6.3)$$

In perturbation theory and at 2-loops (for the  $SU(N_C)$  group),

$$\tilde{\beta}(g) = -\beta_0 g^3 - \beta_1 g^5 + \dots \quad (1.6.4a)$$

$$\beta_0 = 11N_C / 48\pi^2, \quad \beta_1 = (34/3) / (N_C 16\pi^2)^2 \quad (1.6.4b)$$

So, if

$$\Lambda_{\text{lattice}} \equiv a^{-1}(g_0) \exp\left(- \frac{1}{2\beta_0 g_0^2}\right)$$

is a cut-off independent parameter, then:



$$a = \Lambda_{\text{lattice}}^{-1} \exp\left(-\frac{1}{2\beta_0 g^2}\right) (\beta_0 g^2)^{-\frac{\beta_1}{2\beta_0^2}} \quad (1.6.5)$$

On the lattice we calculate (at various  $g$ 's) dimensionless quantities  $m_i a$ , ( $m_i$ =any hadron mass for example) and if we want to be consistent with the continuum limit we should have:

$$m_i a = \text{const.} \exp\left(-\int_{g_0}^g \frac{dg}{\tilde{\beta}(g)}\right) \quad (1.6.6)$$

which implies:

$$(m_i a / m_j a) = \text{constant (Scaling)} \quad (1.6.7)$$

For  $g \rightarrow 0$ ,  $\tilde{\beta}(g)$  should approximate (1.6.4a) and this results to:

$$m a = \text{const.} \exp\left(-\frac{1}{2\beta_0 g^2}\right) (\beta_0 g^2)^{-\frac{\beta_1}{2\beta_0^2}}$$

so,

$$(m a / a(2\text{-loops})) = c \Lambda_{\text{lattice}} = m \text{ (asymptotic scaling)}. \quad (1.6.8)$$

## 1.7 Monte Carlo Theory

Monte Carlo (MC) simulation is a method[5] which is used to approximate integrals by summing over randomly selected points in the integration space.

In field theories, it is applied to the calculation of quantities like

$$\langle O \rangle = \int dU_b O[U_b] e^{-\beta S(U_b)} \quad (1.7.1)$$

where the operator  $O[U_b]$  is a function of the lattice configurations  $\{U_b\}$  (a lattice configuration is a set of  $U_b$  matrices of the gauge group on every link  $b$  of the lattice).

The essence of the method is to generate lattice configurations one after the other in the following sense: let  $\tau$  be the discrete computer time (also called the "fifth time") in the course of which these configurations are generated in a step by step fashion. We define the probabilities:

(a) the normalised transition probability  $P_{ij}$  of going from the configuration  $\{U_{b(i)}\}$  to the configuration  $\{U_{b(j)}\}$  in the computer  $\tau$  time step  $\tau$  and,

(b) the normalised probability of each configuration which for a system in thermal equilibrium is given by the Boltzman distribution

$$\Pi_j = \Pi[\{U_{b(j)}\}] = Z^{-1} e^{-\beta S}.$$

With the M.C. method (1.7.1) is approximated by :

$$O(\tau) = (1/\tau) \sum_{i=1}^{\tau} O[U(i)] \quad (1.7.2)$$

So what we need is to generate in the computer time  $\tau$  a number of lattice configurations and then we calculate  $\langle O \rangle$ .

The method is expected to work if we generate configurations  $\{U_{b(i)}\}$  at each fifth time step  $i$  with the Boltzman distribution (importance sampling). This can be achieved by the Metropolis et.al. algorithm [5]. This involves a generation of states with an initially symmetric transition probability  $P^*_{ij}$ . We then define the transition probability from  $\{U_i\}$  to  $\{U_j\}$  configuration as

$$P_i = P_{ij}^* \Pi_j / \Pi_i \text{ if } \Pi_j / \Pi_i < 1 \quad (1.7.3a)$$

and

$$P_{ij} = P_{ij}^* \text{ if } \Pi_j / \Pi_i > 1 \quad (1.7.3b)$$

with

$$\Pi_j / \Pi_i \sim e^{-\beta \Delta S}, \Delta S = S[U(j)] - S[U(i)].$$

Since it turns out that  $P_{ij}$  satisfies all the requirements of Markov chain theory, all we need to do is ensure that the computer updates configurations, calculates the change in the action  $\Delta S$  and accept or reject the update with criterion (1.7.3).

An important point of the method is the requirement of the detailed balance condition, i.e.,  $\Pi_i P_{ij} = \Pi_j P_{ji}$ . While it is possible to have the general rules on which MC simulations are based, there are some other practical factors which enter in the game, such as the observables we measure, the lattice size, the boundary conditions, the initial configurations and the length of the simulation. For example, the importance of choosing the boundary conditions is seen by the fact that an  $8^4$  lattice has  $8^4 - 6^4 = 2800$  points on its boundary and only 1296 points in its interior. Usually the lattice is assumed to be periodic to avoid finite size effects (even if we have not used a periodic lattice in this work!). Despite the fact that there are specific rules for MC simulations, in practice we have to deal with many other 'experimental' factors.

### 1.8a Lattice Fermion Schemes

In order to have a complete lattice model of QCD we must have a lattice model including fermions. This is quite a difficult problem since the discrete space-time structure of the lattice affects the chiral properties of the theory.

Consider the Dirac action for a fermion field coupled via the minimal subtraction to the gauge field  $A_\mu$  in the continuum:

$$S_F = \sum_{\text{flavors}} \int \bar{\Psi}_f [\not{\partial} + \not{A} + m_f] \Psi_f \quad (1.8a.1)$$

where the index  $f$  stands for the different flavors. Beyond the local gauge symmetries, the action has the following global symmetries with generators acting on the flavor space:

$$\begin{aligned}
\text{i)} \quad & U_V(1): \Psi_f \rightarrow e^{i\omega} \Psi_f \\
\text{ii)} \quad & SU_V(N_f): \Psi_f \rightarrow e^{i\omega \cdot \tau} \Psi_f \\
\text{iii)} \quad & U_A(1): \Psi_f \rightarrow e^{i\omega \Gamma_5} \Psi_f \\
\text{iv)} \quad & SU_A(N_f): \Psi_f \rightarrow e^{i\omega \cdot \tau \Gamma_5} \Psi_f
\end{aligned} \tag{1.8a.2}$$

( $\omega$  is the chiral rotation and  $\Gamma_5$  acts on the spin space). We want to keep these chiral symmetries on the lattice but there is no way to do this[6], and we can have only some remnants of these symmetries, recovering the full symmetries in the continuum limit.

The first step to put fermions on the lattice is to find the lattice approximation to the Dirac operator  $\Gamma^\mu \partial_\mu + m$ . To preserve hermiticity we approximate the derivative  $\partial_\mu$  by the symmetric difference

$$\partial_\mu \Psi(x) \rightarrow \partial_\mu \Psi(x) = (\Psi(n+\mu) - \Psi(n-\mu))/2a$$

where the  $\Gamma$  matrices satisfy  $\{\Gamma_\mu, \Gamma_\nu\} = 2\delta_{\mu\nu}$  with  $\Gamma_5 = \Gamma_1 \Gamma_2 \Gamma_3 \Gamma_4$ .

Under a gauge transformation  $g(n)$  on a lattice site  $n$  we have:

$$\Psi(n) \rightarrow g(n)\Psi(n) \quad \bar{\Psi}(n) \rightarrow \bar{\Psi}(n)g^{-1}(n) \tag{1.8a.3}$$

and the object  $\bar{\Psi}(n)U_\mu(n)\Psi(n+\mu)$  is gauge invariant. The action (1.8.1) can now be written as:

$$S_F = a^4 \sum_n \left[ \left\{ \sum_\mu (1/2a) [\bar{\Psi}(n) \Gamma^\mu U_\mu(n) \Psi(n+\mu) - \bar{\Psi}(n) \Gamma^\mu U^{+\mu}(n) \Psi(n-\mu)] + m \bar{\Psi}(n) \Psi(n) \right\} \right] \quad (1.8a.4)$$

Rescaling  $\Psi(n)$  to  $\Psi(n) = 2^{1/2} a^{3/2} \Psi(n)$  we get

$$S_F = \sum_n \left[ \left\{ \sum_\mu [\bar{\Psi}(n) \Gamma^\mu U_\mu(n) \Psi(n+\mu) - \bar{\Psi}(n) \Gamma^\mu U^{+\mu}(n) \Psi(n-\mu)] + 2ma \bar{\Psi}(n) \Psi(n) \right\} \right] \quad (1.8a.5)$$

which in matrix form is written as  $S_F = \bar{\Psi} [M + 2ma] \Psi$ .

Consider now the free field case ( $U_\mu(n) = 1$ ). The equation for the propagator reads:

$$\sum_\mu \Gamma^\mu [G(n+\mu, 0) - G(n-\mu, 0)] + 2ma G(n, 0) = \delta_{n, 0}$$

which (after usual Fourier transformations) gives:

$$G(q) = (2ma - i \sum_\mu \Gamma^\mu \sin q_\mu) / [(2ma)^2 + \sum_\mu \sin^2 q_\mu] \quad (1.8a.6)$$

and when  $m = 0$ ,  $G(q)$  has poles at  $q_\mu = 0$  or  $\pi$ . So there are 16 poles (in 4-dimensions) and 16 degenerate fermions. This is often called the "doubling problem". We present now a scheme proposed by Wilson which avoids the "doubling problem" at the expense of a non-chirally symmetric action.

### 1.8b Wilson Fermions

In this scheme the chiral symmetry is broken explicitly by a term in the action which is proportional to the lattice spacing  $a$ . For the free field case the action is

$$S_{\text{Wilson}} = 1/2 \sum_{n, \mu} \bar{\Psi}(n) [(\Gamma^\mu - r \mathbf{1}) \Psi(n+\mu) - (\Gamma^\mu + r \mathbf{1}) \Psi(n-\mu)] + m \sum_n \bar{\Psi}(n) \Psi(n) \quad (1.8b.1)$$

where  $r$  is the Wilson  $r$ -parameter. The equation satisfied from the propagator is ( for the free case)

$$1/2 \sum_{\mu} [(\Gamma_{\mu}-r\mathbf{1})G(n+\mu) - (\Gamma_{\mu}+r\mathbf{1})G(n-\mu)] + m(G(n)) = \delta_{n0},$$

hence

$$G(q)=[m+\sum_{\mu}(i\Gamma^{\mu}\sin q_{\mu}-r\cos q_{\mu})]^{-1}$$

So the values of the propagator are:

$$\begin{array}{lll} m+4r & \text{at} & q_{\mu} = (\pi,\pi,\pi,\pi) \\ m+2r & \text{at} & q_{\mu} = (0,\pi,\pi,\pi) \\ m & \text{at} & q_{\mu} = (0,0,\pi,\pi) \\ m-2r & \text{at} & q_{\mu} = (0,0,0,\pi) \\ m-4r & \text{at} & q_{\mu} = (0,0,0,0) \end{array} \quad (1.8b.2)$$

The case  $r = 1$  is special. In this case we have the  $1\pm\Gamma_{\mu}$  projection operators in the action and the free field propagator is recovered for  $m = 4$  or (defining the Wilson's hopping parameter  $k$  as  $k = 1/2m$ )  $k = 1/8$ . We notice that even at  $m=0, r\neq 0$ , there is no chiral symmetry.

### 1.8c *Kogut-Susskind Fermions*

On a lattice with an even number of sites in each direction, we can have 4 degenerate flavors instead of 16. This is done by a unitary site dependent transformation which diagonalises the action in the spin space.

We define

$$\Psi(n) = \Gamma_1^{n_1}\Gamma_2^{n_2}\Gamma_3^{n_3}\Gamma_4^{n_4} X(n), \quad n=(n_1,n_2,n_3,n_4) .$$

Then (18a.4) becomes

$$S_F(\Psi,\bar{\Psi},U)=\sum_n[\sum_{\mu}(-1)^{n_1+n_2+\dots+n_{\mu}-1}\bar{X}(n)U_{\mu}(n)X(n+\mu)-h.c.+m\bar{X}(n)X(n)]. \quad (1.8c.1)$$

The action now is diagonal in the spin space since the  $X$ 's are not spinors but just complex numbers.

### 1.9 Fermion Calculations

The  $X$  fields in the Kogut-Susskind scheme are Grassmannian fields which obey the algebra:

$$\begin{aligned}\{X_i, \bar{X}_j\} &= \delta_{ij} \\ \{X_i, X_j\} &= \{\bar{X}_i, \bar{X}_j\} = 0 \\ \int dX X &= 1, \int dX = 0.\end{aligned}\tag{1.9.1}$$

The action (1.8c.1) can be written as

$$S(X, \bar{X}, U) = \bar{X}[M(U) + 2ma]X,\tag{1.9.2}$$

and the path integral becomes

$$\int dX d\bar{X} [dU_{x,\mu}] e^{-S(U) - S(X, \bar{X}, U)}\tag{1.9.3}$$

Since the  $X$ 's belong to a Grassmannian algebra, it is not practical to use Monte Carlo techniques on the fermionic part of the action. However, since the fermionic part of the action is Gaussian we can integrate out the fermionic degrees of freedom resulting in

$$Z = \int [dU_{x,\mu}] \text{Det}[M(U) + 2ma] e^{-S(U)}.\tag{1.9.4}$$

For the propagator we now have:

$$\begin{aligned}\langle \bar{X}_x X_y \rangle &= \int dX d\bar{X} [dU_{x,\mu}] \bar{X}_x X_y e^{-S(U) - S(X, \bar{X}, U)} = \\ &\int [dU_{x,\mu}] [M(U) + 2ma]^{-1}_{yx} \text{Det}[M(U) + 2ma] e^{-S(U)}\end{aligned}\tag{1.9.5}$$

The determinant describes the creation and annihilation of quark-

antiquark pairs in the vacuum and  $[M(U)+2ma]$  runs over all possible paths from  $x$  to  $y$ . To incorporate fermion loops in the construction of the vacuum we should calculate the determinant  $\text{Det}[M(U) + 2ma]$ .

The matrix  $[M(U) + 2ma]$  is very large and the calculation of the  $\text{Det}[M(U)+2ma]$  is not easy. Most of the calculations have been done in the so-called quenched approximation, i.e.,  $\text{Det}[M(U)+2ma] = 1$ .

### 1.10 Chiral Symmetry Breaking

To test the breaking of chiral symmetry[7], we use as an order parameter the Vacuum Expectation Value (VEV) of  $\bar{X}X$ . Chiral symmetry is broken if  $\lim_{m \rightarrow 0} \langle \bar{X}X(m) \rangle \neq 0$ . Since the lattice is a finite system we have to take care of all the different degenerate minima of the effective potential which lead to  $\langle \bar{X}X(m) \rangle = 0$  even if the symmetry is broken. The correct criterion is:

$$\lim_{m \rightarrow 0} \lim_{\text{volume} \rightarrow \infty} \langle \bar{X}X(m) \rangle \neq 0$$

(the limits do not commute).

We can express  $\langle \bar{X}X(m) \rangle$  in terms of the density of the eigenvalues of  $[M(U)+2ma]$  near to zero[8], i.e.,

$$\lim_{m \rightarrow 0} \lim_{\text{volume} \rightarrow \infty} \langle \bar{X}X(m) \rangle a^3 = 3\pi\rho(0) \quad (1.10.1)$$

which shows that it is the zero modes of the matrix which signal whether or not the chiral symmetry is broken.



## CHAPTER TWO

### 2.1 *An Introduction to Continuum Topology*

In this chapter we present a brief outline of some aspects of the continuum topology. The main framework will be the theory of fibre bundles<sup>[9]</sup>. Some invariants, topological in nature, which have the form of a group (homotopy, cohomology groups) are also discussed.

A bundle is the collection  $(E, \Pi, X, G, U_\alpha)$  where  $E$  is the total space,  $X$  is a topological space (base space),  $\Pi$  is a map from  $E \rightarrow X$ ,  $F$  is the fibre of the bundle and  $G$  is a group of homeomorphisms acting on the elements of the fibre  $F$ .  $U_\alpha$ 's are the covering patches of  $X$  and for each  $U_\alpha$  there is a homeomorphism

$$\Phi_\alpha : \Pi^{-1}(U_\alpha) \rightarrow U_\alpha \times F : \Pi \Phi_\alpha^{-1}(x, f) = x, x \in U_\alpha, f \in F.$$

A physical interpretation of this rather abstract mathematical terminology is as follows:

On the intersection  $U_\alpha \cap U_\beta \neq \emptyset$  we have :

$$\Phi_\alpha \Phi_\beta^{-1} : (U_\alpha \cap U_\beta) \times F \rightarrow (U_\alpha \cap U_\beta) \times F$$

and for fixed  $x \in U_\alpha \cap U_\beta$ ,  $\Phi_\alpha \Phi_\beta^{-1}$  is a homeomorphism from  $F \rightarrow F$ .

The function  $\Phi_\alpha \Phi_\beta^{-1}(x)$  is called a transition function and is denoted by  $g_{\alpha\beta}(x)$ . Later it is shown that it represents, what we call, in physics, the transition function between two overlapping patches. Actually the transition functions represent the change of coordinates between the two patches. The transition functions satisfy the following properties:

$$i) \quad g_{\alpha\alpha}(x) = \text{Identity}, \quad x \in U_{\alpha} \quad (2.1.1a)$$

$$ii) \quad g_{\alpha\beta}(x) = g^{-1}_{\beta\alpha} \quad x \in U_{\alpha} \cap U_{\beta} \quad (2.1.1b)$$

$$iii) \quad g_{\alpha\gamma}(x) = g_{\alpha\beta}(x)g_{\beta\gamma}(x), \quad x \in U_{\alpha} \cap U_{\beta} \cap U_{\gamma} \text{ (cocycle condition)} \quad (2.1.1c)$$

If we fix the coordinate system in the base space and change  $\Phi_{\alpha}$  to  $K_{\alpha}$ , then by defining  $g_{\alpha}(x) = \Phi_{\alpha}K_{\alpha}^{-1}$ ,  $x \in U_{\alpha}$  and  $g_{\beta}(x) = \Phi_{\beta}K_{\beta}^{-1}$ ,  $x \in U_{\beta}$ , we see that:

$$g'_{\alpha\beta}(x) = K_{\alpha}K_{\beta}^{-1} = g_{\alpha}^{-1}(x)g_{\alpha\beta}(x)g_{\beta}(x), \quad x \in U_{\alpha} \cap U_{\beta} \quad (2.1.1d)$$

Before we explain the mathematical terminology used in this work, some other useful points on the theory of bundles are outlined.

In physics we mainly use principal bundles and a principal bundle  $P$  is a bundle where the group  $G$  is identified with the fibre  $F$ . A section from  $U_{\alpha}$  to  $P$  is the map  $S: U_{\alpha} \rightarrow P$  which somehow undoes the work that the map  $\Pi$  does. So, if  $\omega$  is a form on  $P$  as usual  $S^*\omega \in T^*U_{\alpha}$ , where  $\omega \in T^*P$  ( $T^*P$  is the contangent space of  $P$ ). If we denote the coordinates of a point in the bundle as  $(x, g)$ ,  $x \in X$ ,  $g \in G$ , then by defining  $\omega = g^{-1}dg^{-1} + g^{-1}Ag$  ( $\omega \in T^*P$ ), we have (by doing the transformation:  $(x, g) \rightarrow (x', g')$ ,  $x = x'$ ),  $g^{-1}dg + g^{-1}A'g' = g^{-1}dg + g^{-1}Ag$  (i.e. demanding invariance of  $\omega$ ), which implies that:

$$A' = hAh^{-1} + dh h^{-1} \text{ with } g' = hg, \quad h \in G \quad (2.1.2)$$

Relation (2.1.2) gives clearly the identification of the gauge transformation as a map from fibre to fibre.

To give a clearer picture, we write on the overlap of 2 coordinate patches  $U_{\alpha} \cap U_{\beta} \neq \emptyset$ ,  $A_{\mu}^{\alpha}(x) = g^{\alpha\beta}(x)[A_{\mu}^{\beta}(x)]$ , where  $A_{\mu}^{\alpha}(x)$  is the

gauge field in  $U_\alpha$  and  $A_\mu^\beta(x)$  is the gauge field in  $U_\beta$ ,  
 $x \in U_\alpha \cap U_\beta$  and  $g_{\alpha\beta}(x)$  is the transition function on the overlap  
 $U_\alpha \cap U_\beta$ .

The notation  $g^{\alpha\beta}(x)[A_\mu^\beta(x)]$  is the compact notation for

$$g^{\alpha\beta}(x)A_\mu^\beta(x)g^{-1\alpha\beta}(x) - g^{\alpha\beta}\partial_\mu g^{-1\alpha\beta}(x).$$

Then doing a gauge transformation in  $U_\alpha$  and in  $U_\beta$ , we have (the primed fields are the gauged transformed fields):

$$A_\mu'^{(\alpha)}(x) = g^{(\alpha)}(x) [A_\mu^{(\alpha)}], x \in U_\alpha \text{ and}$$

$$A_\mu'^{(\beta)}(x) = g^{(\beta)}(x) [A_\mu^{(\beta)}], x \in U_\beta$$

If  $A_\mu'^{(\alpha)}(x) = g^{\alpha\beta}(x)[A_\mu'^{(\beta)}(x)],$

we get  $g^{\alpha\beta}(x) = g^\alpha(x)g^{\alpha\beta}(x)g^{-1\beta}(x),$  and this reflects the connection with physics of the above terminology. So, using language more familiar to a physicist, we arrive again at (2.1.1d), which was derived previously by the theory of fibre bundles.

We now give some general aspects of the topology in the continuum which refer to the theory of characteristic classes. Generally, using topological arguments (mainly continuity arguments) and differential geometry, we find some topological invariants for various manifolds. The main topological invariants we will use are the homotopy and cohomology groups and the characteristic classes of bundles which are mappings from cohomology groups to cohomology groups.

We start with the well known result

$$\Pi_3(SU(2)) = \Pi_3[S^3] = \mathbb{Z}. \tag{2.1.3}$$

This leads to  $SU(2)$  (and to the extent that  $SU(2)$  is embedded in  $SU(3)$ , to  $SU(3)$  instantons) instantons.  $\Pi_3$  is the third homotopy

group of the SU(2) group space (i.e.  $S^3$ ) and physically shows how many times we go around SU(2) when we have been around  $S^3$  once.

The significance of the above relation comes from the following: we start from the requirement of finite energy solutions to Yang-Mills (Y-M) equations in  $E^4$ .

The action  $S = (1/2) \int d^4x \text{Tr} F_{\mu\nu} F^{\mu\nu}$  must have a finite value at  $|x| \rightarrow \infty$  and for this to happen  $F_{\mu\nu} \rightarrow 0$  as  $|x| \rightarrow \infty$ . This is satisfied by  $A_\mu(x) = 0$  or by the pure gauge  $A_\mu(x) \rightarrow g^{-1}(x) \partial_\mu g(x)$ , where  $g(x)$  is the gauge transformation at  $|x| \rightarrow \infty$ .

We can consider then  $g(x)$  as a map from  $S^3$  [sphere at infinity in  $R^4$  so  $|x| \rightarrow \infty$ ] to SU(2) and we saw above that this map is classified by  $\Pi_3 [SU(2)] = Z$ . We can therefore associate with every  $g(x)$  an integer  $K \in Z$  which we call the winding number. This number actually classifies all the bundles over  $S^4$  with gauge group (fibre) SU(2).

In the case of SU(3), the picture is not so simple but we can consider the SU(3) group as a  $D = 8$  manifold and consider this as a bundle over a  $S^5$  sphere with gauge group SU(3) (the  $S^5$  spheres come from the fact that for every row of an SU(3) matrix with elements  $a, b, c$  we have  $|a|^2 + |b|^2 + |c|^2 = 1$  and this picture of the manifold structure of the SU(3) group is useful when we try to construct the topological charge<sup>[10]</sup> for the SU(3) case).

Now we consider the characteristic classes for the SU(2) bundle over  $S^4$ , i.e. the cohomology classes defined over the  $S^4$  with fibre the SU(2) group. For the cohomology class to be non-trivial it has to consist of closed but non-exact forms.

Some characteristic classes (Pontrjagin, Chern, Euler) are obtained by Lie algebra invariant polynomials of the curvature tensor  $F_{\mu\nu}$  and here we just denote the result. If  $C_i(P)$  is the Chern class ( $P$  is the principal bundle of the SU(2) group) then  $C_{i/2}(P)$

$\in H^i(X, R)$ , where  $H$  is the cohomology group over the base space-time space  $X$  with coefficients in  $R$ , and  $i$  represents the order of the cohomology group. In terms of the above mentioned polynomials of  $F_{\mu\nu}$ , we can write:

$C_i(P) = P_i(F)$  ( $P_i$  = polynomial of  $F_{\mu\nu}$ ) and since  $F_{\mu\nu} = A_\mu A_\nu dx^\mu dx^\nu$  is a 2-form,  $C_i(P)$  must be a 2i-form. The polynomials  $P_i$  appear when we expand the

$$\text{Det}(1 + iF/2\pi) = \sum_{i=0}^{\text{Dimension of the Group}} \frac{1}{i!} P_{m-i}(F) \quad (2.1.4a)$$

and so for the  $SU(2)$  group,  $C_1(P) = 0$ ,  $C_2(P) = -(1/16\pi^2) F \wedge F$ .  
(2.1.4b)

This is the result for which we were looking.  $C_2(P)$  is, what is called in 'instanton physics', the winding number. Integrating  $C_2$  over  $S^4$  and since  $H^4[S^4; \mathbb{Z}] = \mathbb{Z}$ , we get  $C_2 \in \mathbb{Z}$ .

We now give further details on the winding number in the following way:

Define

$$\Omega_\mu = 4\epsilon^{\mu\nu\lambda\rho} \text{Tr}[A_\nu \partial_\lambda A_\rho + (2/3) A_\nu A_\lambda A_\rho] \quad (2.1.5)$$

then

$$\partial_\mu \Omega^\mu = 2 \text{Tr} F_{\mu\nu} \tilde{F}^{\mu\nu} \quad (2.1.6)$$

( $\tilde{F}^{\mu\nu} = (1/2)\epsilon^{\mu\nu\rho\sigma} F_{\rho\sigma}$  ( $F_{\mu\nu}$  is called the dual tensor)). So

$$\int d^4x \text{Tr} F_{\mu\nu} \tilde{F}^{\mu\nu} = (1/2) \int_S d\sigma^\mu \Omega_\mu \quad (2.1.7)$$

and since the winding number is

$$\eta = (1/16\pi^2) \int d^4x \text{Tr} F_{\mu\nu} \tilde{F}^{\mu\nu} \quad (2.1.8)$$

we get

$$\eta = (1/32\pi^2) \int S d\sigma_\mu \Omega^\mu \quad (2.1.9)$$

In the Euclidean space  $(F_{\mu\nu} \pm \tilde{F}^{\mu\nu})^2 = 2(F_{\mu\nu} F^{\mu\nu} \pm F_{\mu\nu} \tilde{F}^{\mu\nu})$   
(since  $\epsilon^{\mu\nu\rho\sigma} = 2\delta^{\mu\nu}_{\rho\sigma}$ ). Hence

$$\text{Tr} \int F^2 d^4x \geq \left| \int \text{Tr} F \tilde{F} d^4x \right| = 16\pi^2 \eta \quad (2.1.10)$$

Since the Euclidean action

$$S_{\text{Euclidean}} = (1/2) \int d^4x \text{Tr} F_{\mu\nu} F^{\mu\nu} \quad (2.1.11)$$

we finally get

$$S_E \geq 8\pi^2/g^2 \quad (2.1.12)$$

So the action is minimized when  $F_{\mu\nu} = \pm \tilde{F}^{\mu\nu}$  and solutions with this property are called (anti)-selfdual solutions. The (anti)-selfdual gauge fields are the most important extrema of the action, i.e. they are always absolute minima for a given winding number. Belavin et al.[11] constructed solutions which satisfy the (anti)-selfduality condition for  $\eta = 1$ . The somewhat hidden point in the construction of the  $\eta = 1$  instanton solution is that the possibility to construct such a solution comes from the fact that we compactify on a sphere.

Now we give the expression for  $\eta$  in terms of the transition functions, which we will use when we discuss the form of  $n$  using twisted boundary conditions (TBC).

Using (2.1.7)

$$\eta = (1/16\pi^2) \int d^4x \text{Tr} F_{\mu\nu} \tilde{F}^{\mu\nu} =$$

$$(1/16\pi^2) \sum_{\mu} \int d^3\sigma_{\mu} [\Omega'_{\mu}(x_{\mu}=a_{\mu}) - \Omega'_{\mu}(x_{\mu}=0)] \quad (2.1.13)$$

and  $\Omega'_{\mu} = 2\Omega_{\mu}$ , ( $\Omega_{\mu}$  as defined in (2.1.5)). Here we work in a finite Euclidean box,  $x_{\mu}$  represents a point in the 4-dimensional Euclidean box and  $a_{\mu}$  are the sizes of the box in the  $\mu$  direction. Denoting by

$$A_{\mu}^{(i)} = U_{ij} A_{\mu}^{(j)} U_{ij}^{-1} + U_{ij} \partial_{\mu} U_{ij}^{-1} \quad (2.1.14)$$

(where  $i, j$  represent 2 coordinate patches which overlap and  $U_{ij}$  is the transition function on the overlap), we get<sup>[12]</sup>

$$\eta = (1/24\pi^2) \sum_{\mu} \int d^3\sigma_{\mu} \epsilon^{\mu\nu\rho\sigma} \{ \text{Tr}[(U^{-1}_{ij} \partial_{\nu} U_{ij})(U^1_{ij} \partial_{\rho} U_{ij})(U^1_{ij} \partial_{\sigma} U_{ij})] \\ + (1/8\pi^2) \sum_{\mu, \nu} \int d^2S_{\mu\nu} \epsilon^{\mu\nu\rho\sigma} \text{Tr}[(U_{ji} \partial_{\rho} U_{ij})(U_{jk} \partial_{\sigma} U_{kj})] \} \} \quad (2.1.15)$$

## 2.2 Introduction to Twisted Boundary Conditions (TBC)

Here we present in a pedagogical way, the basic ideas which concern the twisted boundary conditions. The TBC were first introduced by 't Hooft<sup>[13]</sup>, when he presented a general formulation for the definition of electric ( $\Phi_E$ ) and magnetic ( $\Phi_B$ ) fluxes in the non-Abelian gauge theories in such a way to make them gauge invariant. His definition "gave" them properties characteristic of fluxes (from our experience in the Abelian case), such as additivity, to be covariantly constant and to be related to the space-time topology. These properties distinguish the fluxes from

the Wilson loop which is not necessarily covariantly constant and additive.

TBC have appeared in various papers (see Ref. [14], for example) where it was shown that the QCD vacuum is a condensate of chromomagnetic vortices whose flux is quantized according to the centre of the  $SU(N)$ , i.e.  $Z(N)$ , and the so-called twist transition functions correspond to the phase of the unstable mode of the gauge field.

't Hooft showed that it is possible to have topologically stable fluxes if the space is not simply connected (i.e. the first homotopy group is not trivial). The main idea underlying the TBC is that all physical quantities must be periodic but since the gauge field  $A_\mu$  is not an observable, it can be periodic up to a gauge transformation.

As we saw in section 2.1, Euclidean solutions to the classical Y-M equations were found when we compactified on  $S^4$  and since  $\Pi_1(S^4) = 0$  and  $\Pi_1$  is the 1st homotopy group, we have to seek for a manifold  $M$  with  $\Pi_1(M) \neq 0$  if we want a manifold with non-trivial first homotopy group. So, instead of  $S^4$ , we choose the base space-time manifold  $M$  to be  $T^4 = S^1 \times S^1 \times S^1 \times S^1$  and it is known that  $\Pi_1(S^1 \times S^1 \times S^1 \times S^1) = Z \oplus Z \oplus Z \oplus Z$ .

Now instead of compactifying on  $S^4$ , we work on  $T^4$  (the 4-torus will be labelled by a 4-dimensional hypercube, i.e.  $0 < x_\mu \leq a_\mu$  and inside the space is flat). On the torus, the TBC lead to electric and magnetic fluxes without the necessity to introduce explicit sources (in the form of a quark anti-quark pair at opposite edges of the box to create these fluxes [15]). These fluxes are labelled by 6 integers (in  $D = 4$ ) which are topological invariants and express the non-triviality of the bundle over  $T^4$ . The general form of the TBC is [13]

$$A_V(x_\mu=a_\mu) \equiv \Omega_\mu(x) A_V(x_\mu=0) \Omega_\mu^{-1}(x) - i \Omega_\mu \partial_V \Omega_\mu^{-1} \quad (2.2.1)$$



where  $A_v$  is the gauge field in the  $v$  direction and  $\Omega_\mu$  the transition function in the  $\mu$  direction. Because we must have a single valued gauge field at the corners of the box, we deduce:

$$A_v(x_\mu=a_\mu, x_\lambda=a_\lambda)=\Omega_\mu(x)[A_v(x_\lambda=a_\lambda)]=\Omega_\lambda(x)[A_v(x_\mu=a_\mu)] \quad (2.2.2)$$

where we use the compact notation

$$A_v(x_\mu = a_\mu, x_\lambda = a_\lambda)=\Omega_\mu(x) [A_v(x_\lambda = a_\lambda)]$$

for

$$A_v(x_\mu = a_\mu, x_\lambda = a_\lambda) = \Omega_\mu(x_\mu = 0, x_\lambda = a_\lambda) A_v(x_\mu = 0, x_\lambda = a_\lambda) \\ \Omega_\mu^{-1}(x_\mu = 0, x_\lambda = a_\lambda) - \Omega_\mu(x_\mu = 0, x_\lambda = a_\lambda) \partial_v \Omega_\mu^{-1}(x_\mu = 0, x_\lambda = a_\lambda)$$

This leads to

$$\Omega_\mu(x+a_v) \Omega_v(x) = \Omega_v(x+a_\mu) \Omega_\mu(x) Z_{\mu v} \quad (2.2.3)$$

The factor  $Z_{\mu v}$  enters from the invariance of the gauge field under the  $Z(N)$  Group, i.e.  $A'_\mu = Z A_\mu Z^{-1} = A_\mu$  and so  $Z_{\mu v} \in Z(N)$ , i.e.:

$$Z_{\mu v} = e^{-2i\pi\eta_{\mu v}/N} \quad (2.2.4)$$

where  $N$  corresponds to the order of the  $SU(N)$  group and  $\eta_{\mu v}$  is the antisymmetric twist tensor with integer values. Geometrically,  $\eta_{\mu v}$  labels the different twist bundles over  $T^4$  with gauge group  $SU(N)/Z(N)$  and corresponds to the instanton number which classifies the bundles over  $S^4$ .

We can now define the electric and magnetic fluxes in the following way:

$K_i = \eta_{4i}$  ( $i=1,2,3$ ) ( we are working in 4-dimensions) is the electric flux ( $\Phi_E$ ) and  $M_k = \epsilon_{kij} \eta^{ij}$  ( $i,j=1,2,3$ ) is the magnetic flux ( $\Phi_B$ ) in the  $k$ -direction. This is a very simplified picture and if we want to define the fluxes more rigorously on  $T^4$ , we should define the order and disorder operators of 't Hooft which satisfy the  $Z(N)$  algebra,

i.e.  $A(C)B(C')=B(C')A(C)Z_{\mu\nu}$ , where  $A(C)$  measures  $\Phi_B$  through  $C$  ( $A(C)$  is identified as the usual Wilson loop operator) or  $\Phi_E$  along  $C$  and  $B(C')$  measures  $\Phi_E$  through  $C'$  or  $\Phi_B$  along  $C'$ (Fig.2.2.1). So if  $|m\rangle$  is a state with magnetic flux  $m$ ,

$$A(C)|m\rangle = e^{2i\pi m/N} |m\rangle \text{ and } A(C) B(C') |m\rangle = e^{2i\pi(m+1)/N} B(C')|m\rangle,$$

i.e.  $B(C')$  creates one unit of magnetic flux through  $C'$ .

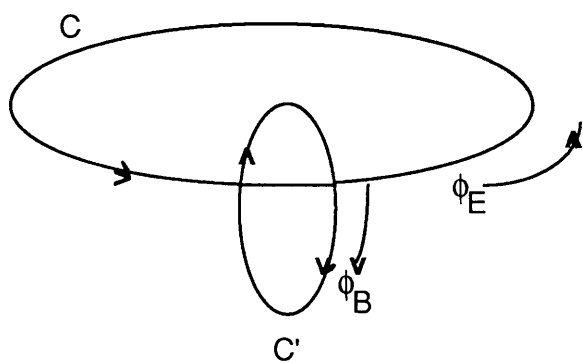


**Fig.2.21 Fluxes à la 't-Hooft**

Here we give a realization of 't Hooft's fluxes in a simple way. Working only in the 1-2 level we have from the consistency condition (2.2.3)

$$\Omega_1(x_1,x_2+a_2)\Omega_2(x_1,x_2) = \Omega_2(x_1+a_1,x_2)\Omega_1(x_1,x_2)Z_{12} \tag{2.2.5}$$

We now define

$$\Phi_{\text{'t-Hooft}} = \Omega^{-1}_1(x_1,x_2)\Omega^{-1}_2(x_1+a_1,x_2)\Omega_1(x_1,x_2+a_2)\Omega_2(x_1,x_2) \tag{2.2.6}$$

which is covariantly constant and additive.

For the  $SU(N)$  groups

$$\Phi_{\text{'t-Hooft}} = e^{2i\pi\eta_{12}/N}. \tag{2.2.7}$$

This reminds us of the definition of the fluxes in the Abelian gauge theories where the fluxes are defined as  $e^{ig\Phi}$ .

We now discuss the effect of the gauge transformation on the transition 'twist' functions  $\Omega_\mu$ .

After a gauge transformation on the gauge field  $A_\mu$  we get:

$$A'_\mu(a_1+x_1, x_2) = g(a_1+x_1, x_2)A_\mu(a_1+x_1, x_2)g^{-1}(a_1+x_1, x_2) - (i/g)(\partial_\mu g(a_1+x_1, x_2))g^{-1}(a_1+x_1, x_2), \quad (2.2.8)$$

where  $g(x)$  represents the gauge transformation.

Using the TBC conditions we get:

$$A'_\mu(a_1+x_1, x_2) = \Omega'_1(x_1, x_2)A'_\mu(x_1, x_2)\Omega'^{-1}_1(x_1, x_2) - (i/g)(\partial_\mu \Omega'_1(x_1, x_2))\Omega'^{-1}_1(x_1, x_2) \quad (2.2.9)$$

and

$$A_\mu(a_1+x_1, x_2) = \Omega_1(x_1, x_2)A_\mu(x_1, x_2)\Omega^{-1}_1(x_1, x_2) - (i/g)(\partial_\mu \Omega_1(x_1, x_2))\Omega^{-1}_1(x_1, x_2) \quad (2.2.10)$$

Solving the above equations we get:

$$\begin{aligned} A_\mu(x_1, x_2) &= (i/g)\Omega_1^{-1}(x_1, x_2)(\partial_\mu \Omega_1(x_1, x_2)) + \\ & (i/g)\Omega_1^{-1}(x_1, x_2)g^{-1}(a_1+x_1, x_2)(\partial_\mu g(a_1+x_1, x_2))\Omega_1(x_1, x_2) + \\ & \Omega_1^{-1}(x_1, x_2)g^{-1}(a_1+x_1, x_2)\Omega'_1(x_1, x_2)g(x_1, x_2) \\ & A_\mu(x_1, x_2)g^{-1}(x_1, x_2)\Omega'^{-1}_1(x_1, x_2)g(a_1+x_1, x_2)\Omega_1(x_1, x_2) - \end{aligned}$$

$$(i/g)\Omega_1^{-1}(x_1, x_2)g^1(a_1+x_1, x_2)[\Omega_1'(x_1, x_2)(\partial_\mu g(x_1, x_2)) + \partial_\mu \Omega_1'(x_1, x_2)]\Omega_1^{-1}(x_1, x_2)g(a_1+x_1, x_2)\Omega_1(x_1, x_2) \quad (2.2.11)$$

which is satisfied for

$$\Omega_1'(x_1, x_2) = g(a_1+x_1, x_2)\Omega_1(x_1, x_2)g^{-1}(x_1, x_2) \quad (2.2.12a)$$

In a similar way :

$$\Omega_2'(x_1, x_2) = g(x_1, x_2+a_2)\Omega_2(x_1, x_2)g^{-1}(x_1, x_2). \quad (2.2.12b)$$

This gives us the freedom to pick up a gauge with  $\Omega_1=1$  or  $\Omega_2=1$  and one such choice which satisfies the TBC is (for the  $SU(2)$  group) :

$$\Omega_1(x_1, x_2) = e^{i\pi\eta_{12}\sigma_3}, \Omega_2 = 1 \quad (2.2.13)$$

In this case  $\Omega_1(x_1+a_1, x_2) = e^{i\pi\eta_{12}}\Omega_1(x_1, x_2)$  and, if we denote by  $h(p)$  a curve in  $SU(N)/Z(N)$  i.e.,

$$h(p) = \Omega_1^{-1}(x_1, x_2)\Omega_1(x_1, x_2+p) \quad a_2 \geq p \geq 0,$$

we see that  $h(p)$  varies from 1 ( $p=0$ ) to  $e^{i\pi\eta_{12}}$  ( $p=a_2$ ). From this example we have a better understanding of the geometrical meaning of  $\eta_{12}$  as a label of the different equivalent classes in  $SU(N)/Z(N)$ , i.e.,  $\eta_{\mu\nu} \in \Pi_1[SU(N)/Z(N)] = Z(N)$  and from the values of  $\eta_{\mu\nu}$  we can classify whether or not a bundle is trivial ( $\eta_{12} = 0$  corresponds to untwisted trivial bundles).

As in the instanton case (transition from one vacuum to the other happens by changing the winding number) here also (using TBC) we

cannot transfer from one homotopic class to the other without changing  $\eta_{\mu\nu}$ .

Some last remarks follow:

(a) When we will apply the TBC on the lattice, the only assumption we will make is the periodicity of the non-local quantities and not of the gauge field itself (demanding periodicity of the gauge field itself excludes the possibility to introduce non-trivial  $\eta_{\mu\nu}$ 's). We present now an example(in  $D = 2$ ) of the periodicity of the non-local Wilson loop operator in a finite box in the continuum[16]:

We use 2 gauges (Fig.2.2.2) :

In Gauge 1:

$$A_1^{(1)}(x) = 0 \quad A_2^{(1)}(0, x_2) = 0$$

and in Gauge 2:

$$A_1^{(2)}(x) = 0 \quad A_2^{(2)}(a_1, x_2) = 0$$

and by relating

$$A_\mu^{(2)} = g(x)[A_\mu^{(1)}(x)] \tag{2.2.14a}$$

we deduce that  $g(x) = g(x_2)$  . From the periodicity of the Wilson loop  $P \exp \int A_\mu dx^\mu$  ( $P$  stands for the path ordering) and using (2.2.14a) :

$$A_2^{(1)}(a_1 + x_1, x_2) = \Omega_1(x_2) [A_2^{(1)}(x_1, x_2)], \tag{2.2.14b}$$

with  $\Omega_1(x_2) = g^{-1}(x_2)$

i.e., the transition function is the inverse of the gauge transformation.

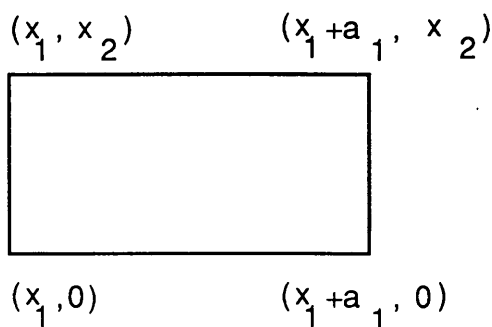


**Fig.2.2.2 Periodicity of the Wilson loop**

(b) The second point we want to refer to is the following:

From the general theory of classical solutions to Y-M equations (Solitons), it is known that these solutions have a quantized flux and a finite energy. We noted earlier that the 't Hooft fluxes were quantized and the quantization comes through the  $Z(N)$  group.

The point which remains to be established is whether the classical energy of the configurations which satisfy the TBC is bounded from below by a positive lower bound.

In Chapter 3, we give the explicit formula for the action under the TBC which shows there could be a positive lower limit, but here we follow [17] to present some arguments, qualitative in nature, for the configurations which satisfy the TBC. Ambjorn and Flyvbjerg [17] showed that it is possible to have magnetic flux different from zero and  $E_{\text{classical}} = 0$  (in the non-Abelian case only). As an illustration, we present their example. Since, under a gauge transformation  $\eta_{\mu\nu}$  is invariant, we choose as

$$\Omega_1 = 1, \Omega_2 = 1 \text{ for } m_3 = 0$$

$$(m_3 = \text{magnetic flux in the } 3_{\text{rd}} \text{ direction}) = \varepsilon_{312} \eta^{12}) \text{ and}$$

$\Omega_1 = i\sigma_1$  ,  $\Omega_2 = i\sigma_3$  for  $m_3 = 1$ .  $\sigma_1, \sigma_2$  are the Pauli matrices.

We can easily check that the configurations  $A_\mu = H(x_1)\delta_{\mu 2}\sigma_3/2$ , with  $H(x_1)$  <sup>anti</sup>periodic in  $x_1$ , and  $A_\mu = 0$  <sup>(for  $A_\mu = 0$ )</sup> can have  $m_3 \neq 0$  (and so non-zero magnetic flux  $\Phi_B$ ) but  $E_{\text{classical}} = 0$ . The mathematical reasoning for this is simple and is attributed to the fact that two constant transition functions on a torus  $T^2$  do not give a trivial bundle but for a sphere we have only one coordinate patch (since a sphere is covered by two patches) at the overlap and a constant transition function maps everything to a single point and of course a bundle over a single point is obviously trivial ( a base space contractible to a point results to trivial bundle).

(c) We now present a simple example of a system which satisfies the  $Z(N)$  algebra.

We work in  $2 + 1$  Dimensions and consider the following Hamiltonian describing a  $Z(N)$  gauge theory (Fig.2.2.3)

$$H = -g \sum_{\text{links}} [A_l^+ + A_l^-] - \sum_{\text{Plaques}} [Q(n_1)Q(n_2)Q(n_3)Q(n_4) + \text{h.c.}] - 2 \tag{2.2.15}$$

The operators  $A_l, Q_l$  are associated with the links of the lattice and obey the  $Z(N)$  algebra

$$A_l^N = Q_l^N = 1, A_l^+ = A_l^{-1}, Q_l^+ = Q_l^{-1} \text{ and}$$

$$A_l Q_{l'} = Q_{l'} A_l e^{2i\pi/N}$$

$(A_l, Q_{l'})$  commute for different links  $l, l'$ ,  $[A_l, Q_{l'}] = 0$  if  $l \neq l'$ ).

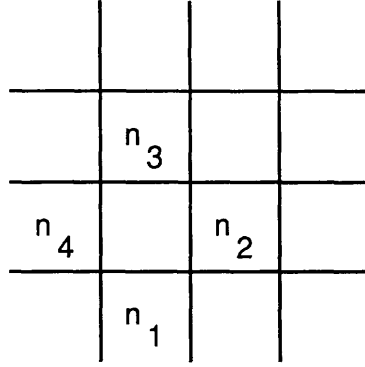


**Fig.2.2.3 A lattice notation**

From the above equations we can have (since  $A_l$  is unitary):

$$A|n\rangle = e^{2i\pi/N}|n\rangle \text{ and } Q|n\rangle = |n+1\rangle, n = 0, 1, \dots, N-1$$

and with the above representation for  $A_l, Q_l$  we get  $QAe^{2i\pi/N} = AQ$ .

If we denote by  $E_l, \tilde{A}_m$  the electric field and the vector potential respectively (with  $[E_l, \tilde{A}_m] = i\delta_{lm}$ ) by writing  $A_l = e(2i\pi/N)E_l$  and  $Q_l = e^{i\tilde{A}_l}$  we get again:

$$A_l Q_l = Q_l A_l e^{2i\pi/N}.$$

From the instanton case we know that there is an operator (call this  $T$ ) which, acting on a vacuum with winding number  $|n\rangle$ , transfers this to  $|n+1\rangle$ , i.e.,  $T|n\rangle = |n+1\rangle$  and this operator commutes with the Hamiltonian. If we then consider the  $\theta$ -vacuum  $|\theta\rangle = \sum_n e^{-in\theta} |n\rangle$ , we have  $T|\theta\rangle = e^{i\theta} |\theta\rangle$ .

In the above example, the corresponding operator to  $T$  is defined as ( $i$  = a lattice site):

$$T(i) = \prod_{i \in l(+)} A^+_{l(+)} \prod_{i \in l(-)} A_{l(-)} \quad (2.2.16a)$$

(+ corresponds to the positive direction - to the negative direction).



$T(i)$  generates a symmetry transformation:

$$\begin{aligned} Q_l &\rightarrow 2i\pi/N, l \in i \\ Q_l &\rightarrow Q_l, l \notin i \\ P_l &\rightarrow P_l \quad \forall i \end{aligned} \quad (2.2.16b)$$

We can easily see that  $[T(i), H] = 0$  and

$$T(i) = e^{(-2i\pi/N)[\sum_{l(+)} E_l - \sum_{l(-)} E_l]} \quad (2.2.16c)$$

with  $[T(i)]^N = 1$ .

In the non-trivial sector of the Hilbert space we have  $T(i) \neq 1$  and this corresponds to  $\nabla \cdot E = \sum_{l(+)} E_l - \sum_{l(-)} E_l \neq 0$ , i.e., the Gauss law.

We now express the Hamiltonian (2.2.15) in terms of  $E_l, A_m$  and this results to

$$H = -g \sum_{\text{links}} [1 - \cos(2\pi E_l/N)] + 2 \sum_{\text{plaques}} [1 - \cos(B_p)] \quad (2.2.17)$$

with  $B_{\text{plaq}} = \tilde{A}_{n_1} + \tilde{A}_{n_2} - \tilde{A}_{n_3} - \tilde{A}_{n_4}$  and from (2.2.17) we can identify a link with  $E_l \neq 0$  as carrying electric flux and a plaquette with  $B_p \neq 0$  as carrying magnetic flux.

d) We now elaborate on the inclusion of a kind of twist on the matter field while we have applied TBC for the gauge field. This is a non-trivial problem since the gauge field while transforming in the adjoint of the group is invariant under  $Z(N)$  transformations (for the  $SU(N)$  case), the  $\Psi$  (matter) field, because it belongs to the fundamental representation, transforms non trivially under  $Z(N)$ . To overcome this problem we introduce a flavor twist for the  $\Psi$ -field in the following sense<sup>[18]</sup>:

$$\Psi(x+L, y, z, t) = \Omega_1^{c(\text{COLOR})}(y, z, t) \Psi(x, y, z, t) \Omega_1^{f(\text{FLAVOR})-1}(y, z, t) \quad (2.2.18a)$$

$$\Psi(x, y+L, z, t) = \Omega_2^{c(\text{COLOR})}(y, z, t) \Psi(x, y, z, t) \Omega_2^{f(\text{FLAVOR})-1}(y, z, t) \quad (2.2.18b)$$

etc.

where (c,f) refer to (color, flavor) indices of  $\Psi$  respectively.

The consistency condition (single-valueness) of the  $\Psi$ -field at the boundary leads to:

$$\begin{aligned} \Psi(x+L, y+L) &= \Omega_1^C(y+L) \Psi(x, y+L) \Omega_1^{f-1}(y+L) = \\ &= \Omega_1^C(y+L) \Omega_2^C(x) \Psi(x, y) \Omega_2^{f-1}(x) \Omega_1^{f-1}(y+L) = \\ &= \Omega_2^C(x+L) \Omega_1^C(x) \Psi(x, y) \Omega_1^{f-1}(x) \Omega_2^{f-1}(x+L) \quad (2.2.19) \\ \Rightarrow \Psi(x, y) &= \Omega_2^{C-1}(x+L) \Omega_1^{C-1}(y+L) \Omega_2^C(x+L) \Omega_1^C(y) \Psi(x, y) \\ &\quad \Omega_1^{f-1}(y) \Omega_2^{f-1}(x+L) \Omega_1^f(y+L) \Omega_2^f(x) \end{aligned}$$

and since

$$\begin{aligned} \Omega_1(a_2+x_2) \Omega_2(x_1) &= \Omega_2(a_1+x_1) \Omega_1(x_2) Z^C_{12} \\ \Rightarrow \eta^C_{12} &= \eta^{f_{12}} \pmod{N}. \quad (2.2.20) \end{aligned}$$

In Chapter 4 we deal with the eigenvalues of the fermion matrix under the inclusion of color and flavor twist.

## CHAPTER THREE

### 3. TOPOLOGY AND LATTICE

Numerical evidence is presented for the existence of non-integer topological charge on a lattice using TBC.

As was shown in the previous chapter, the winding number  $\eta$  (which, from now on, we call topological charge  $Q$ ) is expressed in terms of the transition functions, and we now show that under the TBC, it contains an integer part plus a part which depends on the twist tensor  $n_{\mu\nu}$  and for some combinations of the twist integers ( $n_{\mu\nu}$ ) it leads to a non-integer  $Q$ .

We mainly use non-constant transition  $\Omega_\mu(x)$  but in some cases we also use constant transition functions which still satisfy the twist algebra (2.2.3.). In the case of constant  $\Omega_\mu$ 's we verify what we expected: the action is not bounded from below by a positive bound and it can be lowered to zero. We also have cases where the  $\Omega_\mu$ 's are not constant but by arranging the  $n_{\mu\nu}$ 's in a way to be clear later we again have an action which could reach a zero value. The latter cases are reminiscent of the instanton case where we have a plateau of the action which ends to a zero value. Also, in  $D = 4$  and in the case of the  $SU(2)$  group we capture a topological object of charge  $1/4$  using constant  $\Omega_\mu$ 's in only two directions.

#### 3.1. *Dependence of the Topological Charge on the Twist Transition Functions.*

We start from the expression (2.1.13) and denoting by  $\Omega_\mu$  the transition functions we get [19]:

$$Q = (1/24\pi^2)\Sigma_{\mu}\int d^3\sigma^{\mu}\epsilon_{\mu\nu\rho\sigma}(1/3)\{Tr[(\Omega_{\mu}\partial_{\nu}\Omega_{\mu}^{-1}]$$

$$[\Omega_{\mu}\partial_{\rho}\Omega_{\mu}^{-1}][\Omega_{\mu}\partial_{\sigma}\Omega_{\mu}^{-1}]+\partial_{\nu}Tr[(1/i)(\Omega_{\mu}^{-1}\partial_{\rho}\Omega_{\mu})A_{\sigma}(x_{\mu}=0)]\}$$

$$(3.1.1)$$

$$+ (1/8\pi^2)\Sigma_{\mu,\nu}\int d^3S_{\mu\nu}\epsilon^{\mu\nu\rho\sigma}\{Tr[\Omega_{\nu}^{-1}\partial_{\rho}\Omega_{\nu}][\Omega_{\mu}\partial_{\sigma}\Omega_{\mu}^{-1}]\}_{x_{\mu}=a_{\mu}}\}$$

Using the consistency condition (2.2.3) we can calculate the  $\partial_{\nu}$  derivative term as the difference between  $x_{\nu} = a_{\nu}$  and  $x_{\nu} = 0$  with  $x_{\mu} = 0$  (fixed) and we get:

$$Tr[(1/i)[\Omega_{\mu}^{-1}\partial_{\rho}\Omega_{\mu}]|_{x_{\nu}=a_{\nu}}A_{\sigma}(x_{\mu}=0, x_{\nu}=a_{\nu}) -$$

$$(1/i)[\Omega_{\mu}^{-1}\partial_{\rho}\Omega_{\mu}]|_{x_{\nu}=0}A_{\sigma}(x_{\mu}=0, x_{\nu}=0)] - (\mu \leftrightarrow \nu) =$$

$$Tr[(\Omega_{\nu}^{-1}\partial_{\rho}\Omega_{\nu})|_{x_{\mu}=a_{\mu}}[\Omega_{\mu}\partial_{\sigma}\Omega_{\mu}^{-1}]|_{x_{\nu}=0} - (\mu \leftrightarrow \nu).$$

Using this we end up with:

$$Q=(1/24\pi^2)\Sigma_{\mu}\int d^3\sigma^{\mu}\epsilon_{\mu\nu\rho\sigma}\{Tr[(\Omega_{\mu}\partial_{\nu}\Omega_{\mu}^{-1})[\Omega_{\mu}\partial_{\rho}\Omega_{\mu}^{-1}][\Omega_{\mu}\partial_{\sigma}\Omega_{\mu}^{-1}]$$

$$+ (1/8\pi^2)\Sigma_{\mu,\nu}\int d^3S_{\mu\nu}\epsilon^{\mu\nu\rho\sigma}\{Tr[\Omega_{\nu}^{-1}\partial_{\rho}\Omega_{\nu}]|_{x_{\mu}=a_{\mu}}[\Omega_{\mu}\partial_{\sigma}\Omega_{\mu}^{-1}]|_{x_{\nu}=0}\}$$

$$(3.1.2)$$

with

$$d^3S_1 = \int_0^{a_2} dx^2 \int_0^{a_3} dx^3 \int_0^{a_4} dx^4, \quad d^2S_{12} = \int_0^{a_3} dx^3 \int_0^{a_4} dx^4, \quad \text{etc...}$$

We now present some comments on the general form of the "twist" transition functions as well as the general method of constructing the transition functions for the constant and non-

constant twist.

In the case of constant transition functions, the general method is based on the existence of matrices  $A, B$  with the property  $A.B=B.A.e^{2i\pi/N}$ , where  $A, B$  are  $N \times N$  matrices which belong to the  $SU(N)$  group. The method consists of finding the  $\Omega_\mu$ 's by taking the powers of some specially chosen  $U, V$  matrices<sup>[17]</sup>. For the case of the  $SU(2)$  group we have the matrices

$$U = \begin{bmatrix} 0 & 1 \\ 1 & 0 \end{bmatrix} \quad V = \begin{bmatrix} e^{i\pi} & 0 \\ 0 & 1 \end{bmatrix}$$

and

$$\Omega_1=U^{u_1}V^{v_1}, \Omega_2=U^{u_2}V^{v_2}, \Omega_3=U^{u_3}V^{v_3} \tag{3.1.3a}$$

where  $u_1, u_2, u_3, v_1, v_2, v_3 \in Z(2)$ .

This leads to 8 combinations in 3 dimensions (generally there are  $N^{D(D-1)/2}$  different classes for  $N$  = dimension of the group under consideration and  $D$  = dimension of space-time).

Two of the eight classes are:

$$\begin{bmatrix} u_1 \\ u_2 \\ u_3 \end{bmatrix} = \begin{bmatrix} 1 \\ 1 \\ 0 \end{bmatrix}, \quad \begin{bmatrix} v_1 \\ v_2 \\ v_3 \end{bmatrix} = \begin{bmatrix} 0 \\ 0 \\ 1 \end{bmatrix}$$

with twist functions

$$\Omega_1 = \sigma_1, \Omega_2 = \sigma_1, \Omega_3 = -\sigma_3 \tag{3.1.3b}$$

i.e., we are using twists only in the 1-3, 2-3 levels.

and

$$\begin{bmatrix} u_1 \\ u_2 \\ u_3 \end{bmatrix} = \begin{bmatrix} 1 \\ 1 \\ 0 \end{bmatrix}, \quad \begin{bmatrix} v_1 \\ v_2 \\ v_3 \end{bmatrix} = \begin{bmatrix} 1 \\ 0 \\ 1 \end{bmatrix}$$

with twist functions

$$\Omega_1 = -\sigma_1, \Omega_2 = \sigma_1, \Omega_3 = -\sigma_3 \quad (3.1.3c)$$

i.e. we have twists only in the 1-2, 2-3, 1-3 levels.

In the case of the SU(3) group and in 3-dimensions we have 27 classes, two of which are:

$$\Omega_1 = \begin{bmatrix} 0 & 1 & 0 \\ 0 & 0 & 1 \\ 1 & 0 & 0 \end{bmatrix}, \quad \Omega_2 = \begin{bmatrix} 0 & 0 & 1 \\ 1 & 0 & 0 \\ 0 & 1 & 0 \end{bmatrix}, \quad \Omega_3 = \begin{bmatrix} e^{2i\pi/3} & 0 & 0 \\ 0 & e^{-2i\pi/3} & 0 \\ 0 & 0 & 0 \end{bmatrix}$$

(3.1.3d)

and :

$$\Omega_1 = \begin{bmatrix} 0 & e^{-2i\pi/3} & 0 \\ 0 & 0 & 1 \\ e^{2i\pi/3} & 0 & 0 \end{bmatrix}$$

$$\Omega_2 = \begin{bmatrix} 0 & 0 & 1 \\ 0 & 0 & 1 \\ 0 & 1 & 0 \end{bmatrix}, \quad \Omega_3 = \begin{bmatrix} e^{2i\pi/3} & 0 & 0 \\ 0 & e^{-2i\pi/3} & 0 \\ 0 & 0 & 1 \end{bmatrix} \quad (3.1.3e)$$

with spatial twists at all levels.

Following [20] we write  $\Omega_\mu = P^{S_\mu} Q^{t_\mu}$  with

$$P = \begin{bmatrix} 0 & 1 & \dots & \dots & 0 \\ & 0 & 1 & \dots & 0 \\ & & & \ddots & \\ & & & & 1 \\ 1 & \dots & \dots & \dots & 0 \end{bmatrix}$$

$$Q = e^{\frac{i\pi(1-N)}{N}} \begin{bmatrix} 1 & 0 & 0 \\ 0 & e^{2i\pi/N} & 0 \\ 0 & 0 & e^{2i\pi(1-N)/N} \end{bmatrix}$$

and  $PQ = QPe^{2i\pi/N}$  ( $Z(N)$  algebra).

Then :

$$\Omega_\nu \Omega_\mu = P^{S_\nu} Q^{t_\nu} P^{S_\mu} Q^{t_\mu} = P^{S_\nu} [Q^{t_\nu}, P^{S_\mu}] Q^{t_\mu} -$$

$$P^{S_\nu} [Q^{t_\nu}, P^{S_\mu}] Q^{t_\mu} + P^{S_\mu} Q^{t_\mu} P^{S_\nu} Q^{t_\nu} \Rightarrow$$

$$\Omega_\mu \Omega_\nu = \Omega_\nu \Omega_\mu Z^{-(t_\mu s_\nu - t_\nu s_\mu)},$$

where we used:

$$[Q^m, P^n] = (1 - Z^{mn}) Q^m P^n \text{ and } Z = e^{2i\pi/N}.$$

We identify  $\eta_{\mu\nu}$  as  $\eta_{\mu\nu} = s_\mu t_\nu - s_\nu t_\mu \pmod{N}$ .

From (3.1.2) it can be shown that [19,20]

$$Q = (g^2/16\pi^2) \int_{\text{box}} d^4x \text{Tr} F_{\mu\nu} \tilde{F}^{\mu\nu} = v - k/N \quad v \in \mathbb{Z} \quad (3.1.4)$$

and

$$k = (1/8) \epsilon^{\mu\nu\rho\sigma} \eta_{\mu\nu} \eta_{\rho\sigma} = \eta_{12} \eta_{34} + \eta_{13} \eta_{42} + \eta_{14} \eta_{23} \quad (3.1.5).$$

From

$$S_E = (1/2) \int \text{Tr} F_{\mu\nu} F^{\mu\nu} \geq |(1/2) \int \text{Tr} F_{\mu\nu} \tilde{F}^{\mu\nu}| \Rightarrow$$

$$S_E \geq \min(8\pi^2/g^2) |v - k/N|, \quad (3.1.6)$$

(where the equality holds for  $F_{\mu\nu} = \pm \tilde{F}_{\mu\nu}$  i.e (anti)-selfdual configurations), we notice that for only spatial twist we have  $k = 0$  and the action can be lowered to zero (i.e.,  $F_{\mu\nu} = 0$ ). A solution to  $F_{\mu\nu} = 0$  is, of course,  $A_\mu = 0$  and in this case the transition functions must be constant for the inhomogeneous term in (2.2.1) to vanish (we use the gauge  $\partial_\mu \Omega^\mu = 0$ ).

We now deal with the construction of the non-constant transition functions[20]. The method consists of decomposing the  $SU(N)$  group into a direct sum of smaller  $SU(N)$  groups and applying the twists in every subgroup, i.e., we decompose

$$SU(N) \supset SU(k) \oplus SU(l) \oplus U(1) \text{ with } k+l = N.$$



Using

$$\omega = 2\pi \begin{bmatrix} 1 & & & & \\ & 1 & & & \\ & & \ddots & & \\ & & & 1 & \\ & & & & -k \\ & & & & -k & \\ & & & & & \ddots \\ & & & & & & -k \end{bmatrix}$$

k-times

l-times

and denoting by the subscripts 1, 2 the two smaller sub-groups of SU(N), we write

$$\tilde{P}_1 = \left[ \begin{array}{c|c} P_1_{k \otimes k} & 0 \\ \hline 0 & 1_{l \otimes l} \end{array} \right]$$

$$\tilde{Q}_1 = \left[ \begin{array}{c|c} Q_1_{k \otimes k} & 0 \\ \hline 0 & 1_{l \otimes l} \end{array} \right]$$

$$\tilde{P}_2 = \begin{bmatrix} 1_{k \otimes k} & 0 \\ 0 & P_{2l} \otimes 1 \end{bmatrix}$$

$$\tilde{Q}_2 = \begin{bmatrix} 1_{k \otimes k} & 0 \\ 0 & Q_{2l} \otimes 1 \end{bmatrix}$$

with

$$P_1 Q_1 = Q_1 P_1 e^{2i\pi/k}, \quad P_2 Q_2 = Q_2 P_2 e^{2i\pi/l}.$$

Hence the commutation relations for  $P_{1,2}, Q_{1,2}$  are

$$\tilde{P}_1 \tilde{Q}_1 = \tilde{Q}_1 \tilde{P}_1 e^{2i\pi/N + i\omega/Nk}$$

$$\text{and} \quad \tilde{P}_2 \tilde{Q}_2 = \tilde{Q}_2 \tilde{P}_2 e^{2i\pi/N - i\omega/Nl} \quad (3.1.8)$$

Defining :

$$\Omega_{\mu}(x) = \begin{bmatrix} \tilde{P}_1^S & \tilde{Q}_1^t & 0 \\ 0 & \tilde{P}_2^u & \tilde{Q}_2^v \end{bmatrix} e^{i \omega \sum_{\lambda} a_{\mu\lambda} \frac{x_{\lambda}}{a_{\lambda}}} \quad (3.1.9)$$

( $s_{\mu}, t_{\mu}, u_{\mu}, v_{\mu} \in \mathbb{Z}$  and  $a_{\mu\nu} = -a_{\nu\mu} \in \mathbb{R}$ ) and using (2.2.2)  $\Rightarrow$

$$a_{\mu\nu} - a_{\nu\mu} = \eta_{\mu\nu}^{(2)} / (Nl) - \eta_{\mu\nu}^{(1)} / (Nk) \quad (3.1.10)$$

with

$$\eta_{\mu\nu} = \eta_{\mu\nu}^{(2)} + \eta_{\mu\nu}^{(1)} \quad (3.1.10a)$$

and

$$\eta_{\mu\nu}^{(1)} = s_{\mu} t_{\nu} - s_{\nu} t_{\mu} + \text{integer} \quad (3.1.10b)$$

$$\eta_{\mu\nu}^{(2)} = u_{\mu} v_{\nu} - u_{\nu} v_{\mu} + \text{integer} \quad (3.1.10c)$$

We now present some examples of non-constant  $\Omega_{\mu}$ 's, which were used when we applied the TBC on the lattice.

**A)** SU(2) case with  $k = 1$ , i.e.,  $(k/N) = 1/2$  :

We choose  $\eta_{12}^{(1)} = -1, \eta_{34}^{(2)} = 1$ , other  $\eta_{\mu\nu}^{(1,2)}$ 's zero, with:

$$s^{\mu} = (-1, 0, 0, 0), t^{\mu} = (0, 1, 0, 0), u^{\mu} = (0, 0, 1, 0), v^{\mu} = (0, 0, 0, 1).$$

This choice leads to :

$$\Omega_1(x) = e^{2i\pi\sigma_3 a_{12} x_2/a_2},$$

$$\Omega_2(x) = e^{-2i\pi\sigma_3 a_{12} x_1/a_1} \quad (3.1.11)$$

$$\Omega_3(x) = e^{2i\pi\sigma_3 a_{34} x_4/a_4}$$

$$\Omega_4(x) = e^{-2i\pi\sigma_3 a_{34} x_3/a_3}, \quad a_{12} = a_{34} = (1/4).$$

Clearly

$$\Omega_1(x_2 = a_2) \Omega_2(x_1 = 0) = \Omega_2(x_1 = a_1) \Omega_1(x_2 = 0) e^{i\pi}$$

and  $Z_{12} = -1$ .

In this case we expect the action to be bounded from below, i.e.

$$S_E \geq (8\pi^2/g^2) |v^{-1/2}|.$$

**B)** SU(2) group with  $k = -3$ ,  $(k/N) = 3/2$

We choose:

$$\eta^{(1)}_{12} = -1, \quad \eta^{(1)}_{13} = -1, \quad \eta^{(1)}_{14} = -1$$

$$\eta^{(2)}_{34} = 1, \eta^{(2)}_{42} = 1, \eta^{(2)}_{23} = 1, \text{ other } \eta^{(1,2)}_{\mu\nu} \text{'s zero,}$$

with

$$s^\mu = (-1, 0, 0, 0), \quad t^\mu = (0, 1, 1, 1), \quad u^\mu = (0, 0, -1, 1), \quad v^\mu = (0, 1, 0, -1),$$

and we get :

$$\begin{aligned}
\Omega_1(x) &= e^{(i\pi/2)\sigma_3 \{ (x_2/a_2) + (x_3/a_3) + (x_4/a_4) \}}, \\
\Omega_2(x) &= e^{(i\pi/2)\sigma_3 \{ -(x_1/a_1) + (x_3/a_3) - (x_4/a_4) \}}, \\
\Omega_3(x) &= e^{(i\pi/2)\sigma_3 \{ -(x_1/a_1) - (x_2/a_2) + (x_4/a_4) \}}, \quad (3.1.12) \\
\Omega_4(x) &= e^{(i\pi/2)\sigma_3 \{ -(x_1/a_1) + (x_2/a_2) - (x_3/a_3) \}},
\end{aligned}$$

which satisfy the twist algebra (2.2.3) .

**C)** Now we proceed to the  $SU(3)$  group with:  $k = -1$ ,  $(k/N) \Rightarrow 1/3$ .

Then

$$\begin{aligned}
\Omega_1(x) &= \begin{bmatrix} 0 & 1 & 0 \\ 1 & 0 & 0 \\ 0 & 0 & 1 \end{bmatrix} e^{(i\pi/6) (x_2/a_2) \omega} \\
\Omega_2(x) &= \begin{bmatrix} e^{(-i\pi/2)} & 0 & 0 \\ 0 & e^{(i\pi/2)} & 0 \\ 0 & 0 & 1 \end{bmatrix} e^{(-i\pi/6) (x_1/a_1) \omega} \\
\Omega_3(x) &= e^{(i\pi/3) (x_4/a_4) \omega} \quad (3.1.13) \\
\Omega_4(x) &= e^{(-i\pi/3) (x_3/a_3) \omega},
\end{aligned}$$

and

$$\omega = \begin{bmatrix} 1 & 0 & 0 \\ 0 & 1 & 0 \\ 0 & 0 & -2 \end{bmatrix}$$

where  $\omega$  is a  $3 \times 3$  matrix,  $\omega_{ij}$  is the  $i$ -th row and  $j$ -th column of  $\omega$ . The matrix  $\omega$  is the same as the one in case C above.

**D)  $SU(3)$ ,  $k = 2$ ,  $(k/N) = 2/3$**

Here

$$\Omega_1(x) = e^{(-i\pi/3)(x_2/a_2)\omega},$$

$$\Omega_2(x) = \begin{bmatrix} e^{(-i\pi/2)} & 0 & 0 \\ 0 & e^{(i\pi/2)} & 0 \\ 0 & 0 & 1 \end{bmatrix} e^{(i\pi/3)(x_1/a_1)\omega}$$

$$\begin{aligned} \Omega_3(x) &= e^{(i\pi/3)(x_4/a_4)\omega} \\ \Omega_4(x) &= e^{(-i\pi/3)(x_3/a_3)\omega} \end{aligned} \tag{3.1.14}$$

with  $\omega$  the same as in case C above.

In this case we pick  $\eta^{(1)}_{12} = 2$ ,  $\eta^{(2)}_{34} = 1$  and the other  $\eta^{(1,2)}_{\mu\nu}$ 's zero. We used the above four cases when we apply the TBC on the lattice and we discuss our results in Section 3.3.

### 3.2 Topological properties of the Pure Gauge Field on the Lattice

From the strict point of view, topology is lost on the lattice, firstly because of the loss of continuity (which is recovered only in the continuum limit for the lattice spacing  $a \rightarrow 0$ ), and also since there are no surface terms on the lattice which contribute

to the winding number (topological charge  $Q$ ) in the continuum. Despite these not too encouraging factors for looking for topological "freaks" on the lattice, there have been considerable efforts to put topology on the lattice and the indications we have show a rather optimistic picture. Until now, efforts on the lattice have concentrated on the existence or non-existence of instantons, the measurement of the topological susceptibility  $\chi_t$  and the resolution of the  $U(1)$  problem (we refer to these just as an indication of the various lattice topological explorations). The methods devised to compute these topological "freaks" on the lattice, provide an example of how MC simulation and pure mathematics can be "married" in a nice way.

A long standing problem on the lattice is the definition of the topological charge density. Its calculation is plagued by technical and conceptual difficulties. The first attempts to attack this problem used as [21]  $Q^{\text{lattice}}(n)$ ,  $n = a$  lattice site, the following expression :

$$Q^{\text{lattice}}(n) = -(1/32\pi^2) \epsilon^{\mu\nu\rho\sigma} \text{ReTr}[U_{\mu\nu}(n)U_{\rho\sigma}(n)] \xrightarrow{a \rightarrow 0} a^4 Q(x) \quad (3.2.1a)$$

( $U_{\mu\nu}$  is the elementary plaquette at the  $\mu$ - $\nu$  level) and (3.2.1) is a direct "translation" on the lattice of the continuum expression:

$$Q(x) = -(1/32\pi^2) \epsilon^{\mu\nu\rho\sigma} \text{Tr}[F_{\mu\nu}(x)F_{\rho\sigma}(x)] \quad (3.2.1b)$$

The analogy comes from the expansion of

$$U_{\mu\nu}(n) = e^{iA_\mu(n)} e^{iA_\nu(n+\mu)} e^{-iA_\mu(n+\nu)} e^{iA_\nu(n)} \underset{a \rightarrow 0}{=} 1 + ga^2 F_{\mu\nu}(n) + g^2 a^4 F_{\mu\nu}^2 + \dots, g = \text{coupling constant of the simple gauge group under consideration.}$$

The consequences<sup>[21]</sup> of using (3.2.1) to measure the topological

charge are bad since in this expression the perturbative terms contribute (in the form of powers of  $ga^2$ ) to making the search for the contribution of the more important non-perturbative modes quite difficult. To resolve this problem various methods have appeared in the literature and the situation seems to be like baroque (for a general review (c.f.[22]). The advantage of one method over the other is not clear yet. For example, the geometric method based on the interpolation of the gauge field in adjacent cells of the lattice, while seeming to be rather rigorous and mathematically elegant, does not give "good" results for  $x_t(R)$ [23].

In this work we have used the cooling method [24] which we now describe. The main idea is to minimise the action (the standard Wilson action) in a systematic way and so to reduce the fluctuations of the original Monte-Carlo generated configuration and at the same time to produce quite stable configurations. By using the cooling method it is believed that the main difficulty in measuring  $Q^{\text{lattice}}(n)$  referred above, (i.e., the contribution of the perturbative modes) is resolved, since this procedure renders the configurations smoother (by minimising the action), and so (3.2.1) can be safely used to a good approximation during the cooling process. The algorithm for minimising the action consists of concentrating at one link  $U_\mu(n)$  of the lattice and changing this link to  $U'_\mu(n)$ , (while all the other links which multiply the  $U_\mu(n)$  at the six plaquettes around  $U_\mu(n)$  are kept fixed) in such a way that  $S[U'_\mu(n)] \leq S[U_\mu(n)]$ . We make this change for every link of the lattice (1 sweep) and repeat this process several times until the action plateaus at a value and remains there for a number of cooling sweeps. The configuration at the point where the action reaches a plateau is a solution to the equations of motion and by measurement of the action we find the value of the topological charge. As an act of faith we believe that when the action plateaus and gets its minimum the contributions to  $Q^{\text{lattice}}$  (i.e. the so-called lattice artefacts) from the perturbative modes have disappeared and only long-distance modes are left. In the case of the instantons, in a periodic lattice it has been observed that the action gets a plateau after a few cooling sweeps and remains there for some time[24], before decaying to a zero value. The reason for this is that the instanton action on the lattice is quite different from the  $S^{\text{continuum}}_{\text{instanton}}$  at scales where the instanton



size is smaller than the lattice spacing, i.e., when  $\rho$  (instanton size)  $\ll a$  ( $a$  = lattice spacing) then  $S^{\text{lattice}}_{\text{instanton}} \rightarrow 0$ , while in the continuum

$$S^{\text{continuum}}_{\text{instanton}} = [8\pi^2/g^2(\rho)]_{\rho \rightarrow 0} \rightarrow \infty.$$

When  $\rho \gg a$ ,  $S^{\text{lattice}}_{\text{instanton}} \rightarrow S^{\text{continuum}}_{\text{instanton}}$  and if  $\rho \sim 0(a)$  the instanton shrinks through the lattice sites and disappears, while at the same time its action drops to zero.

The lesson from the instanton search on the lattice is that if we want to have a clear picture of what is going on, we must have instanton sizes larger than the lattice spacing and the larger the instanton size the longer the lifetime of the object on the lattice. When the action plateaus

$$S = [8\pi^2/g^2]Q \tag{3.2.3}$$

and we find the topological charge by measuring the action.

The technical points of the algorithm for the minimization are as follows:

The SU(2) case is simple since the staple which multiplies the link we cool consists of a sum of SU(2) matrices, which is still an SU(2) matrix if we divide it by its determinant. Using the Lagrange's multiplier method we find that, if the staple matrix is denoted by  $A$ , the choice

$$U_\mu = A^+ / \text{Det} A \text{ minimises the action.}$$

The SU(3) case is not so simple, since the sum of SU(3) matrices is not generally an SU(3) matrix. The main idea of our algorithm is to find a matrix which belongs to SU(3) and is very close to  $A$ . We have checked the algorithm for the SU(3) case by comparing the results using the NAG Library, and this confirmed that, after a number of hits, we reached the minimum of the action.

### 3.3 Numerical Results

We now present our MC results and comments on them.

Figs. A<sub>1</sub> to A<sub>4</sub> refer to the SU(2) case, where we set up the twists  $\eta_{\mu\nu}$ 's in such a way to get topological charge of 3/2. Fig. A<sub>1</sub> was taken with 600 thermalized sweeps from a configuration obtained by a hot start while Fig. A<sub>2</sub> was taken from a configuration with a cold start (gauge links were fixed equal to the unit matrix). We observe that in the Fig. A<sub>1</sub> we get topological charge of 1/2 instead of 3/2 as in Fig. A<sub>2</sub>, despite the fact that the  $\eta_{\mu\nu}$ 's are the same in both the cases. Comparing these results with other results we will present next leads us to interpret this as coming from the integer part of the twist, i.e. the integer  $v$  in relation (3.1.4). We conclude that when we thermalize a configuration the instanton(s) can always be there and from the previous paragraph we know that their existence depends (among other things) on the lattice size and that after some cooling sweeps they shrink through the lattice. So it could be the case that the integer  $v$  in (3.1.4) is 1 for the configuration of A<sub>2</sub> case. Fig. A<sub>2</sub> shows a somewhat unstable plateau at 3/2, which decays to 1/2, which seems to be quite pertinent. From Fig. A<sub>1</sub> we also observe that the topological structure we get does not disappear, even after about 160 cooling sweeps, which leads us to believe that the topological objects with TBC seem to have a size larger than the instanton size (even if we have not any analytical reasoning for this).

Figs. A<sub>3</sub> and A<sub>4</sub> have been obtained by cooling from a cold start ( $U=1, \beta=\infty$ ) and their twist was set up for  $Q=3/2$ . We got exactly  $Q=3/2$ , and so all the topological charge is attributed to the twist part of (3.1.4) (i.e. the  $k/N$  of this relation).

Fig. B refers to an object of topological charge  $Q=1/4$ . This was created by using constant twist matrices, along the 1 and 2 directions. The physical analogue of this is a magnetic flux at a link pointing in the third direction in space. This is quite similar to a  $Z(N)$  solution to the equations of motion [25,26]. In this case the action does not decay to zero and this can be explained using

the Schwartz's identity for the U(1) subgroup of the SU(2) group, i.e.,

$$E_{\text{classical}} = (1/2) \int (F^{12})^2 d^4x \geq (1/2) |(\int F^{12} dS)^2 / (a_1 a_2 a_3 a_4)| \quad (3.3.1a)$$

The action for such a configuration is

$$S = \cos(F_{12})^{-1}, \quad (3.3.1b)$$

where  $F_{12} = \pi/a_1 a_2$ , so  $E = (1/2)\pi^2/(a_1 a_2)^2$ .

A configuration, in the continuum, which has the same action as in (3.3.1), is given by  $A_\mu = [(\pi x_1/a_1 a_2), 0, 0, 0]$ , which corresponds to a magnetic field  $B^3 = \pi/a_1 a_2$ . We justify that  $Q = 1/4$  (for the above case) by comparing the value of the action with that for  $Q = 1$  on the same lattice. To measure the topological charge on the lattice we are using the relation (for the SU(2) group, and for a  $6^4$  lattice in 4-dimensions):

$$(4/g^2)6^4 x_6 x(1 - S_{\text{plaq}}) = [8\pi^2/g^2]Q \quad (3.3.2)$$

where  $S_{\text{plaq}}$  is the plaquette at one level.

For  $Q=1$ ,  $1 - S_{\text{plaq}} = [\pi^2/(6^4 \cdot 3)]$ .

For the U(1) group, if we consider the action (which corresponds to a configuration with a twist only in 2 directions)

$$\cos(F_{12})^{-1} \equiv (1/2)\pi^2/(a_1 a_2)^2,$$

we get  $\pi^2/(2 \times 6^4) = 6(1 - S_{\text{plaq}})$  and so  $(1 - S_{\text{plaq}}) = \pi^2/(2 \times 6^5)$ .

Compared with  $1 - S_{\text{plaq}} = \pi^2/(6^4 \cdot 3)$ , (for  $Q = 1$ ) we see that for the U(1) subgroup of SU(2) we get

$$Q_{U(1)} = 1/4 \quad (3.3.3)$$

(with constant twists in 2 directions).

Category C contains results for SU(2) with  $Q = 1/2$  on a  $6^4$  lattice, where the matrices of (3.1.11) were used.

Fig. C<sub>1</sub> shows clearly that the action plateaus to  $Q = 1/2$  after  $\sim 50$  cooling sweeps and remains there for  $\sim 350$  cooling sweeps. This shows again that this topological object is quite stable. We could speculate that the "size"  $\rho$  of these objects is significantly larger than the instanton size, since their stability leads us to believe that even after a large number of cooling sweeps their size is  $\rho \gg a$  ( $a$  = lattice spacing). Of course, we expect that after a number of cooling sweeps the action will go to zero, but our observation is that we need a lot of sweeps for the action to decay to zero.

Figs. C<sub>2</sub> and C<sub>3</sub> are taken by cooling from a cold start ( $\beta = \infty$ ). We see again  $Q = 1/2$ . C<sub>3</sub> is taken by fixing the gauge so that  $\Omega_2 = \Omega_4 = 1$ ,  $\Omega_1 \neq 1$ ,  $\Omega_3 \neq 1$ , and still preserving the twist algebra (2.2.3).

Category D contains results for an  $8^4$  lattice. In this case twists for  $Q = 1/2$  were used.

Fig. D<sub>1</sub> was taken from a configuration which was thermalized for 1000 thermalization sweeps starting from a cold start at  $\beta = 2.2$ . We observe that at around the  $\sim 140$ th cooling sweep we have a plateau for  $Q = 1/2$ . When we thermalized this configuration again, for 2020 thermalization sweeps, starting from a cold start, we got Fig. D<sub>2</sub> where we have two quite stable plateaus at  $Q = 3/2$  and  $Q = 1/2$ . We interpret this as the appearance of an instanton in the lattice since we now have a larger lattice than the one in Fig. A<sub>2</sub>.

Fig. D<sub>3</sub> shows that at  $\beta = \infty$  on the same lattice we have only the "pure" twist case, i.e.  $Q = 1/2$ .

Class (E) contains graphs concerning the cases where we have to use non-constant twists so that  $k/N = 1$ , i.e. a twisted instanton. If we want a (anti)-selfdual solution we have of course to satisfy,

$F_{\mu\nu} = \pm \tilde{F}_{\mu\nu}$ . From the analysis of 't-Hooft [20], we know that in order to satisfy the (anti)-selfduality condition of the gauge field, we have to arrange the ratio  $a_1 a_2 / a_3 a_4$  ( $a_1, a_2, a_3, a_4$  are the lattice sizes in  $D = 4$ ). This restricts the lattice size we can use (depending always on the twists we use), and, for example, for the  $SU(2)$  group and for  $Q=1$ , we should use a lattice with  $(a_1 a_2 / a_3 a_4) = 2$  (for the (anti)-selfduality condition to be satisfied).

The case  $Q = 1$  for a  $12 \times 6^3$  lattice at  $\beta = 0$  is shown in Fig. E<sub>1</sub>. From the graph we see clearly two small plateaus close to  $Q = 3$  and  $Q = 2$ , respectively, and a stable plateau at  $Q = 1$ .

Fig. E<sub>2</sub> was taken for  $\beta = \infty$ , and again we obtained  $Q = 1$ .

Fig. E<sub>3</sub> refers to a case where our lattice ( $6^3 \times 12$ ) does not satisfy the (anti)-selfduality condition and was obtained by 1000 thermalization iterations at  $\beta = 2.2$ . Again, we see a small curvature at  $Q \cong 2$ , and quite a stable plateau at " $Q$ "  $\cong 1.2$ , which decays to zero (before it decays to zero it stays for some time at  $Q = 0.1$ ). In the case of Figs. E<sub>1</sub> and E<sub>2</sub> the lattice ( $12 \times 6^3$ ) satisfied the (anti)-selfduality condition and  $Q$  was exactly 1, but this is unlikely in this case of Fig. E<sub>3</sub> where we have small fluctuations around  $Q = 1$ . Similarly, in Fig. E<sub>4</sub> we see that (using 3.2.3) " $Q$ "  $\cong 0.6$  despite the fact that we arranged the twists to correspond to  $Q = 1/2$ .

In all the above cases we plot the value of the average plaquette versus the number of cooling sweeps, and we use (3.2.3) to measure the topological charge. When the configuration does not satisfy the (anti)-selfduality condition it is not legitimate to use (3.2.3), since this holds only for (anti)-selfdual configurations. This explains why " $Q$ "  $\cong 0.6$  for the case plotted in Fig. E<sub>4</sub>.

Now we present a more formal "proof" why " $Q$ "  $\cong 0.6$ .

The twists  $\eta_{\mu\nu}$ 's were arranged such that

$$\eta_{12} = -1, \eta_{34} = 1, \text{ i.e. } Q = 1/2.$$

Then

$$\begin{aligned} \text{Tr} F_{\mu\nu} \tilde{F}^{\mu\nu} &= (1/2) \epsilon^{\mu\nu\rho\sigma} \text{Tr} F_{\mu\nu} F_{\rho\sigma} = \\ &= (16\pi^2/a_1 a_2 a_3 a_4) [\eta_{\mu\nu} \tilde{\eta}_{\mu\nu}] / (4N), \quad N = 2. \end{aligned}$$

So for the above choice of  $\eta_{\mu\nu}$ 's  $\text{Tr} F_{\mu\nu} \tilde{F}^{\mu\nu} = (8\pi^2/a_1 a_2 a_3 a_4)$  and this value corresponds to topological charge  $Q = 1/2$ . If the configuration is (anti)-selfdual then

$$S = (1/2) \int \text{Tr} F F d^4x = 4\pi^2,$$

but if the configuration does not satisfy

$$\begin{aligned} F_{\mu\nu} &= \pm \tilde{F}^{\mu\nu}, \quad \text{Tr} F_{\mu\nu} F^{\mu\nu} = 2(\text{Tr} F_{12}^2 + \text{Tr} F_{34}^2) = \\ &= 4\pi^2 [1/(a_1 a_2)^2 + 1/(a_3 a_4)^2] \end{aligned}$$

and

$$S = 2\pi^2 (x + (1/x)), \quad x = a_1 a_2 / a_3 a_4.$$

Comparing the actions for (anti)-selfdual and non-(anti)-selfdual configurations we have:

$$(S_{\text{(anti)-selfdual}} / S_{\text{non-(anti)-selfdual}}) = 2/(x + (1/x)). \quad (3.3.4)$$

If  $x = 1$  then  $S_{\text{anti(self)-dual}} = S_{\text{non-(anti)-selfdual}}$ .

From (3.3.4) we can now deduce that " $Q$ "  $\cong 0.6$ , provided we accept that even for a non-(anti)-selfdual configuration  $S$  is still proportional to  $Q$ . Then

$$(S_{\text{(anti)-selfdual}} / S_{\text{non (anti)-selfdual}}) = 2/(x + (1/x)) = 0.5/0.6 =$$

$Q_{\text{(anti)-selfdual}} / "Q"_{\text{non (anti)-selfdual}}$ , and for this to hold  $x \cong 1.2$ , i.e., we

should have a  $6^3 \times 12$  lattice.

Therefore using (3.2.3) with a  $6^3 \times 12$  lattice and twists for  $Q = 1/2$  we should expect to find " $Q$ "  $\cong 0.6$ . With the same logic we can justify the value " $Q$ "  $\cong 1.2$  for the case shown in Fig. E<sub>3</sub>.

We now present the results of our numerical study for the SU(3) group.

Figs. F<sub>1</sub> and F<sub>2</sub> refer to the case with topological charge  $Q = 1/3$ , where in order to satisfy (anti)-selfduality condition, we have to use a lattice with  $a_1 a_2 / a_3 a_4 = (1/2)$ . We see clearly  $Q = 1/3$ .

Fig. F<sub>3</sub> refers to the case where we constructed the twists  $\eta_{\mu\nu}$ 's for  $Q = 4/3$ , but we find again  $Q = 1/3$ . Our interpretation of this is that an instanton was lost or, by the modulus law of the twist in (3.1.4), there is a possibility that  $Q = 1/3$  can actually be the same as  $Q = 4/3$ . In (3.1.4) we think  $k/N$  is equal to  $(k/N) \bmod N$  and so  $Q = 4/3$  belongs to the same topological class as  $Q = 1/3$ .

Fig. G<sub>1</sub> shows a very interesting sequence of plateaus. We set up the  $\eta_{\mu\nu}$ 's for  $Q = 2/3$  in a  $6^4$  lattice (using a configuration obtained by 790 thermalization sweeps) starting with a hot start at  $\beta = 5.5$ . The graph shows topological charges with values at  $Q = 1/3, 4/3, 7/3$ . This is not surprising since the occurrence of instantons is quite probable when we use a thermalized configuration. This interplay between the instantons and the TBC can be justified also by graph G<sub>2</sub>. We used the "twisted" thermalized configuration of G<sub>1</sub>, and cooled it without the twist. If instantons exist they would be seen by a small plateau (or curvature) of the graph, since they are unstable. This was actually the case, and in Fig. G<sub>2</sub> there is an indication of  $Q = 1$  at around 25 cooling sweeps, which is about the time that the first plateau of Fig. G<sub>1</sub> occurs.

Class H contains the graphs which refer to  $Q = 2/3$ , where our Monte Carlo generated configuration was obtained after 650 thermalization sweeps from a hot start on a  $6^4$  lattice.

Now the action plateaus at  $Q = 2/3$ , where there is an indication of a small plateau at  $Q = 5/3$ . In contrast, at  $\beta = \infty$  (Fig. H<sub>2</sub>), there are

no instantons and  $Q = 2/3$ . Of course  $Q=(1/3,4/3,7/3)$  does not belong to the same vacuum as  $Q=(2/3,5/3)$ . Here we have an example of how the initial conditions (in this example the number of thermalization sweeps) affect the topological nature of the gauge field.

The choice for the twist transition functions, for a particular set of  $\eta_{\mu\nu}$ 's, is not unique. For example, it is possible to have 2 different  $\Omega_\mu$ 's which correspond to the same twist (i.e., the same topological charge  $Q$ ), but they have different  $\eta_{\mu\nu}$ 's. To give an example: the  $\Omega_\mu$ 's

$$\Omega_\mu^{(1)}(x) = e^{\frac{2i\pi}{N}} \begin{bmatrix} k & & & & \\ & N-k \text{ times} & & & \\ & & \ddots & & \\ & & & k & \\ & & & & k-N & k\text{-times} \\ & & & & & k-N \\ & & & & & & k-N \end{bmatrix}$$

$$\Omega_\mu^{(2)}(x) = e^{\frac{2i\pi k}{N}} \begin{bmatrix} 1 & & & & \\ & \ddots & & & \\ & & \ddots & & \\ & & & 1 & \\ & & & & 1-N \end{bmatrix}$$

both correspond to the same twist  $k$ , but



$$E_{\text{classical}}^{(1)} - E_{\text{classical}}^{(2)} \sim (k^2 - k)$$

and in general is different from zero.

If we consider the case of the SU(3) group for  $Q = 2/3$ , we see that if instead of  $\omega$  in (3.1.14), we use

$$\omega = \begin{bmatrix} 2 & 0 & 0 \\ 0 & -1 & 0 \\ 0 & 0 & -1 \end{bmatrix}$$

then the transition functions  $\Omega_\mu$  have the form

$$\Omega_1(x) = e^{(-2i\pi/3)(x_2/a_2)\omega}$$

$$\Omega_2(x) = e^{(2i\pi/3)(x_1/a_1)\omega},$$

$$\Omega_3(x) = \begin{bmatrix} 1 & 0 & 0 \\ 0 & 0 & 1 \\ 0 & 1 & 0 \end{bmatrix} e^{(i\pi/6)(x_4/a_4)\omega}$$

(3.3.5)

$$\Omega_4(x) = \begin{bmatrix} 1 & 0 & 0 \\ 0 & -i & 0 \\ 0 & 0 & i \end{bmatrix} e^{(-i\pi/6)(x_3/a_3)\omega}$$

and still satisfy the twist algebra (2.2.2) for  $Q = 2/3$ . Obviously, the action of this "twist" choice is different from the action chosen in (3.1.14) and in addition to this the choice (3.3.5) cannot be used to measure the topological charge via (3.2.3) on a 64 lattice, since it is not (anti)- selfdual on this lattice.

Cases  $l_1, l_2, l_3$  refer to a twisted instanton for the SU(3) case at  $\beta \neq 0$ ,  $\beta = \infty$ ,  $\beta = \infty$ , where the third graph was taken by changing the number of hits on the link during the cooling method from 20 to 1. Clearly there is a strong indication of  $Q = 1$  in the SU(3) case.

We also used constant  $\Omega_\mu$ 's for the SU(2) and SU(3) groups using the matrices (3.1.3,b,c,d,e) and we found  $Q = 1$  (we do not present the plots here).

It has been seen from Section 3.1 that for  $k \neq 0 \pmod{N}$ , we have to use non-constant  $\Omega_\mu$ 's (see also Ref.[27]). When  $k = 0 \pmod{N}$  we can have "twisted" instantons with constant and non-constants  $\Omega_\mu$ 's.

It has been argued[28] that the effect of the twist for the SU(2) case can be incorporated in a factor  $Z_{\mu\nu}$  in front of the elementary plaquette in the action, i.e.

$$S_{\text{twisted}} = \sum_{n,\mu,\nu} \text{Tr}[1 - Z_{\mu\nu} S_{\text{plaq}}]$$

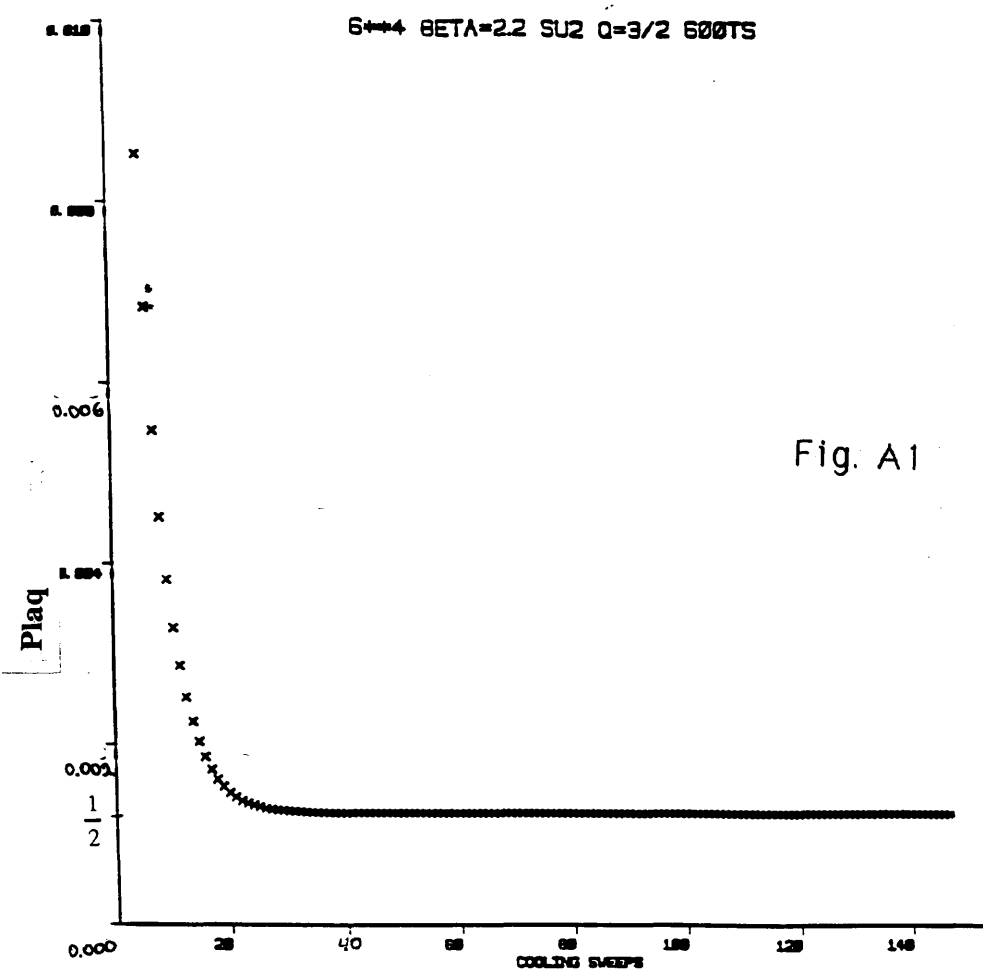
where  $Z_{\mu\nu} = e^{2i\pi\eta_{\mu\nu}/N}$ .

The author of [28] used anisotropic lattices and found topological charges 1/2, 3/2 (for the SU(2) group). It is not clear to us that by incorporating the twisted boundary condition on the lattice the Wilson action has an overall factor  $Z_{\mu\nu}$  in front of  $S_{\text{plaq}}$ . We could only see a minus sign at the right corner plaquette (Fig. K) when we used constant twist matrices for  $\eta_{12} = -1$  in 2-dimensions for the SU(2) group.

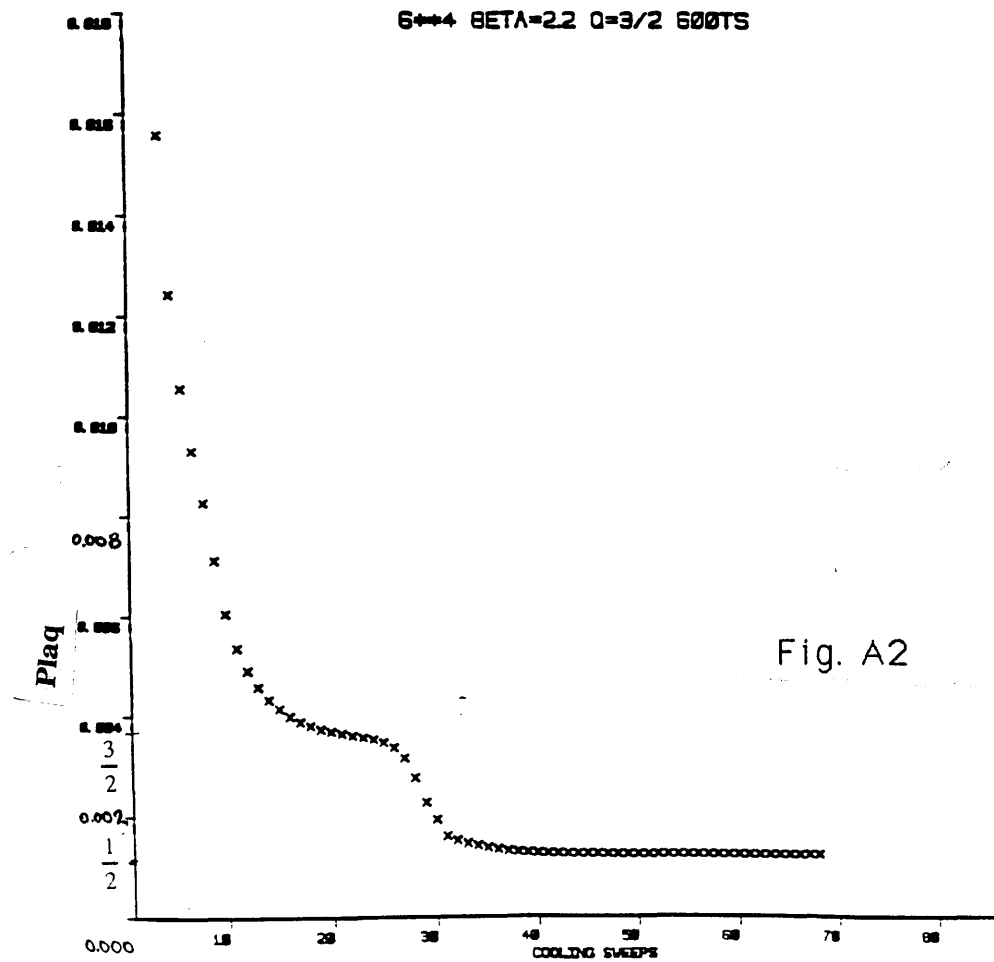
			x

**Fig. K**     *TBC with constant in  $D = 2$*

6444 BETA=2.2 SU2 Q=3/2 600TS



6444 BETA=2.2 Q=3/2 600TS



SU2 6\*\*\*4 BETA=  $\infty$  Q=3/2

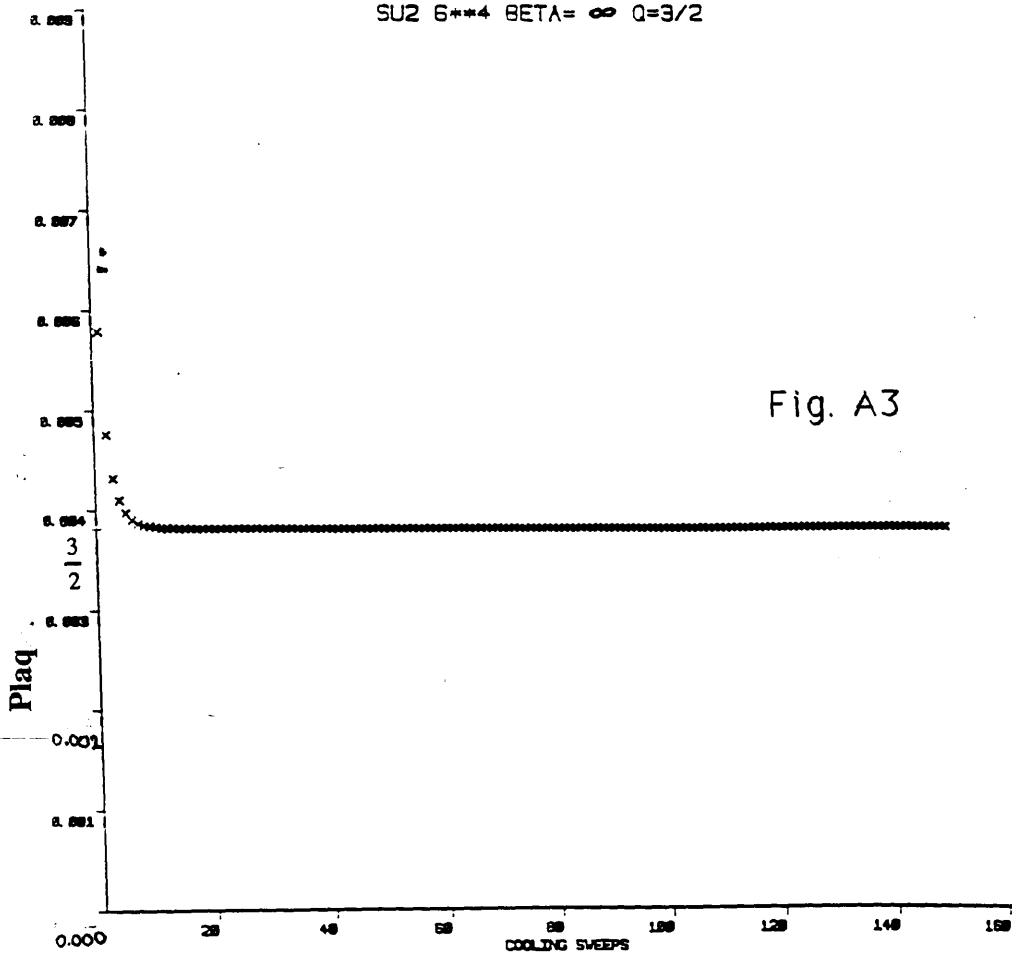


Fig. A3

SU2 8\*\*\*4 BETA=  $\infty$  Q=3/2

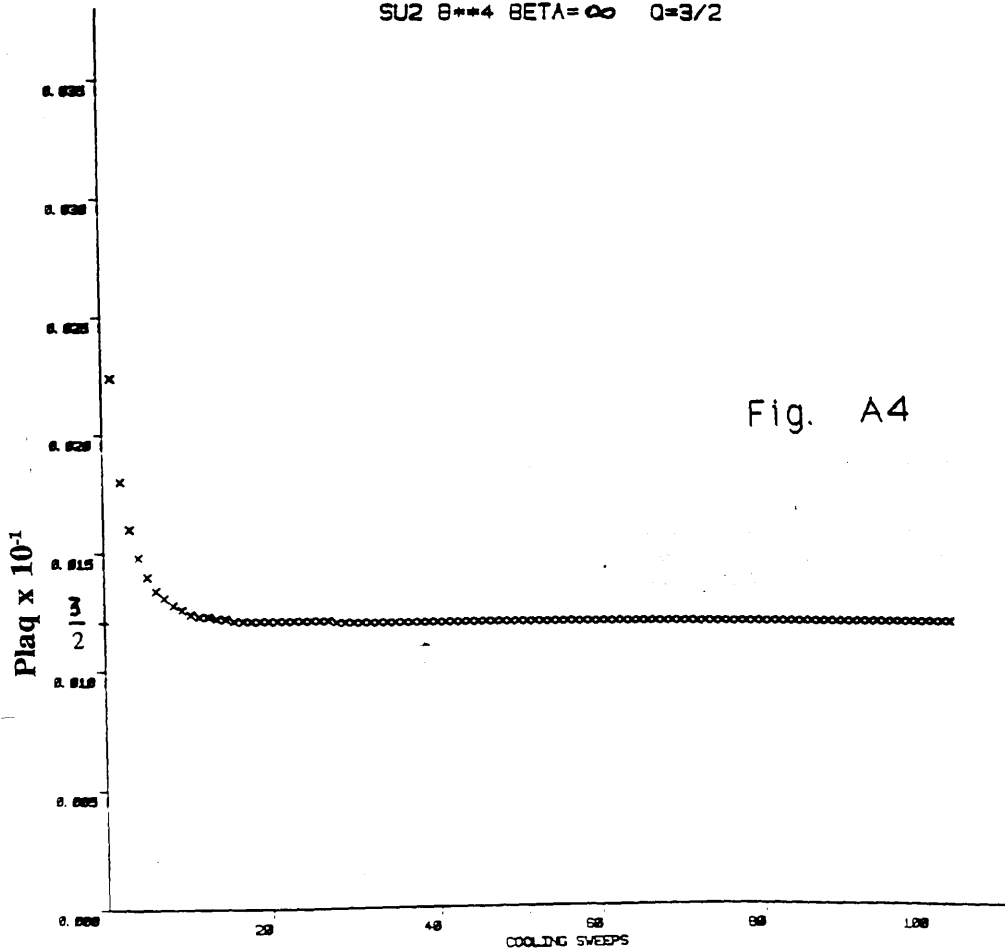


Fig. A4

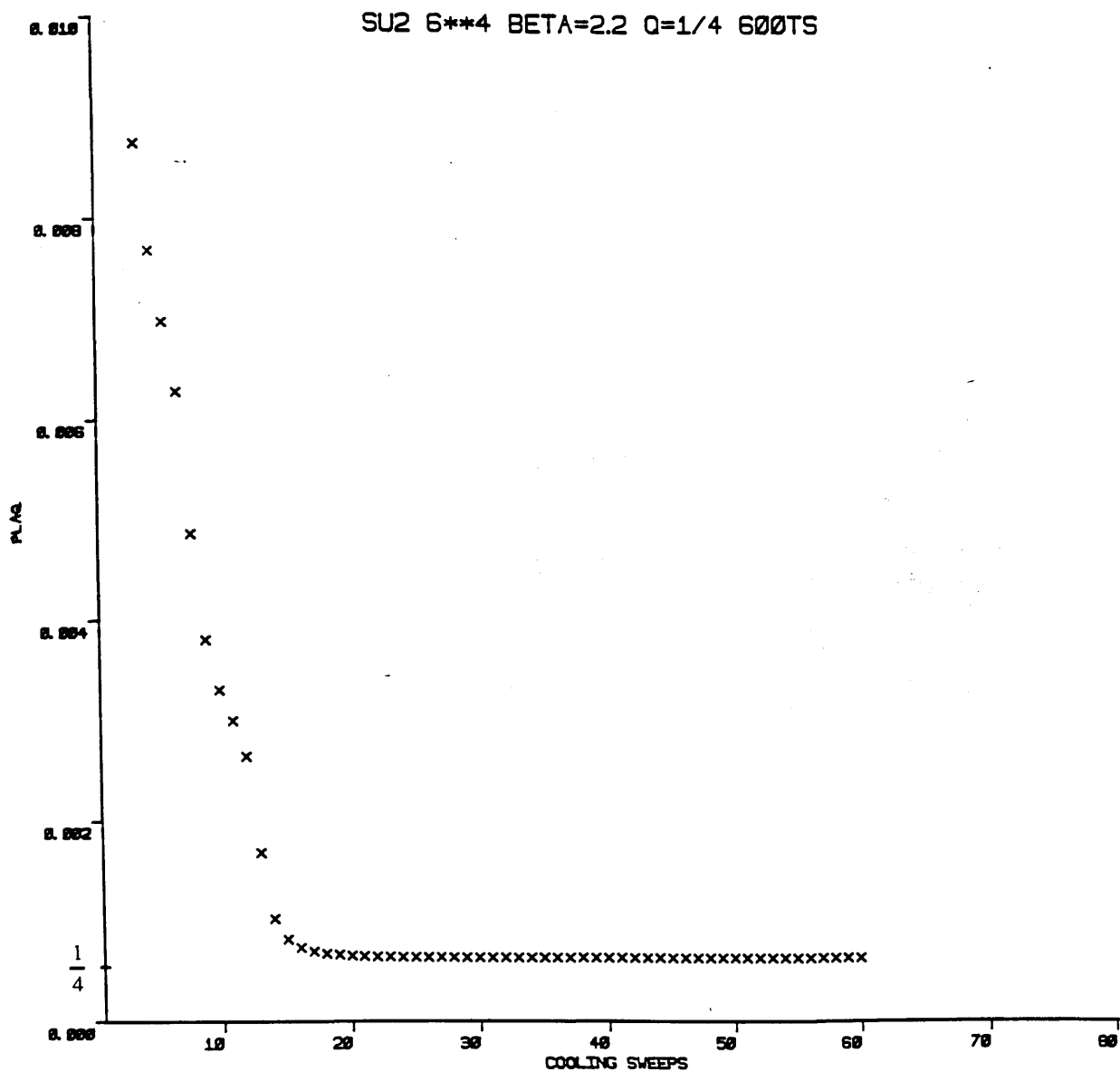
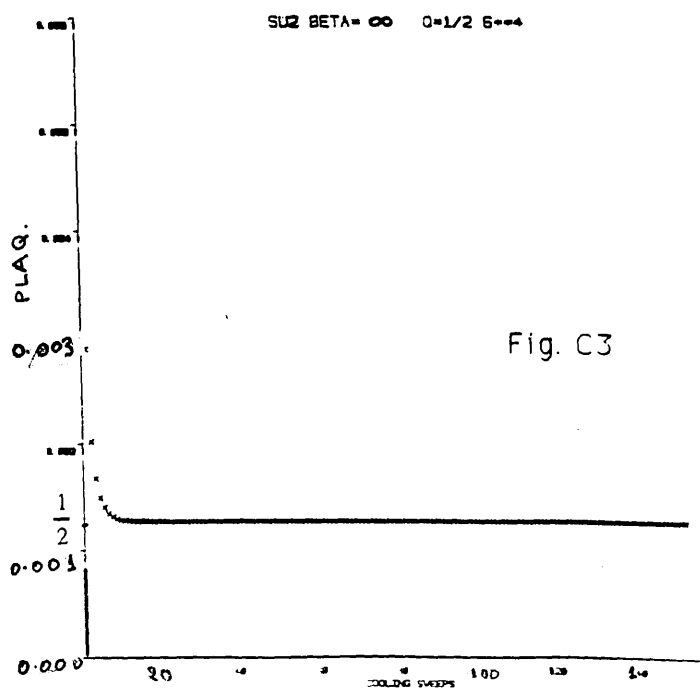
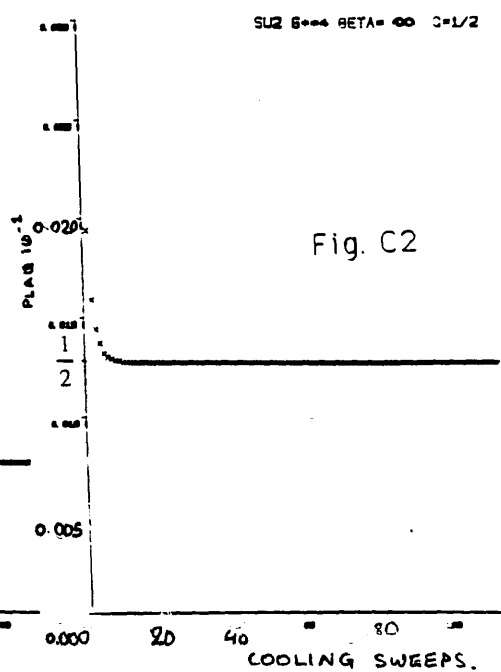
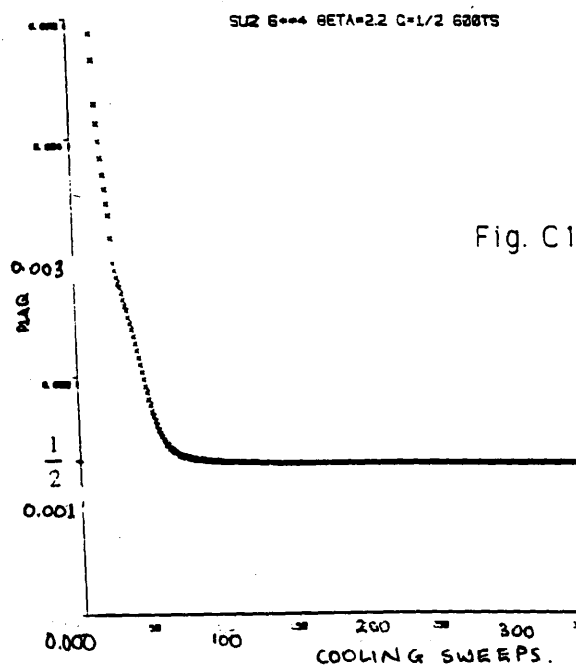
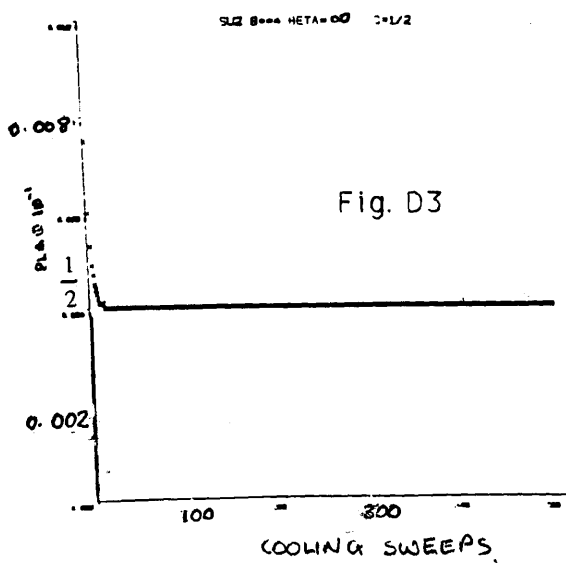
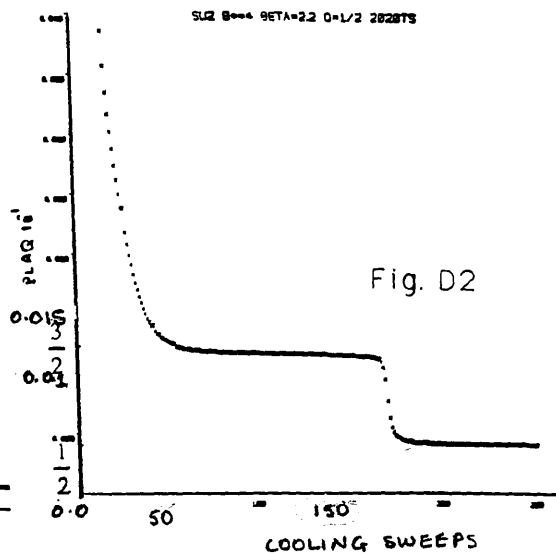
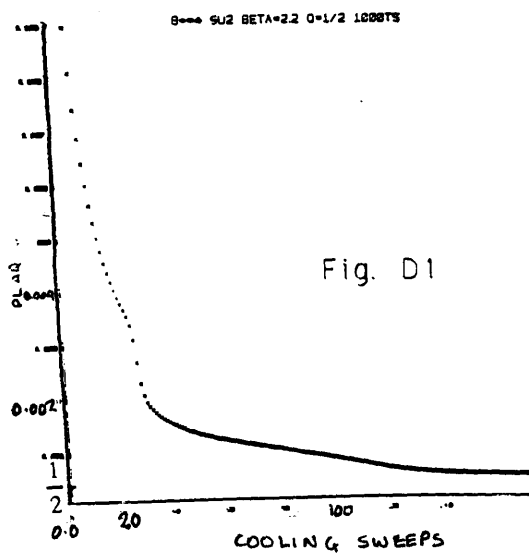


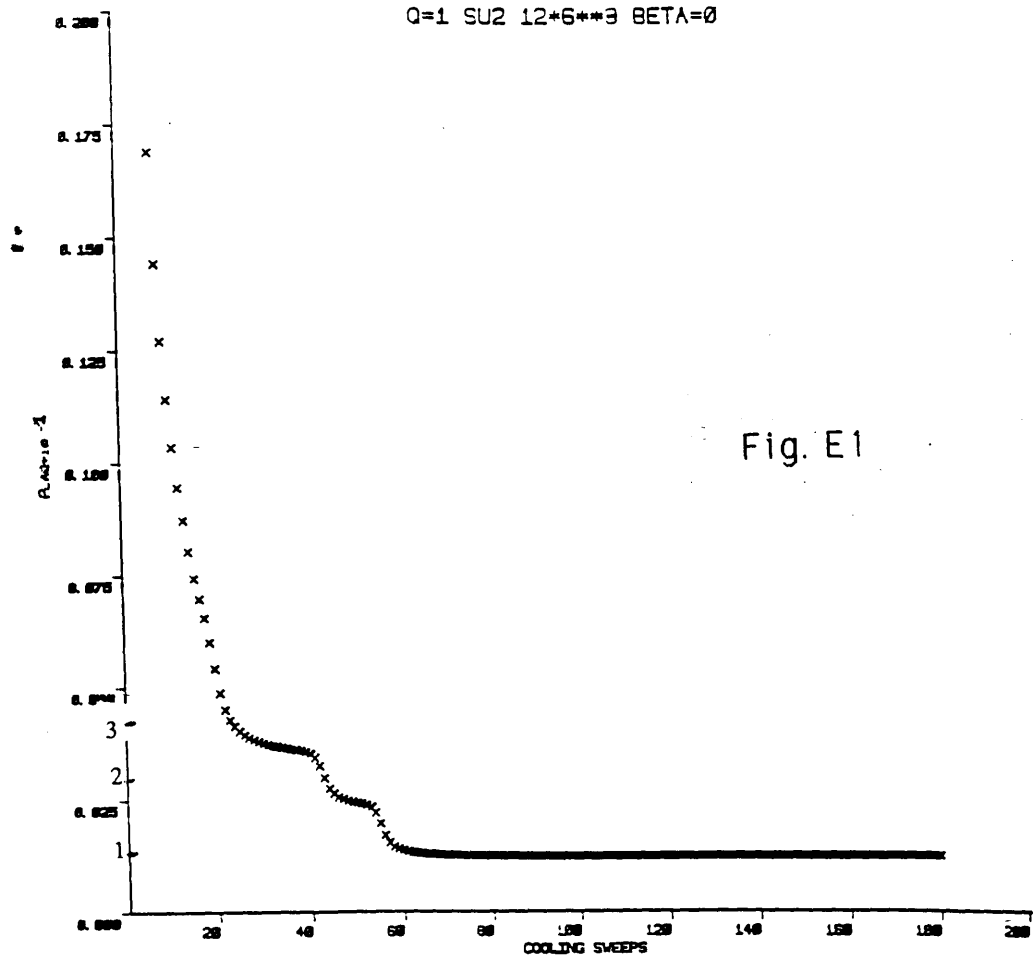
Fig. B



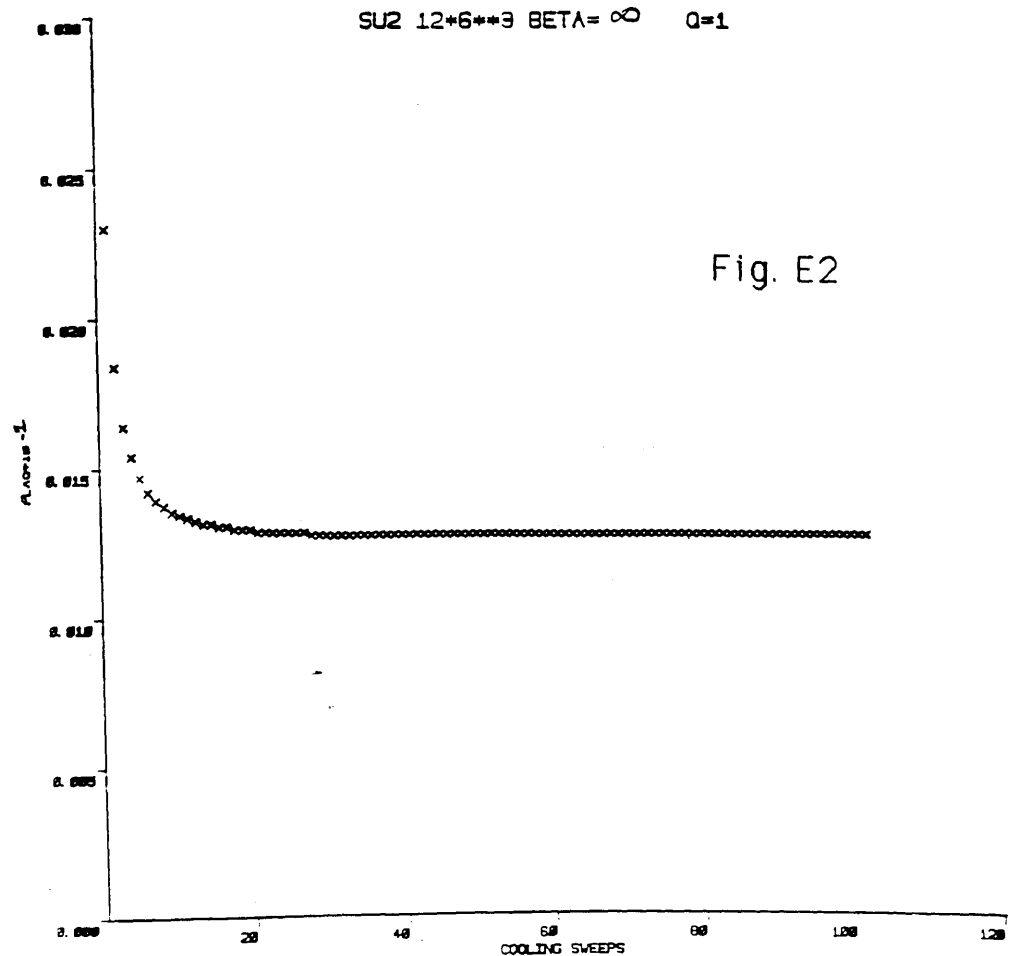




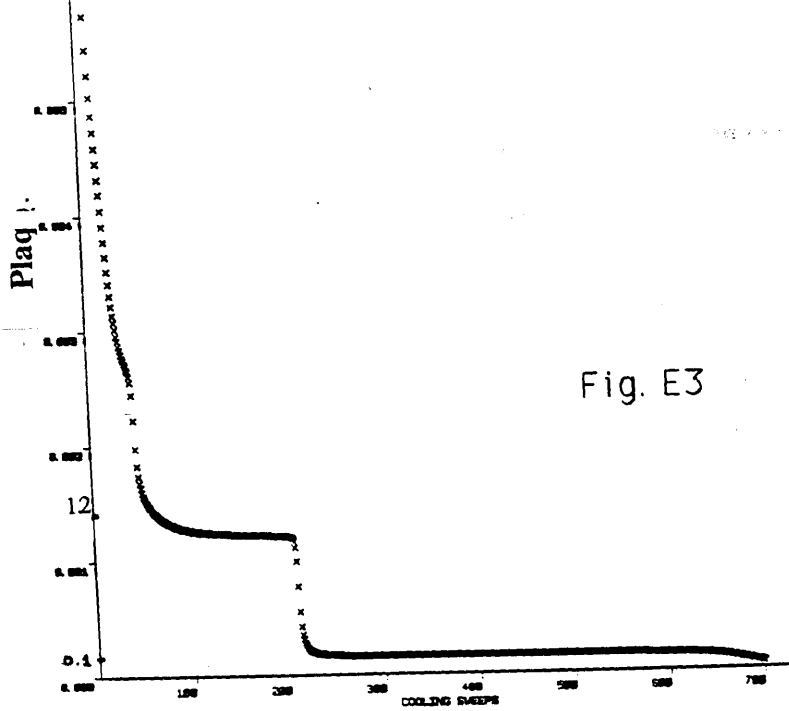
Q=1 SU2 12\*6\*\*\*3 BETA=0



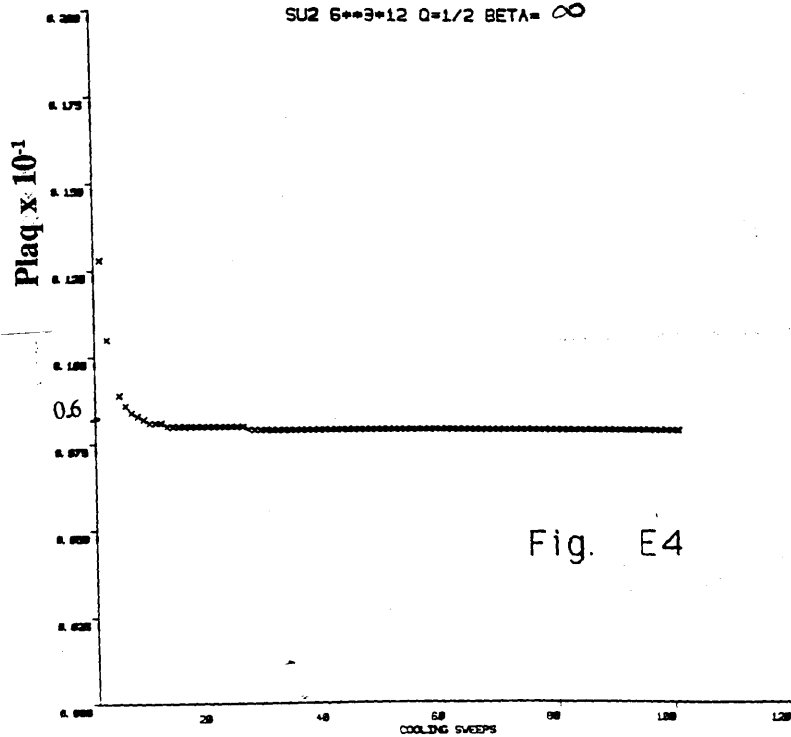
SU2 12\*6\*\*\*3 BETA=∞ Q=1

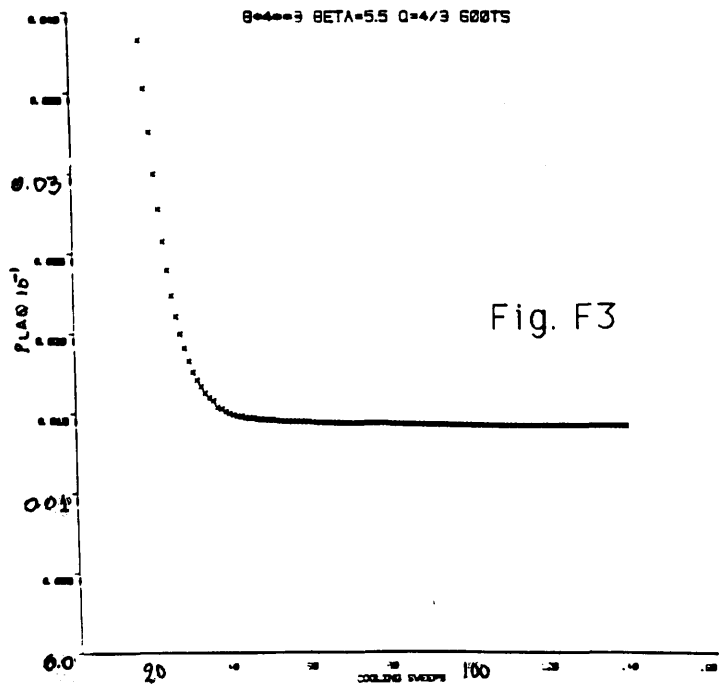
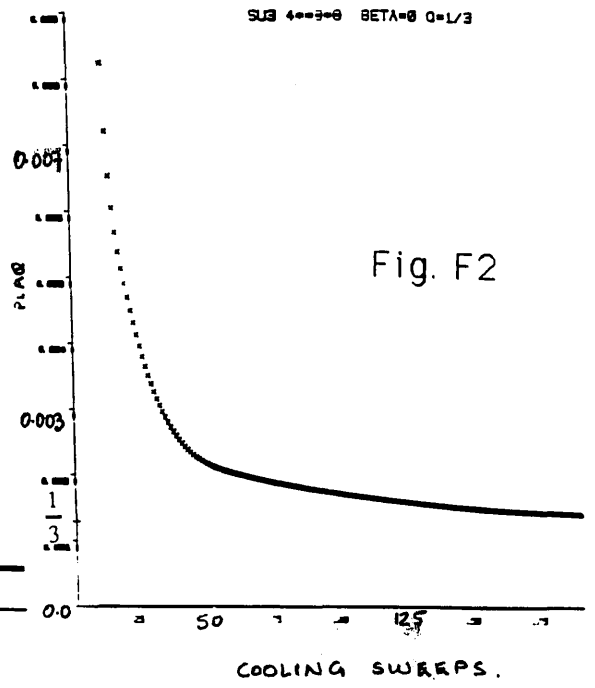
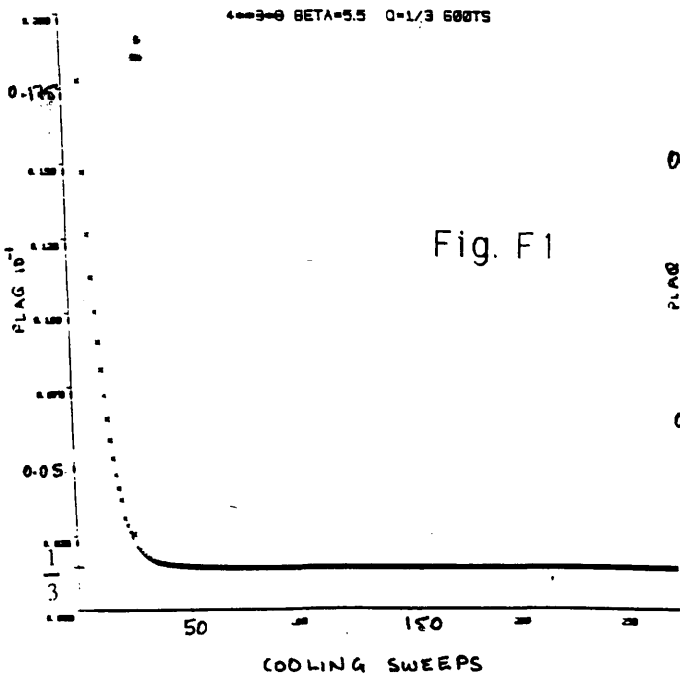


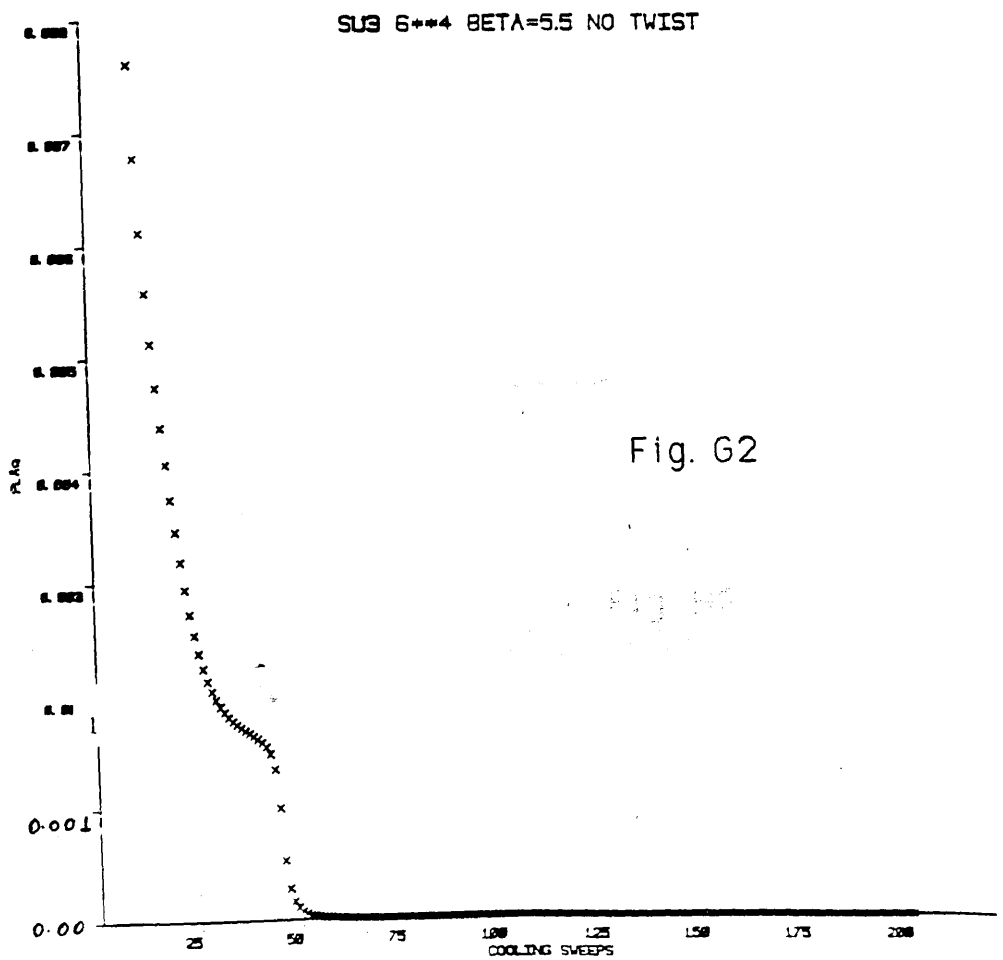
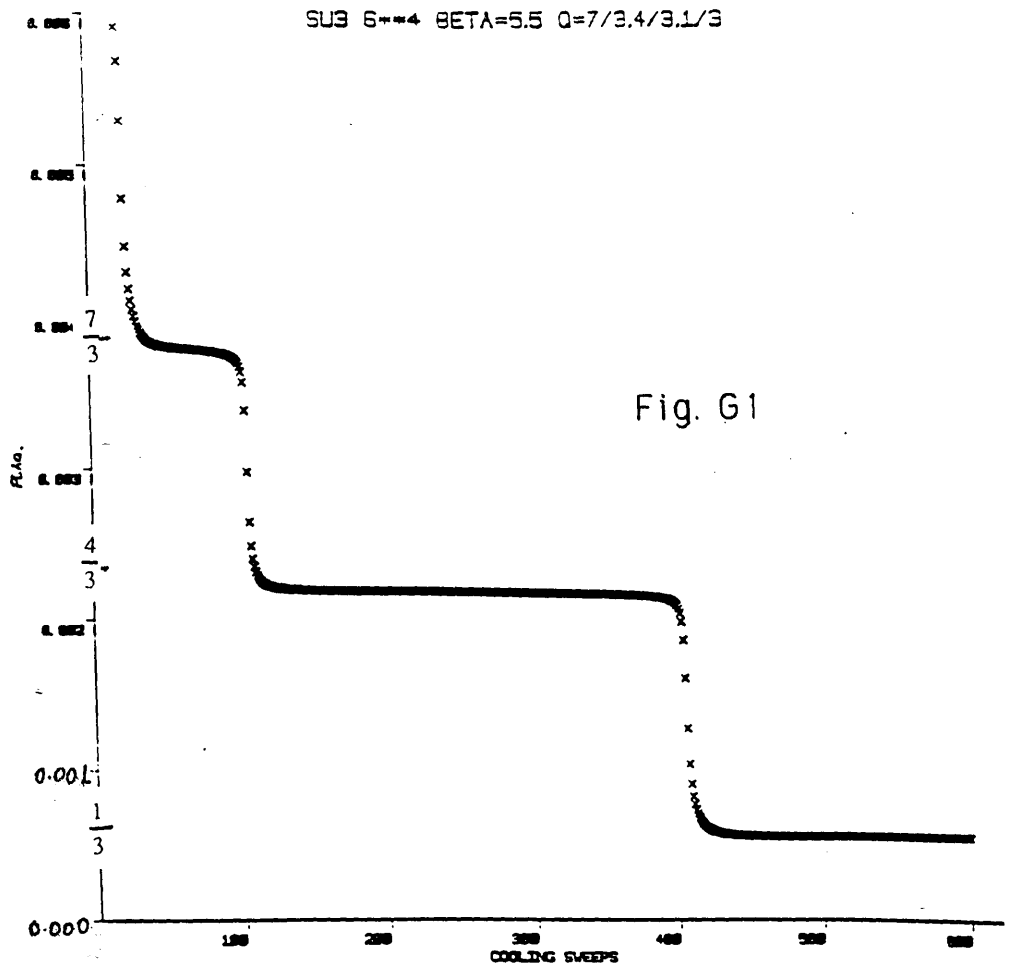
TOPOLOGICAL CHARGE FOR SU2 P=1 1000TS BETA=2.2 6\*\*3\*12

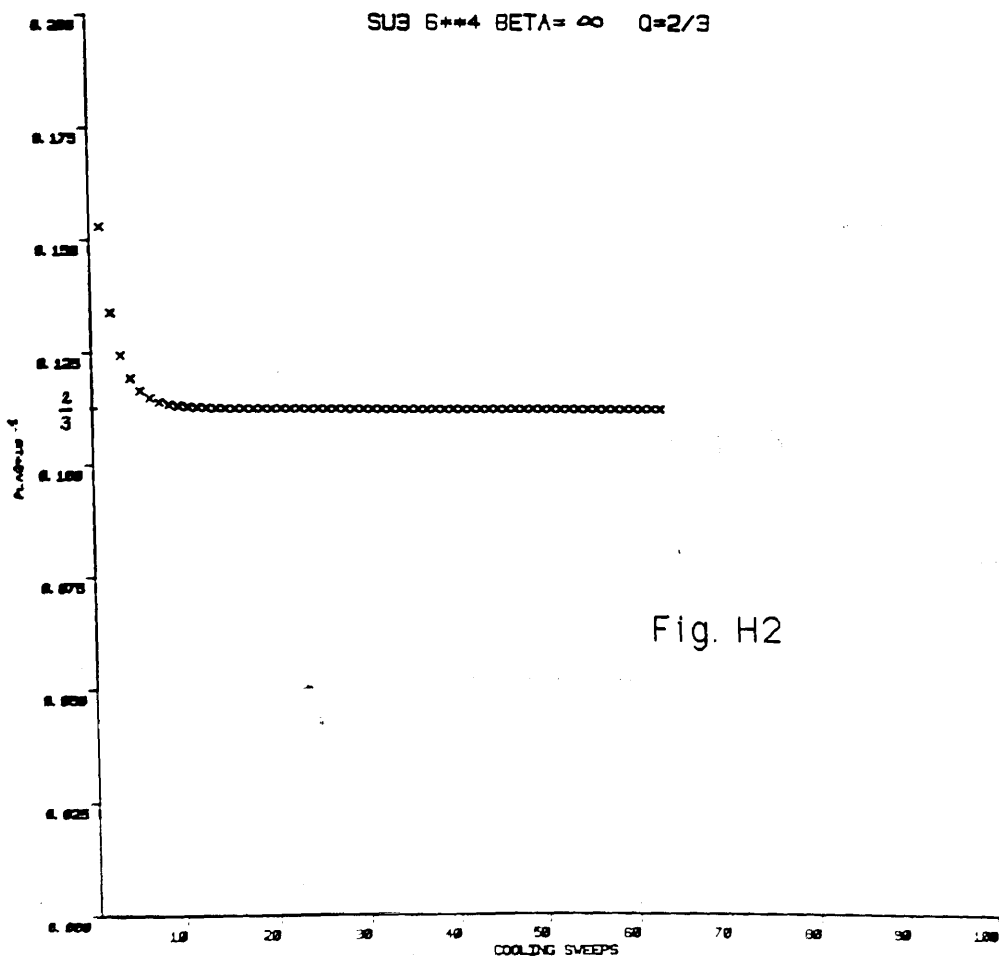
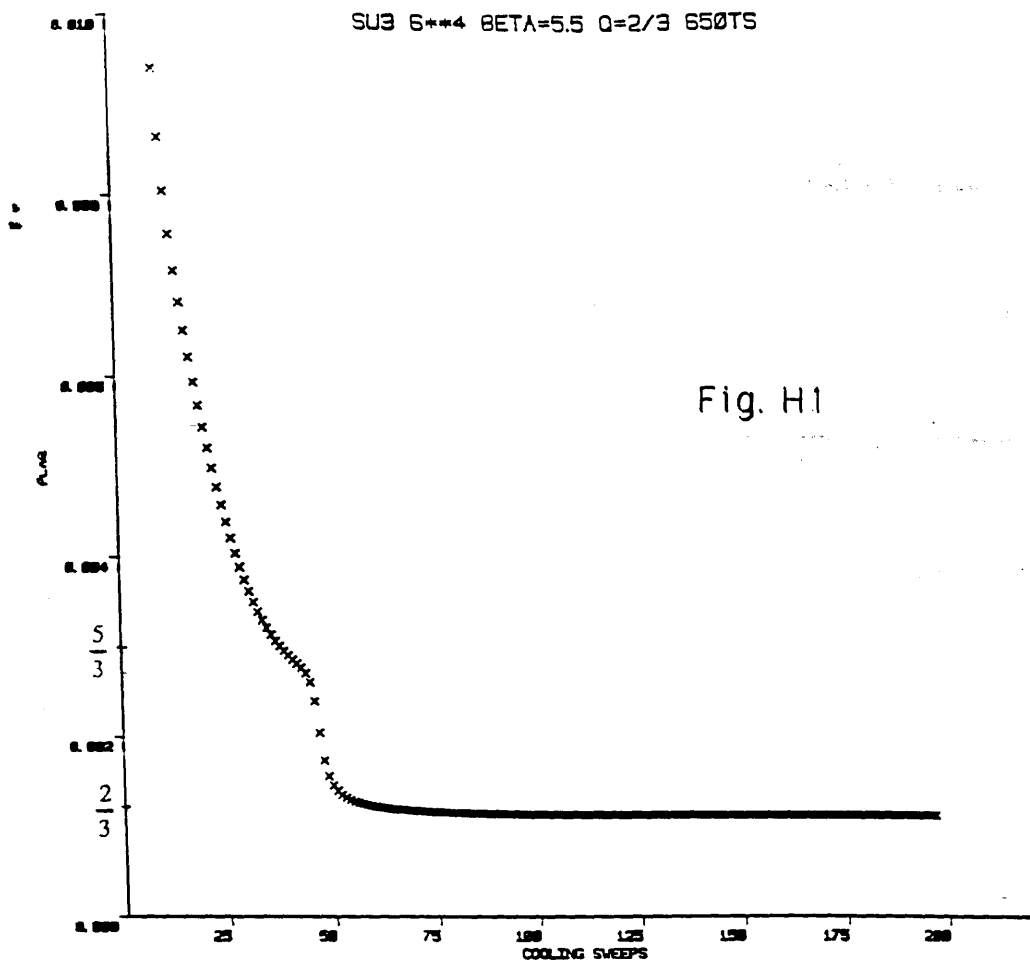


SU2 6\*\*3\*12 Q=1/2 BETA=  $\infty$









## CHAPTER FOUR

### 4.1 Generalities on the Index Theorem

In this chapter we deal with the index theorem and its verification on a lattice. We start, firstly, by giving a general outline of the index theorem in the continuum.

The index theorem basically reflects the non-trivial topological properties of the gauge field and remarkably connects these properties with the number of zero modes of the Dirac operator[29].

We discuss briefly the "proof" of the index theorem and we comment on some points referring to the conditions under which it is applicable.

It is well known[30] that the Eculidean path - integral measure is not invariant under the chiral transformation, and it gives rise to an anomalous Jacobian factor  $\sum_n \Psi_n^+(x) \Gamma_5 \Psi_n(x)$  (where  $\Psi_n(x)$  are the eigenfunctions of the Dirac operator) which is not well defined and may be regularised with a Gaussian cut-off, i.e.,

$$\sum_n \Psi_n^+(x) \Gamma_5 \Psi_n(x) = \lim_{M \rightarrow \infty} \Psi_n^+(x) \Gamma_5 \exp(-\not{D}^2/M^2) \Psi_n(x) =$$

$$\lim_{M \rightarrow \infty} \text{Tr} \Gamma_5 \exp(\not{D}^2/M^2) \sum_n \int_{x \rightarrow y} \Psi_n^+(x) \Psi_n(y) = (1/16\pi^2) \text{Tr} F_{\mu\nu} \tilde{F}^{\mu\nu}.$$

So the factor in the path integral which gives the anomaly is

$$\int dx \omega(x) \sum_n \Psi_n^+(x) \Gamma_5 \Psi_n(x) = \int dx \omega(x) (1/16\pi^2) \text{Tr} F_{\mu\nu} \tilde{F}^{\mu\nu},$$

( $\omega(x)$  is the chiral rotation of  $\Psi(x) \rightarrow e^{i\omega(x)\Gamma_5} \Psi(x)$ ).

In the limit in which  $\omega(x)$  becomes a constant we can use this result to generate a proof of the index theorem for the Dirac

operator. To see this we note that  $\int d^4x \sum_n \Psi_n^+(x) \Gamma_5 \Psi_n(x) = 0$  for eigenfunctions with eigenvalues  $\lambda_n \neq 0$  so the only contribution is from the zero modes of  $\Gamma_5$  and :

$$\int d^4x (\sum_{i=1}^{\text{positive chirality zero modes}} \Psi_+^i(x) \Gamma_5 \Psi_+^i(x) - \sum_{i=1}^{\text{negative chirality zero modes}} \Psi_-^i(x) \Gamma_5 \Psi_-^i(x)) = n_+ - n_- ,$$

so

$$n_+ - n_- = (1/16\pi^2) \int \text{Tr} F_{\mu\nu} \tilde{F}^{\mu\nu} \tag{4.1.1}.$$

The chirality is defined by the eigenfunctions of  $\Gamma_5$ :

$$\Gamma_5 \Psi = \pm \Psi \tag{4.1.2}.$$

We now discuss some points concerned with the index theorem.

1) Most of the work so far, in the continuum, and on the lattice, has been restricted to the case of the instanton field and the number of zero modes of  $D$  in the presence of the instanton field in various simple compact groups. Obviously, when we consider the case of the instantons we deal with  $S^4$  as our base space (compact space), or, using the conformal mapping from  $R^4 \cup \{\infty\}$  to  $S^4$ ,  $R^4$ . This justifies attempts to verify the index theorem on a lattice, considering the lattice as a compact flat space.

2) Solving the equation

$$F_{\mu\nu} = \pm \tilde{F}_{\mu\nu} \tag{4.1.3}$$

for fixed winding number, provides the number of parameters on which the instanton solution depends. For example, for the  $SU(2)$  case with Pontryagin number  $P$  (in this chapter we will denote sometimes the topological charge  $Q$  by  $P$ ) the number of parameters for the instanton solution is  $8P-3$ . For the  $SU(3)$  case

for  $P = 1$  we have 5 parameters and for  $P > 1$  we have  $12P-8$  parameters. The fluctuation problem (expansion around known instanton solutions which preserves (4.1.3)) has been considered for the instanton case and it should be formulated also using TBC. For the instanton case there are known solutions for the gauge field, for example, for  $Q=1$  the solution was found in [31], and by expanding around it we are able, in principle, to find the spectrum of the Dirac operator for a general gauge field, as well as the number of parameters on which this gauge field depends.

While much work has been done concerning instantons, in the case of the TBC the only known solution is that of [20] and we should formulate the fluctuation problem by expanding around the Abelian solutions of [20].

3) The form (4.1.1) is a special case of the index theorem for an elliptic operator. Generally, the index is defined as  $\sum (-1)^i (h_i)$ , where every Betti number  $h_i$  is the dimension of the coset [32]

$H_i = \text{Ker } D_i / \text{Image } D_{i-1}$  and  $D_i$ 's form a complex [33,34] which, in the case of gauge theories, can be represented by

$$\begin{array}{ccccccc} D_{-1} & D_0 & D_1 & D_2 \\ 0 \rightarrow \Gamma_0 \rightarrow \Gamma_1 \rightarrow \Gamma_2 \rightarrow 0 \end{array}$$

where  $\Gamma_0$  = the space of scalar fields,  $\Gamma_1$  = the space of vector fields, and  $\Gamma_2$  = the space of (anti)-selfdual tensors  $F_{\mu\nu}$ , and  $D_{i+1}D_i = 0$ . Physically,  $H^1$  gives the number of non-gauge equivalent solutions to Yang-Mills equations which satisfy duality and  $H^0$  the dimension of the holonomy group of the gauge group. The number  $h^2$  for the case of the sphere is zero. The number  $h^0 - h^1$  is what we call the index of the operator  $D$  which maps  $\Gamma_0 + \Gamma_1$  to  $\Gamma_2$  and the index

$$D = \dim \text{Ker } D - \dim \text{Ker } D^* = h^0 - h^1.$$

4) Atiyah et al. [35] have shown that



$$\text{index } D = a_V Q + c\tau \quad (4.1.4)$$

where  $a_V$  = the Dynkin index of the representation of the fermion field and  $\tau$  = the signature of the base-space manifold. In the case of the sphere and the torus  $\tau = 0$  and  $a_V = s(s-1)(s+1)/6$  where  $s$  is the dimension of the fermion representation. For the case of the SU(2) group with the fermions in the fundamental representation, index  $D = n_+ - n_- = P$ , where  $P$  = topological charge  $Q$ .

## 4.2 The Index Theorem on a Lattice

We applied the MTBC (Multi Twisted Boundary Conditions of Section 2.2) on a lattice both for Wilson and Kogut-Susskind fermions. We used thermalised configurations as well as explicit configurations with constant field strength  $F_{\mu\nu}$  which were constructed according to [20]. We start by giving some of the explicit solutions for the gauge field which we used to find the eigenvalues of the fermion matrix.

For the SU(2) group a configuration with  $P = 1/2$  is given by [20].

### 4.2A

$$\begin{aligned} A_1(x) &= (\pi/2)x_2\sigma_3/a_1a_2, & A_2(x) &= -(\pi/2)x_1\sigma_3/a_1a_2, \\ A_3(x) &= (\pi/2)x_4\sigma_3/a_3a_4, & A_4(x) &= -(\pi/2)x_3\sigma_3/a_3a_4, \end{aligned} \quad (4.2.1)$$

where  $A_\mu$  denotes the gauge field in the continuum,  $a_1, a_2, a_3, a_4$  are the sizes of a 4-dimensional Euclidean box along the 4 directions,  $x_1, x_2, x_3, x_4$  are the coordinates of a point and  $\sigma_3$  is the Pauli  $\sigma_3$ -matrix. The twists  $\eta_{\mu\nu}$ 's which were used for (3.1.11) were used also to construct (4.2.1). This solution has constant field strength in the 1-2,3-4 levels and satisfies the Yang-Mills equations of motion:

$$\therefore D_\mu F^{\mu\nu} = \partial_\mu F^{\mu\nu} + i[A_\mu, F^{\mu\nu}] = 0.$$

It has been shown [36], that stable extrema of the action (for compact manifolds) are always (anti)-selfdual. Since the solutions of [20] are constant (they have constant field strength), we should expect them to be stable.

Another example of an explicit configuration is:

#### 4.2B Group $SU(2)^{\text{color}} \times SU(4)^{\text{flavor}}$

In this example we have the peculiar characteristic that the number of colors is different from the number of flavors, but the MTBC still apply.

In this case, to be consistent with (2.2.20), we chose

$$\eta_{12}^{(\text{color})} = \frac{1}{2} \eta_{12}^{(\text{flavor})}$$

The gauge field is now the same as in (4.2.1) since it depends only on the color twist, but we have to change the flavor twist transition functions for them to match the  $\eta_{12}^{(\text{flavor})} = 2$ .

So we construct the  $\Omega_\mu^{(\text{flavor})}$ 's such that

$$\Omega_1^f(x) = \begin{bmatrix} p^* & & & \\ & p^* & & \\ & & p & \\ & & & p \end{bmatrix}, \Omega_2^f(x) = \begin{bmatrix} -iq & & & \\ & iq & & \\ & & q^* & \\ & & & q^* \end{bmatrix},$$

$$\Omega_3^f(x) = \begin{bmatrix} z \\ & z \\ & & z^* \\ & & & z^* \end{bmatrix}, \Omega_4^f(x) = \begin{bmatrix} \lambda \\ & \lambda \\ & & -i\lambda^* \\ & & & i\lambda^* \end{bmatrix}.$$

(4.2.2)

In (4.2.2)

$$p = e^{i\pi x_2/2a_2}$$

$$q = e^{i\pi x_1/2a_1}$$

$$z = e^{i\pi x_4/2a_4}$$

$$\lambda = e^{-i\pi x_3/2a_3}$$

We now give an explicit configuration for the  $SU(3)$  group for  $P = 2/3$ .

**4.2C** Using the twists for  $Q = 2/3$  (c.f 3.1.14) we have

$$A_1(x) = (\pi/3)x_2\omega/a_1a_2, \quad A_2(x) = -(\pi/3)x_1\omega/a_1a_2,$$

$$A_3(x) = (\pi/3)x_4\omega/a_3a_4, \quad A_4(x) = -(\pi/3)x_3\omega/a_3a_4,$$

(4.2.3)

where

$$\omega = \begin{bmatrix} 1 & 0 & 1 \\ 0 & 1 & 0 \\ 0 & 0 & -2 \end{bmatrix}$$

When we apply the color-flavor twist on the lattice we do this in the following way. Every time we reach a boundary site of the lattice; i.e., when for example the coordinate of a lattice site in the x-direction is  $N_x+1$  ( $N_x$  = lattice size in the x-direction), we multiply the gauge field matrix with the matrix we obtain after the application of the color-flavor twist on the  $\Psi$  field. We now present, as an example, the application of the color-flavor twist for the group  $SU(2)^{(\text{color})} \times SU(2)^{(\text{flavor})}$ .

If  $\begin{bmatrix} a & b \\ -b^* & a^* \end{bmatrix}$ , represents the  $SU(2)$  gauge field matrix,

then the application of the color-flavor twist on the  $\Psi$ -field results in:

1st flavor

$$\mu=1 \quad \begin{bmatrix} a & b \\ -b^* & a^* \end{bmatrix} \begin{bmatrix} 1 & 0 \\ 0 & p^{*2} \end{bmatrix} = \begin{bmatrix} a & bp^{*2} \\ -b^* & a^*p^{*2} \end{bmatrix}$$

(4.2.4a)

For the other directions (and using  $\Omega_\mu^c(x) = \Omega_\mu^f(x)$ )

we replace  $p = e^{i\pi x_2/2a_2}$  by (c.f.3.1.11)

$$q = e^{-i\pi x_1/2a_1} \quad (\mu = 2)$$

$$z = e^{i\pi x_4/2a_4} \quad (\mu = 3) \quad (4.2.4b)$$

$$\lambda = e^{-i\pi x_3/2a_3} \quad (\mu = 4),$$

For the 2nd flavor we have:

$$\therefore \mu=1 \begin{bmatrix} a & b \\ -b^* & a^* \end{bmatrix} \begin{bmatrix} p^2 & 0 \\ 0 & 1 \end{bmatrix} = \begin{bmatrix} ap^2 & b \\ -b^*p^2 & a^* \end{bmatrix} \quad (4.2.4c)$$

(for the other directions we replace p by q,z,l of (4.2.4b)).

Since we use a local flavor twist(without introducing "flavor bosons"), we have to specify the coordinates x of  $\Omega_\mu^f(x)$  for every particular flavor we deal with. In the case of Wilson's fermions this does not seem to create any conceptual problem since each flavor field lives on one lattice site.

For the K-S fermions we have really to think about the argument to be used for the flavor twist functions, since each flavor is spread over the 16 (in D=4) corners of the hypercube. For a periodic lattice the X fields on the boundary sites of the lattice are identical to the ones in the interior of the lattice. Under the MTBC of section 2.2 we have to take into account the influence of the twist on the X - fields, and this can be done by constructing the flavor field in terms of the X-fields and then applying the color-flavor twist on the flavor field.

We label the sites of each flavor box as in Fig.4.2.2 and using

$$q^{\mu f} = \sum_n \Gamma_n^{\mu f} U U_n X_n, \text{ where } \mu = \text{Dirac index, } f = \text{flavor index}$$

(c.f. Appendix A) we arrive at :

$$q^1 = \begin{bmatrix} X'(1) & +iUU'(1')X'(1') \\ X'(2)UU'(2) & +iUU'(2')X'(2') \end{bmatrix} \quad q^2 = \begin{bmatrix} X'(1) & -iUU'(1')X'(1') \\ X'(2)UU'(2) & -iUU'(2')X'(2') \end{bmatrix} \quad (4.2.5)$$

where the prime(') fields refer to the boundary flavor box, i.e., box

1 at Fig.4.2.1 and we work in  $D=2$ .

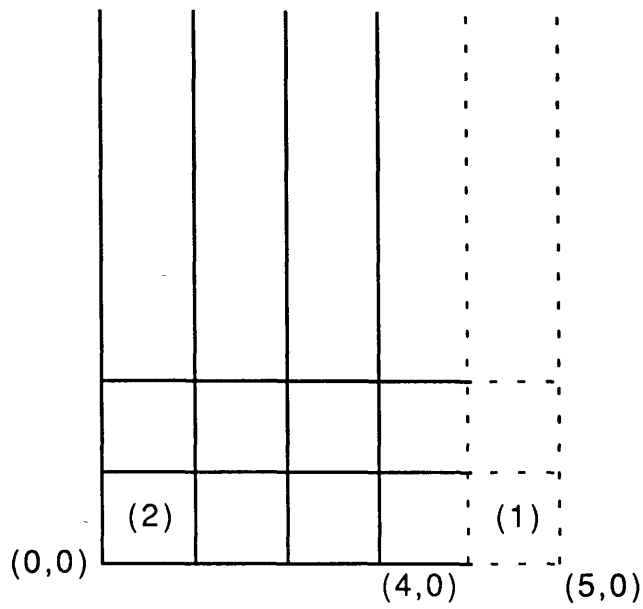


**Fig. 4.2.1**     *Flavor boxes on a lattice for the K-S fermions in  $D=2$*

In Fig. 4.2.1 we suppose that along the  $x$ - axis the lattice has four sites and so the sites of box 1 do not belong in the lattice. In (4.2.5) we label the four sites of any flavor box as in Fig.4.2.2., and this relation without the primes on the  $U$ 's and the  $X$ 's can also be used for every flavor box of the lattice and not only for the boundary flavor boxes.

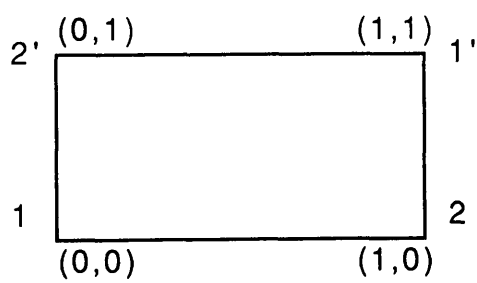


**Fig.4.2.2**     *A flavor box for K-S fermions in  $D=2$*

The indices 1,2 on the q's correspond to the 2 flavors in  $D = 2$  and we used representation of the  $\Gamma$  matrices

$$\Gamma_0 = \begin{bmatrix} 0 & 1 \\ 1 & 0 \end{bmatrix}, \Gamma_1 = \begin{bmatrix} 0 & -i \\ i & 0 \end{bmatrix}$$

Also

$$\begin{aligned} UU(1) &= 1 & UU'(1) &= 1 \\ UU(2) &= U_1(00) & UU'(2) &= U_1(40) \\ UU(2') &= U_2(00) & UU'(2') &= U_2(40) \\ UU(1') &= U_1(00)U_2(10) & UU'(1') &= U_1(40)U_2(50) . \end{aligned}$$

We now perform a flavor twist on  $(q^1, q^2)$  and we get:

$$\begin{bmatrix} X'(1) + iUU'(1')X'(1') & X'(1) - iUU'(1')X'(1') \\ X'(2)UU'(2) + iUU'(2')X'(2') & X'(2)UU'(2) - iUU'(2')X'(2') \end{bmatrix} =$$

$$\begin{bmatrix} X(1) + iUU(1')X(1') & X(1) - iUU(1')X(1') \\ X(2)UU(2) + iUU(2')X(2') & X(2)UU(2) - iUU(2')X(2') \end{bmatrix} \begin{bmatrix} p & 0 \\ 0 & q \end{bmatrix} \quad (4.2.6)$$

In (4.2.6) the matrix

$$\begin{bmatrix} p & 0 \\ 0 & q \end{bmatrix}$$

is equal to  $\Omega_{\mu}^f(x)$  with argument  $x$  of  $\Omega_{\mu}^f(x)$  the center of the particular flavor box being considered. Solving (4.2.6) for the primed fields and applying the color twist on the gauge field, if it is at the boundary, we express the  $X$  fields on the boundary flavor boxes in terms of the  $X$  fields of the flavor boxes in the lattice. If we concentrate on boxes 1,2 of Fig. 4.2.1 then we find  $X(4,1)$ ,

which in the notation of Fig.4.2.2 is the  $X'(2)$  site,  $X(4,0)$ ,  $X(5,0)$ ,  $X(5,1)$  in terms of  $X(0,0)$ ,  $X(1,0)$ ,  $X(0,1)$ ,  $X(1,1)$ .

We now consider the interaction:  $\bar{X}(3,1) U_1(3,1) X(4,1)$ . For a periodic lattice with antiperiodic boundary conditions for the  $X$ - fields it equals  $-\bar{X}(3,1) U_1(3,1) X(0,1)$ . Now, using (4.2.6),

$$X(41) = (1/2i)\Omega_1(3/2)U_2^+(00)(p-q)X(10)U_1(00)+ \\ (1/2)\Omega_1(3/2)(p+q)X(01)$$

and finally

$$\bar{X}(31)U_1(31)X(41)= \\ (1/2i)\bar{X}(31)U_1(31)\Omega_1(3/2)U_2^+(00)(p-q)X(10)U_1(00)+ \\ (1/2)\bar{X}(31)U_1(31)\Omega_1(3/2)(p+q)X(01)$$

From this we notice that the first term is not a neighbour interaction.

We can proceed to the calculation of  $q\bar{q}$  in  $D = 2$  for each flavor after the inculsion of the MTBC.

We present the condensate  $qq$  in  $D = 2$  for one of the flavor boxes. Without twist (using (4.2.5))

$$\bar{q}^1 q^1 = \bar{X}(00)X(00) + i\bar{X}(00)U_1(00)U_2(10)X(11) - \\ i\bar{X}(11)U_2^+(10)U_1^+(00)X(00) + \bar{X}(11)X(11) + \bar{X}(10)X(10) + \\ i\bar{X}(10)U_1^+(00)U_2(00)X(01) - i\bar{X}(01)U_2^+(00)U_1(00)X(10) + \\ \bar{X}(01)X(01)$$

and



$$\begin{aligned}
\bar{q}^2 q^2 = & \bar{X}(00)X(00) - i\bar{X}(00)U_1(00)U_2(10)X(11) + \\
& : \\
& i\bar{X}(11)U_2^+(10)U_1^+(00)X(00) + \bar{X}(11)X(11) + \bar{X}(10)X(10) - \\
& i\bar{X}(10)U_1^+(00)U_2(00)X(01) + i\bar{X}(01)U_2^+(00)U_1(00)X(10) + \\
& \bar{X}(01)X(01).
\end{aligned}$$

In the presence of the twist (color-flavor for the same flavor box) we have, by solving (4.2.6),

$$X(40) = \Omega_1^{\text{color}(1/2)} \{ \cos\theta X(00) + \sin\theta U_1(00)U_2(10)X(11) \}$$

$$X(51) = \Omega_1^{\text{color}(3/2)} \{ \cos\theta X(11) - \sin\theta U_2^+(00)U_1^+(00)X(00) \}$$

$$X(50) = \Omega_1^{\text{color}(1/2)} \{ \cos\theta X(10) + \sin\theta U_1^+(00)U_2(00)X(01) \}$$

$$x(41) = \Omega_1^{\text{color}(3/2)} \{ \cos\theta X(01) - \sin\theta U_2^+(00)U_1(00)X(10) \}$$

$$\text{with } \cos\theta = \frac{1}{2}(p+q) \text{ and } \sin\theta = \frac{1}{2i}(p-q)$$

Finally ,after some algebra ,we find that:

$$q\bar{q}_{\text{twisted}} = q\bar{q}_{\text{without twist}} \quad (4.2.7)$$

and this holds for each flavor separately.

We should expect that (4.2.7) is independent of the incorporation of the twist, since  $q\bar{q}$  is a local quantity and it must not be affected by the global effects of topology. In contrast,

$\langle q\bar{q} \rangle_{\text{twisted}} \neq \langle q\bar{q} \rangle_{\text{untwisted}}$ , since when we consider the VEV of  $\langle q\bar{q} \rangle$ , we take into account the updating of the gauge field under the TBC, which affects  $\langle q\bar{q} \rangle$  (c.f. 1.9.5). In all the cases on which MTBC were applied on the lattice we did not consider the flavor group to be gauged, as this would require the introduction of "flavor" bosons. The flavor twist is used in this work purely as a transformation

which acts on the flavor indices of the  $\Psi$  field. Gauging the flavor group should make the flavor index into a gauge quantum number.

### 4.3 Numerical Results

From the Section 4.1 we expect that, since for the SU(3) case  $a_V=4$  and for the SU(2) case  $a_V=1$ ,

$$n_+ - n_- = 4N_f P \quad \text{for the SU(3) group} \quad (4.3.1a)$$

and

$$n_+ - n_- = N_f P \quad \text{for the SU(2) group} \quad (4.3.1b)$$

We now discuss our numerical results. In the numerical analysis the Lanczos algorithm (Appendix B) was employed and we worked in the quenched approximation. We now present the plots for the K-S fermions.

Figs. 4.3.1a,b,c show the eigenvalues of the fermion matrix for the configuration of Fig. G1. (G1 was taken for the SU(3) group at  $\beta=5.5$  for a  $6^4$  lattice). We have plotted only the first six small eigenvalues and we used antiperiodic boundary conditions for the fermion field, i.e. a minus sign in front of (2.2.18).

Comparing Figs. 4.3.1a,b,c and  $G_1$ , makes it clear that the distribution of the small eigenvalues is correlated with the sequence of plateaus in  $G_1$ . One is now tempted to ask whether the index theorem (4.3.1) is verified by the above figures. We believe that this is not achieved convincingly. Certainly, the eigenvalues follow the behaviour of the pure gauge action, and in the sweeps where the changes of the topological charge occur (where we lose one unit of topological charge), we are able to see an induced change in the form of the eigenvalues.

We now consider the case of periodic twisted boundary conditions, (Figs. 4.3.2a,b,c.)

Here we observe a rather different behaviour, in the sense that the first and the second flavors seem to follow the same pattern, while the 3rd flavor does not "suffer" very sharp changes at the critical sweep numbers (about 25, 100, 400). We therefore

conclude that no significant insight can be gained into the exact reproduction on the lattice of (4.3.1) using periodic MTBC.

In Figs. 4.3.3a,b,c we examined the influence on the eigenvalues of the  $H_1$  configuration. We recall that  $H_1$  refers to the pure gauge action for the SU(3) group for a  $6^4$  lattice at  $\beta = 5.5$  and  $Q = 2/3$ . Although we have deviations from (4.3.1) we believe that our results show that there are some remnants of the index theorem on the lattice. There are zero modes which remain even after about 200 cooling sweeps. We also observe the similarities between the first and the second flavors. Where the first plateau ( $Q \cong 5/3$ ) appears, at around the 44th sweep, the 5th and the 6th eigenvalues for the third flavor rapidly disappear, and at the same time we lose the last four eigenvalues for the first and second flavors. At the final and stable plateau, at  $Q = 2/3$ , we are left with eight small eigenvalues, in agreement with (4.3.1).

Fig.4.3.4 presents the case where we found the eigenvalues for the SU(2) group using antiperiodic boundary conditions for the configuration of Fig. D<sub>2</sub>. Again there is a correspondence between these two graphs.

When one instanton disappears at about the 50th sweep and we move from the  $Q = 3/2$  to the  $Q = 1/2$  vacuum, we lose zero modes. In this plot we give the results for only the 1st flavor, since the 2nd flavor behaved identically. The fact that the form of the eigenvalues does not distinguish between the flavors is explained by the existence of the following similarity transformation (c.f.4.2.4a,c):

$$\begin{bmatrix} a & bp^{*2} \\ -b^{*} & a^{*}p^{*2} \end{bmatrix} = \{ \sigma_2 \begin{bmatrix} ap^2 & b \\ -b^{*}p^2 & a^{*} \end{bmatrix} \sigma_2 \}^{*}$$

and  $\sigma_2$  is the Pauli  $\sigma_2$  matrix.

We now study the eigenvalues for the case of the Wilson's fermions for the SU(3) group. In all the cases we studied to find the eigenvalues, we used the Hermitian  $\Gamma_5 M$  matrix, and, of course, the zero modes of this matrix are the same as the zero modes of  $M$  ( $M$

is the fermion matrix) and vice versa.

Figs. 4.3.5a to 4.3.5g deal with the eigenvalues of the first flavor using antiperiodic boundary conditions and all the figures correspond to the  $G_1$  configuration. We examine the behaviour of the eigenvalues by again varying the sweep number and also studying the variation of the form of the eigenvalues with respect to the Wilson parameter  $k$ .

We notice there are no zero modes at  $k = 0.125$ , while at the sweep numbers (about 25,100,400) and even at  $k = 0.125$ , all the eigenvalues show small "curvature" effects. At  $k = 0.130$  we have reached the real eigenvalues of  $M$  and there is a strong indication of zero modes, which actually appear at  $k = 0.135$  and at about the 25th and 400th sweeps, where the plateaus occur. Counting the number of zero modes of  $\Gamma_5 M$  at each  $k$  we verify that the number of small eigenvalues is different at around the 25th, the 100th and 400th sweeps. So, at every cooling sweep, we have a choice of one particular  $k$ , such that the eigenvalues  $\lambda$  of  $M$  are  $\lambda = 1/k$ <sup>[37]</sup>.

Going from  $k=0.130$  to  $k=0.135$  we observe a "tunnelling" of a whole line of eigenvalues from the left to the right of the axis. As we go to higher  $k$ 's we reach a point where there is no zero mode. For the other two flavors the behaviour is about the same. The above figures indicate that "a form" of the index theorem is satisfied on a lattice.

We now discuss the case of the  $H_1$  configuration. (Figs. 4.3.8a to 4.3.10g). Obviously there is a dramatic change at about the 44th sweep, i.e. when the instanton disappears. Remarkably again at  $k=0.125$  there is no zero mode and as we go to higher  $k$ 's we find the movement of whole lines of eigenvalues through the axis. Again we have exact zero modes (c.f. at  $k=0.140$  for the 2nd flavor for example). There are no substantial differences in the behaviour of the eigenvalues for the three flavors.

We now give a description of our results for the cases where explicit configurations were used.

Figs. 4.3.11a,b,c and Figs. 4.3.12a,b,c ( $P = 2/3$  at both cases) show that at  $k = 0.131$  there are zero modes for all the flavors, while in

both cases the eigenvalue distribution for the third flavor differs from that of the first two flavors. At  $k = 0.131$  there are four eigenvalues of  $\Gamma_5 M$  very close to zero.

Figs. 4.3.13a,b,c and 4.3.14a,b,c correspond to results for a  $P=4/3$  configuration. We therefore conclude that even although there are zero modes for  $k = 0.139$  and  $k = 0.141$  there is a deviation from (4.3.1).

Figs. 4.3.15a,b were obtained by setting only color twist for the  $\Psi$  - field. This, of course, leads to a non single-valued fermion field and comparison with Figs. 4.3.11 and 4.3.12 shows that the number of small eigenvalues is significantly less when we apply only a color twist. In all the above cases our lattice size was  $6^4$ , with the exception of the case with  $P = 4/3$  where the lattice size was  $8 \times 4^3$ .

Results for the  $SU(2)$  group are as follows:.

Fig.4.3.16 shows the dependence of the small eigenvalues on  $k$ . Again we do not plot the 2nd flavor, since it behaves exactly as the 1st one. Our lattice size is  $6^4$  and we see one mode very close to zero at  $k = 0.129$ .

Figs. 4.3.17a,b are for the case where we had only a color twist (the lattice size is still  $6^4$ ) . No zero modes were seen.

We now present the case of a "twisted" instanton configuration on a  $12 \times 6^3$  lattice. In 4.3.18, where we had a color-flavor twist there were zero modes, while at Fig.4.3.19 (only a color twist) no zero modes were observed.

The final graph (Figs. 4.3.20a,b,c,d) is for the group  $SU^c(2) \times SU^f(4)$ . There are no small eigenvalues for the first two flavors but there are small ones for the third and the fourth flavors.

In this case, since the  $\Psi$ - field belongs to the fundamental representation of the  $SU(2)$  group, we expect that  $a_V=1$  and, from (4.3.1) that  $n_+ - n_- = 2$ . This was found to be the case.

In all the cases, where Wilson fermions were referred, we kept the Wilson  $r$ - parameter equal to 1, but we also ran some cases with  $r = 0.50$  and  $r = 0.25$  for explicit configurations only. Since as  $r \rightarrow 0$  the Wilson term (c.f. 1.8b.1) in the action goes to zero too, the chiral symmetry is restored and there are no zero modes. We confirmed this although the results are not presented here.

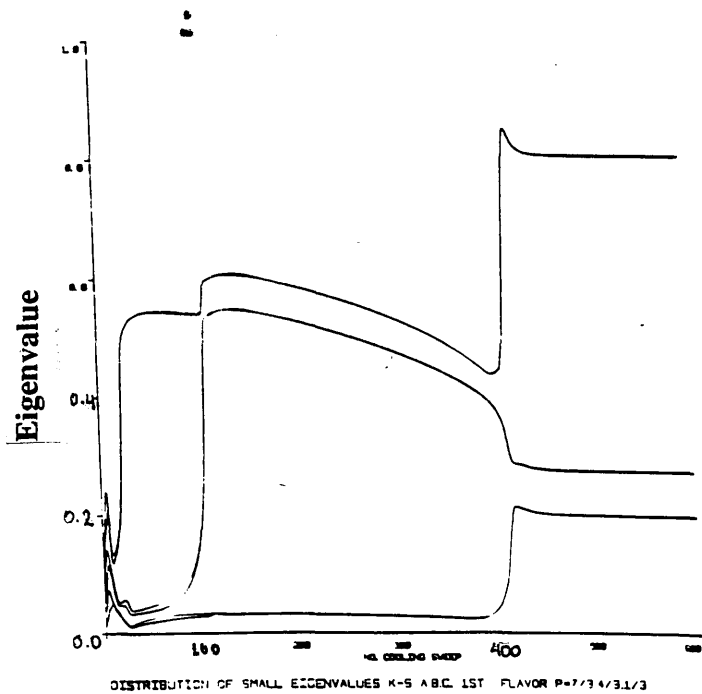


Fig. 4.3.1a

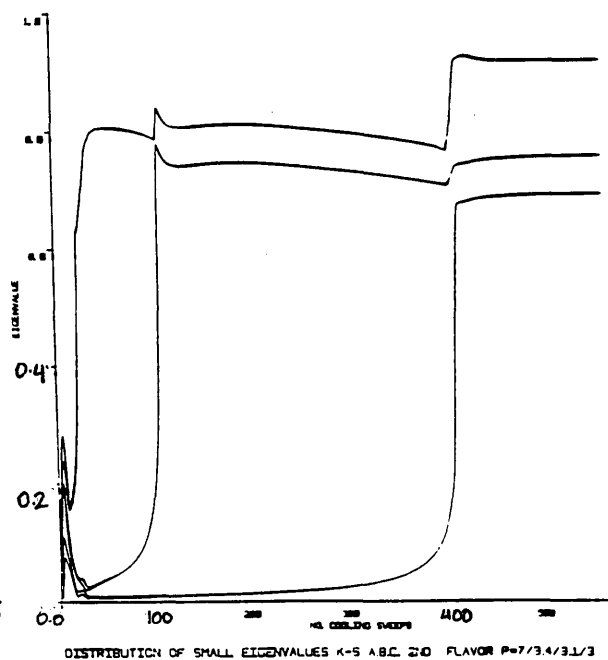


Fig. 4.3.1b

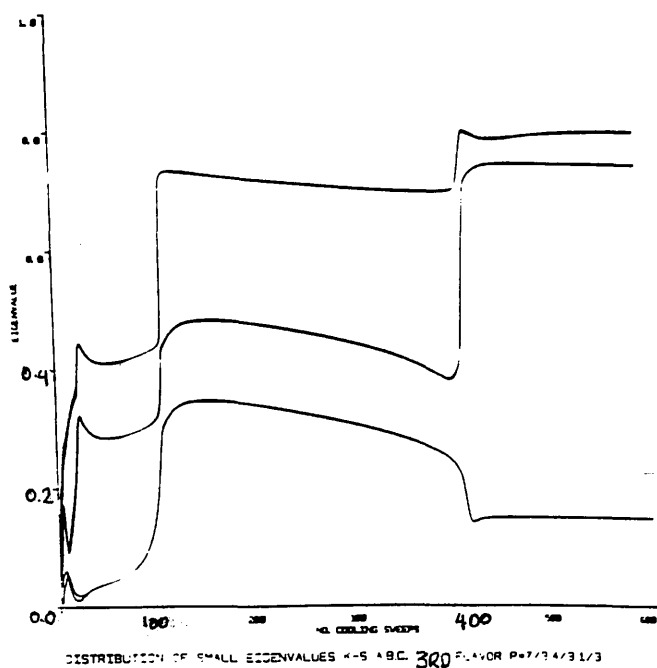


Fig. 4.3.1c

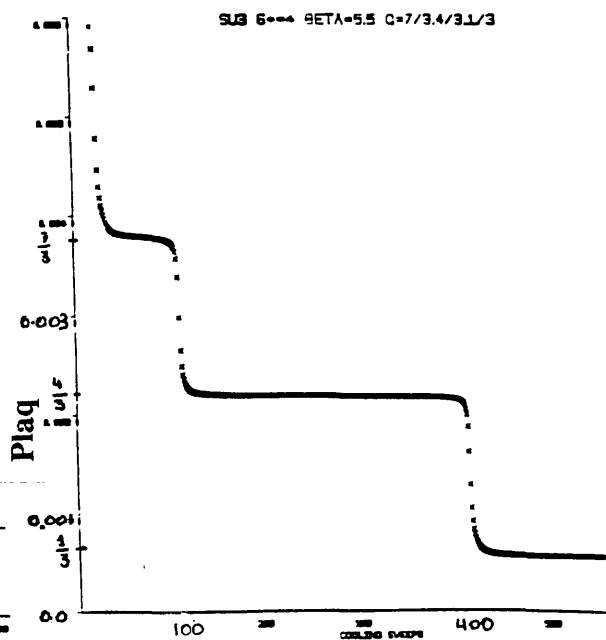


Fig. 11

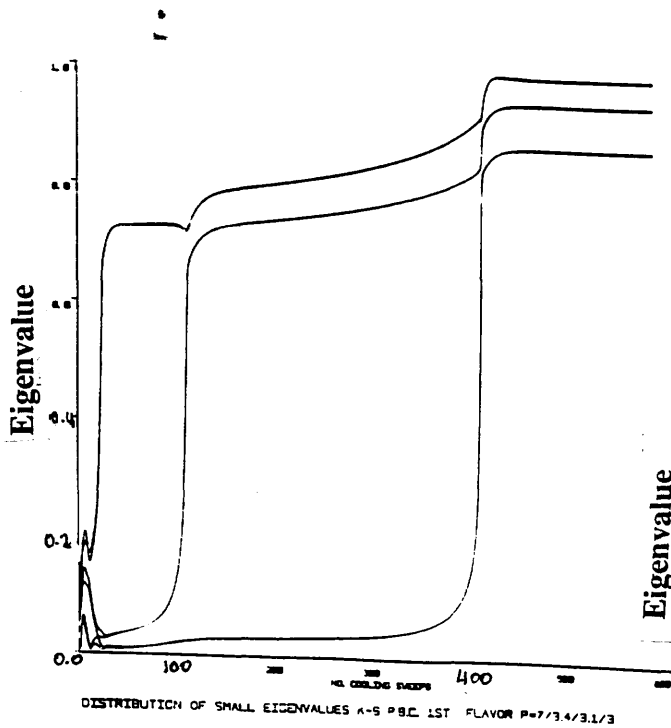


Fig. 4.3.2a

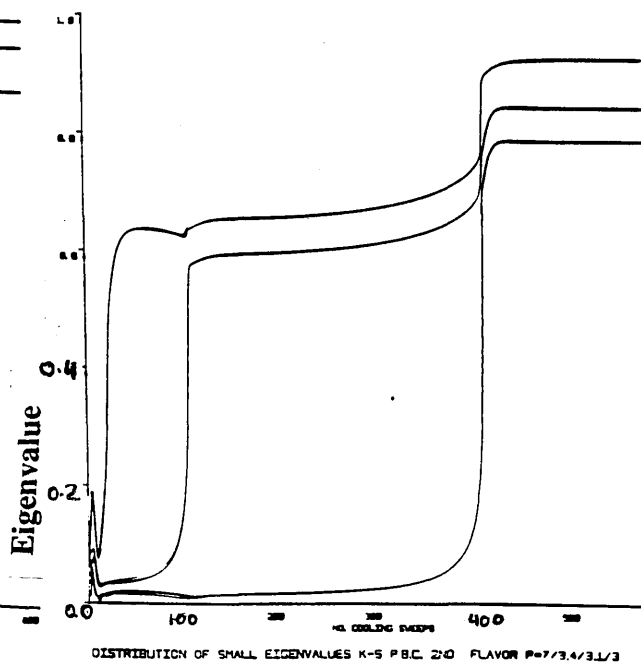


Fig. 4.3.2b

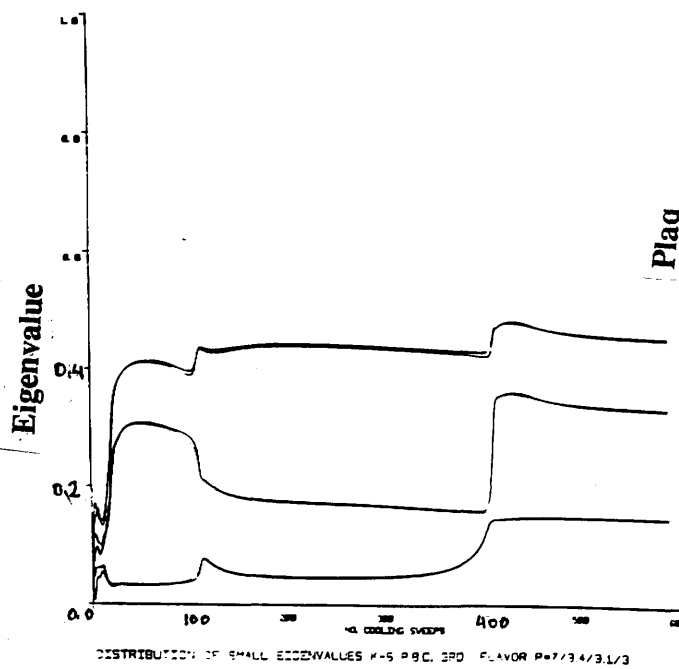


Fig. 4.3.2c

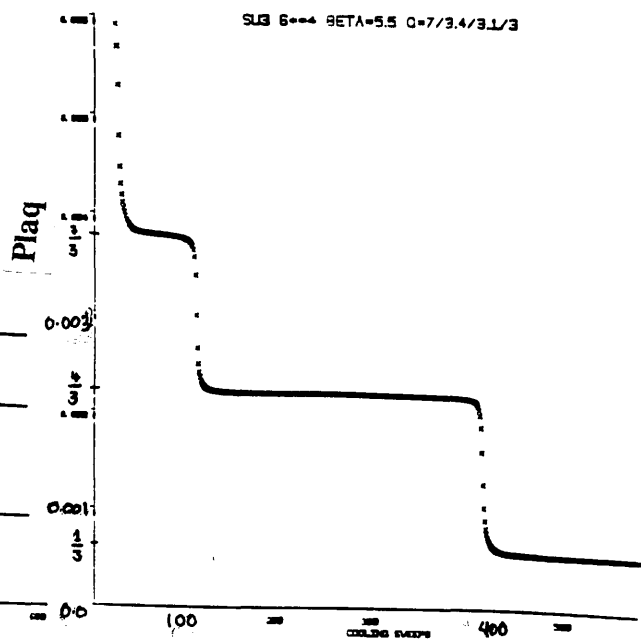


Fig. 11



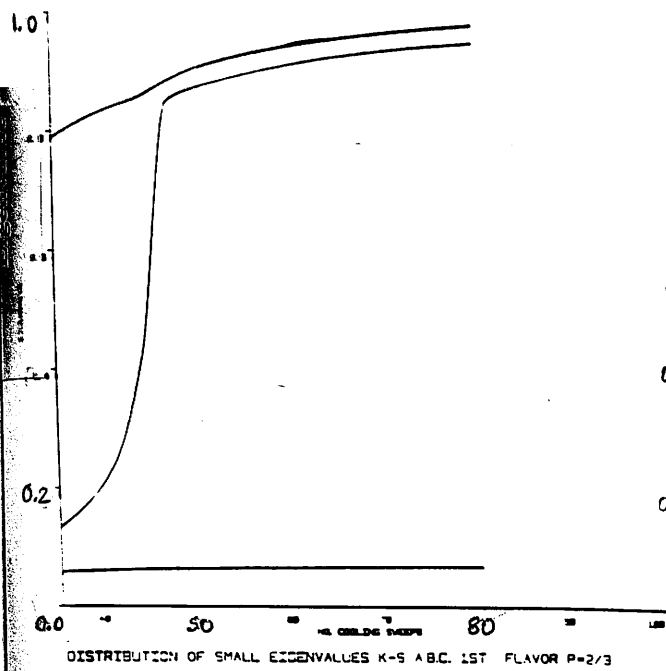


Fig. 4.3.3a

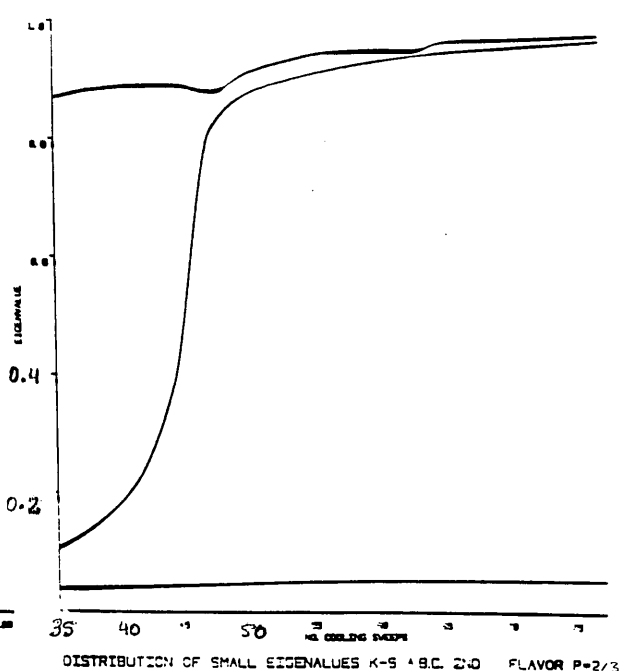


Fig. 4.3.3b

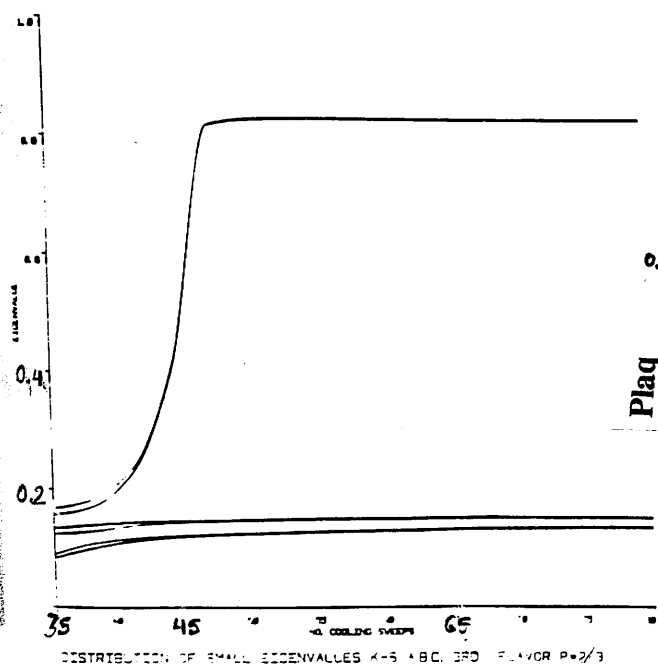


Fig. 4.3.3c

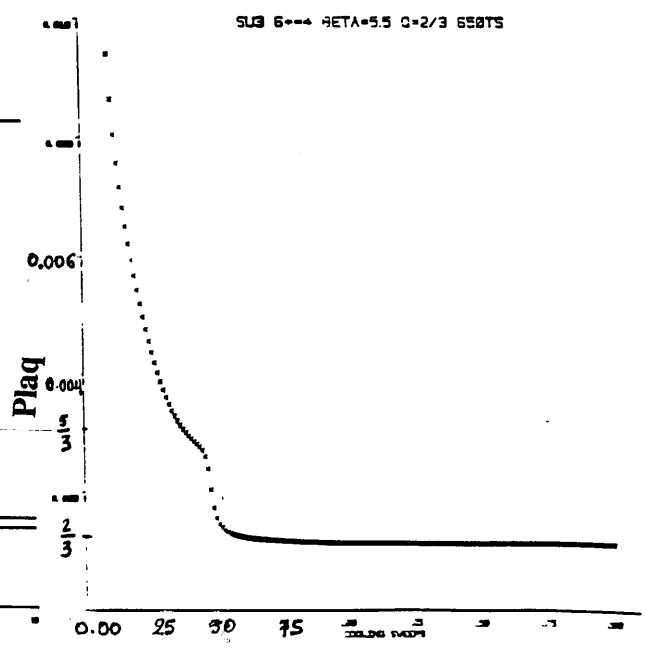


Fig. H1

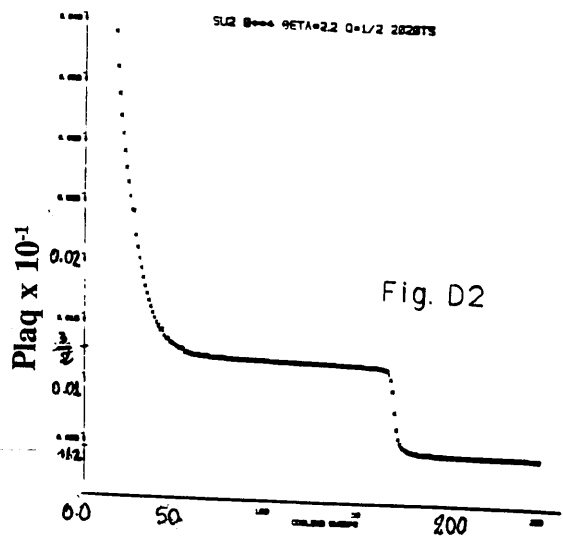


Fig. 4.3.4

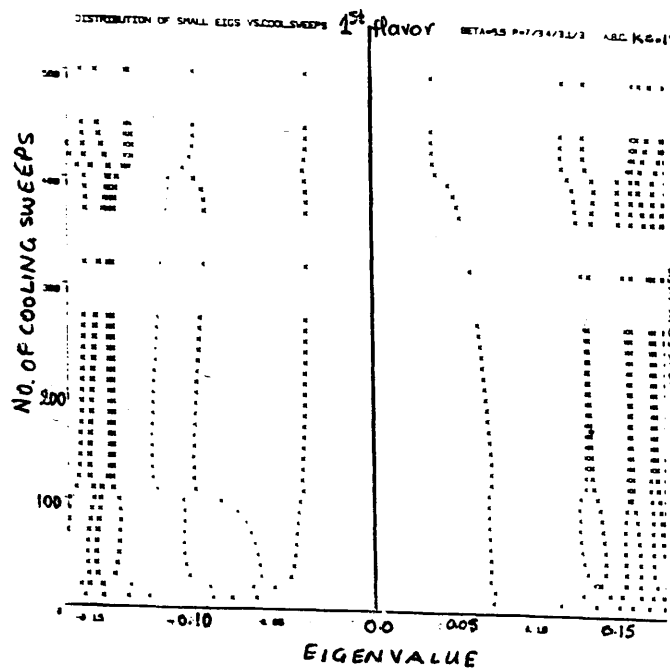


Fig. 4.3.5a

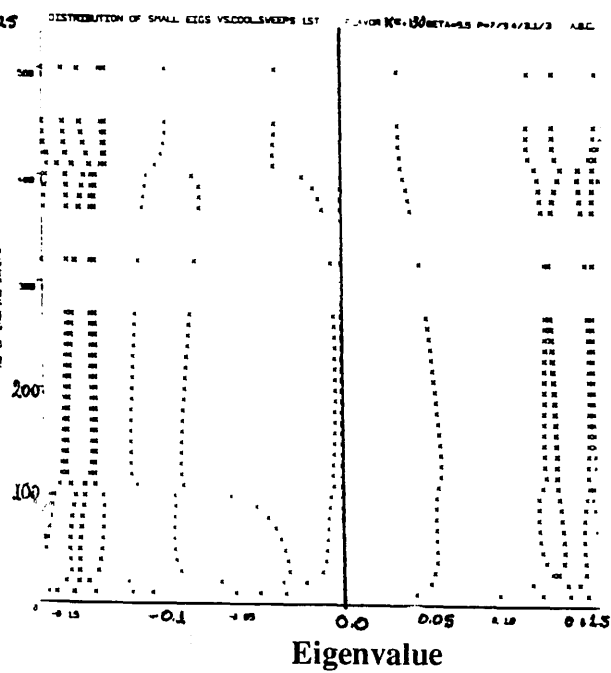


Fig. 4.3.5b

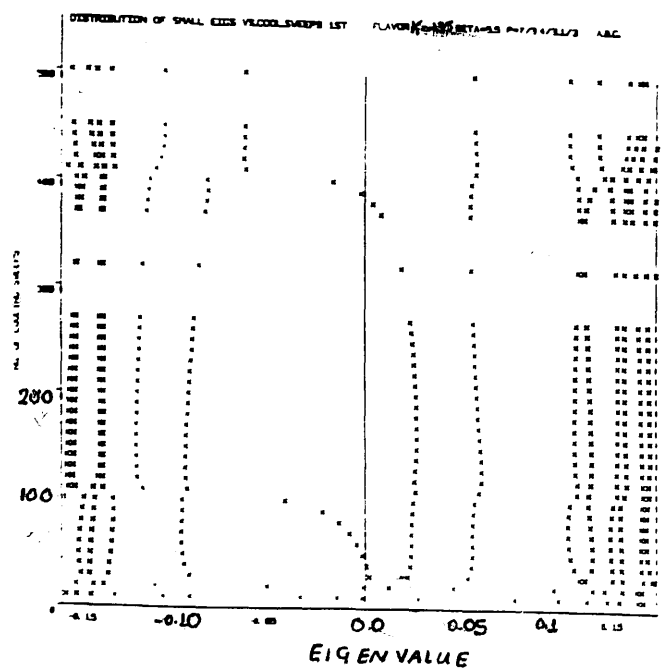


Fig. 4.3.5c

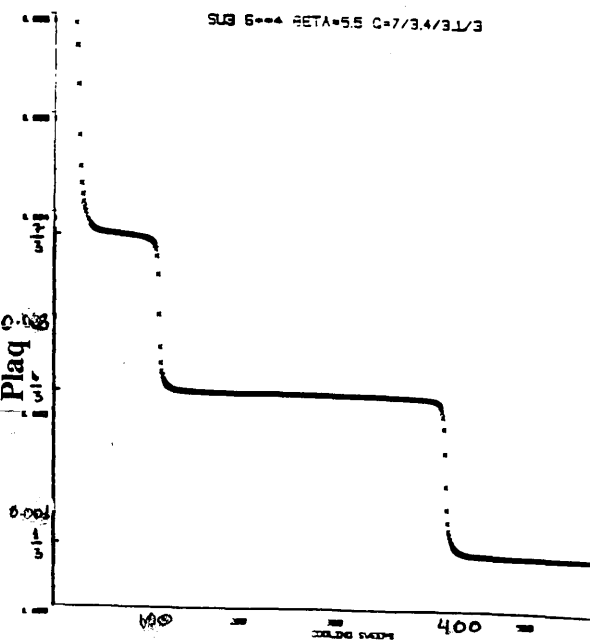


Fig. 11

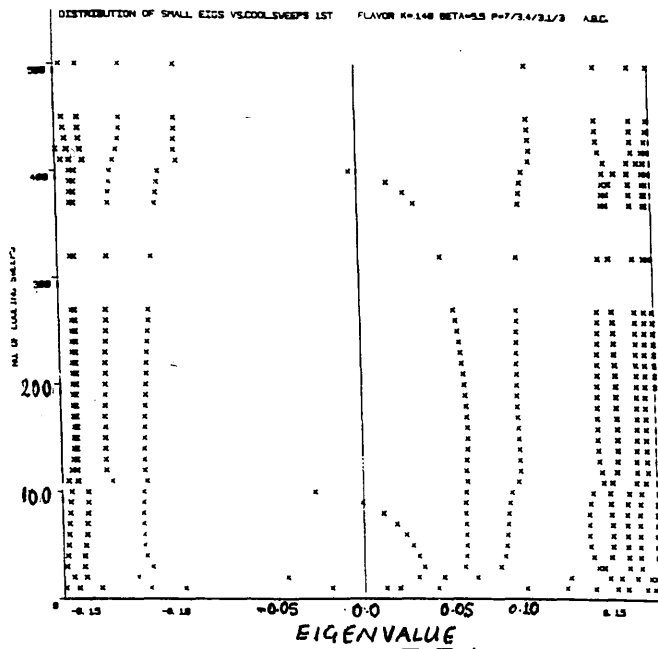


Fig. 4.3.5d

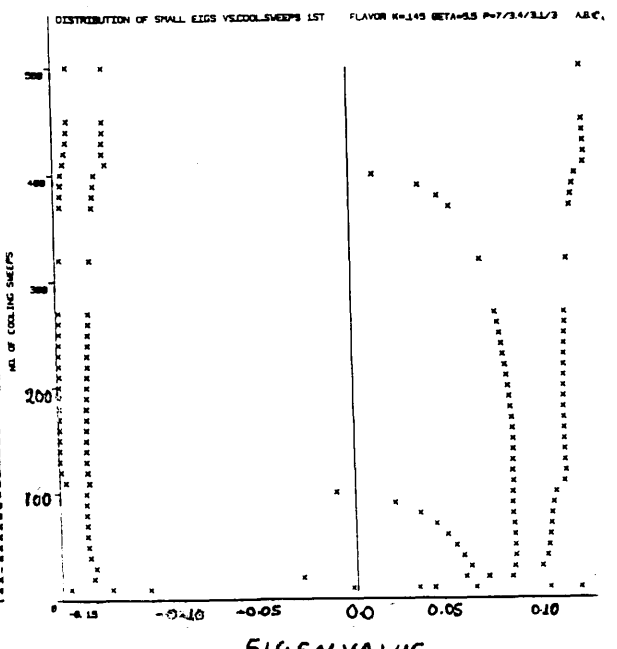


Fig. 4.3.5e

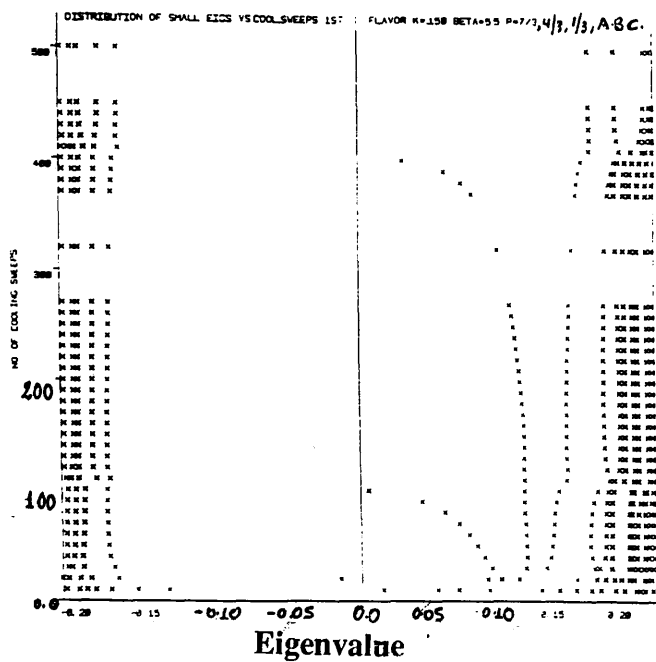


Fig. 4.3.5f

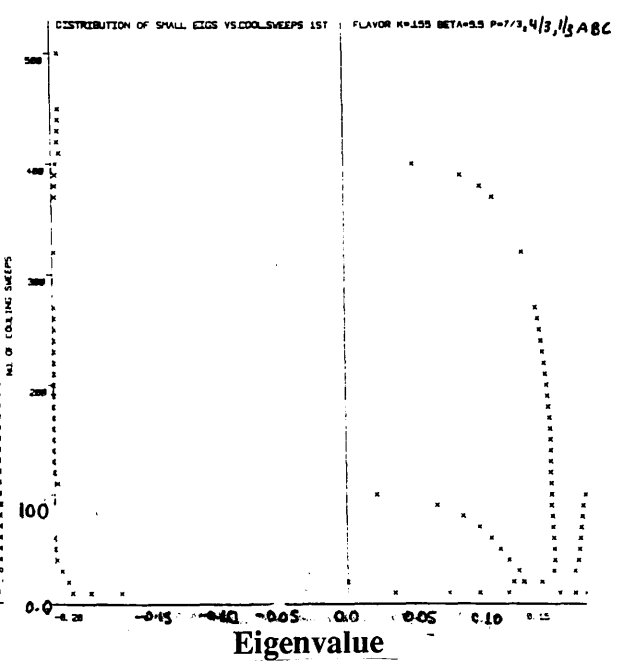


Fig. 4.3.5g

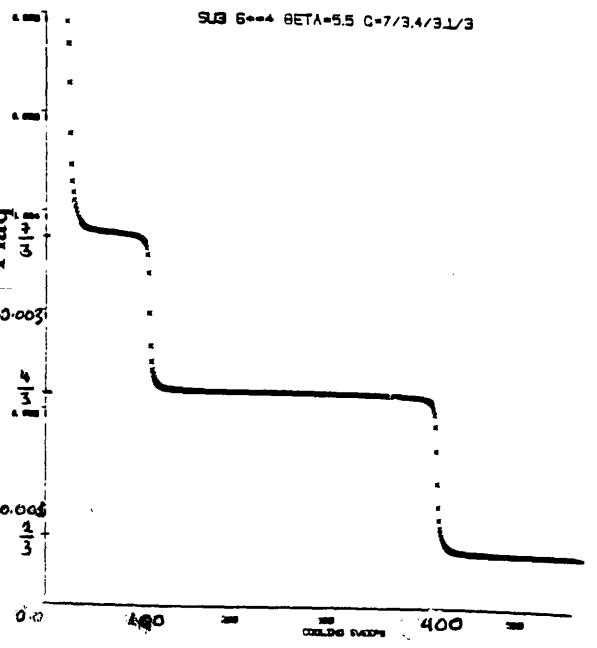
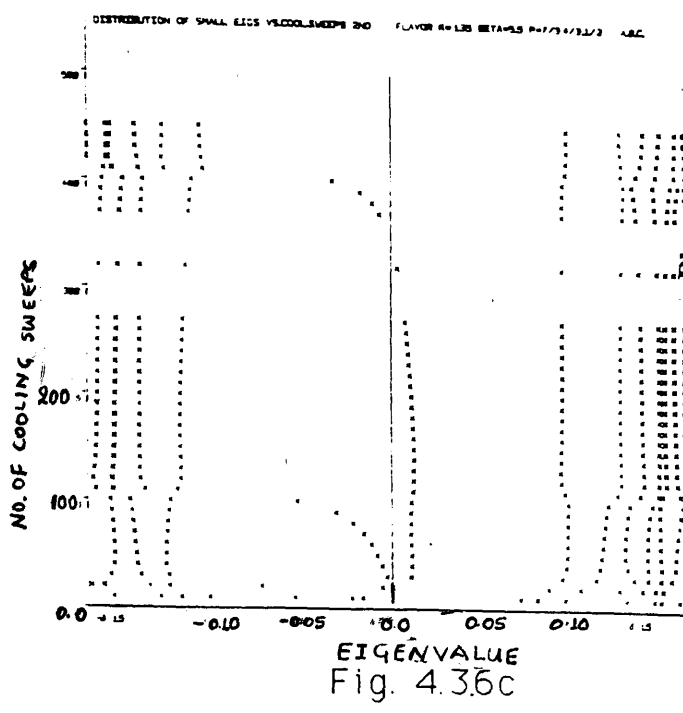
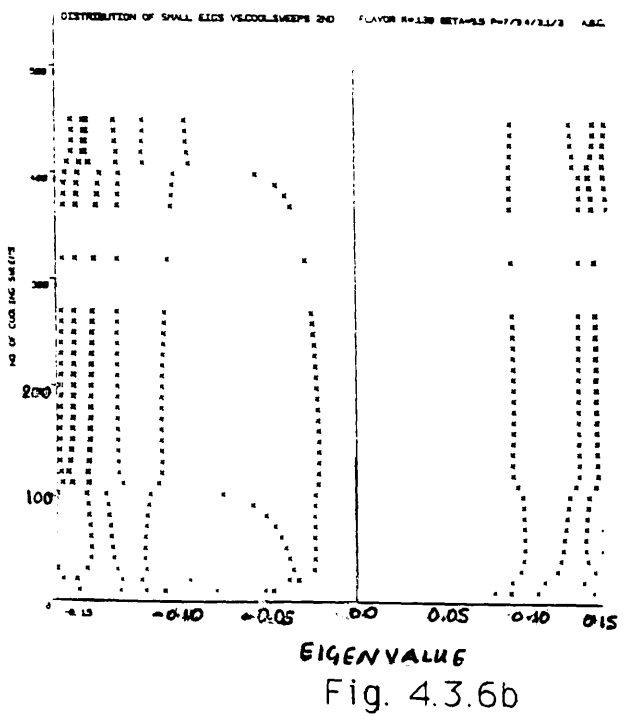
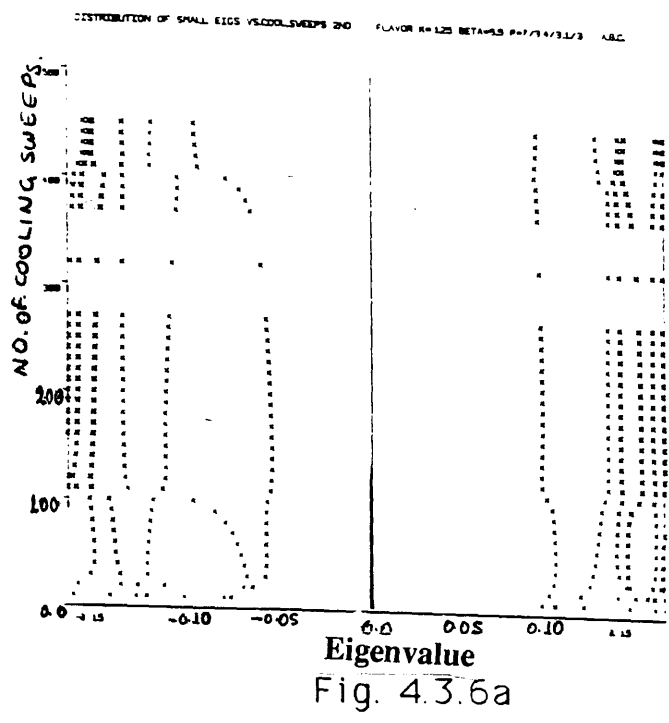


Fig. 11

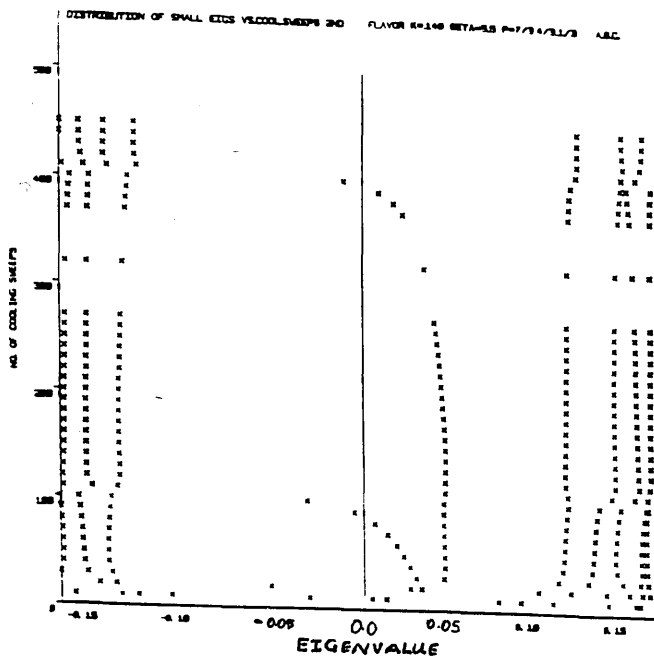


Fig. 4.3.6d

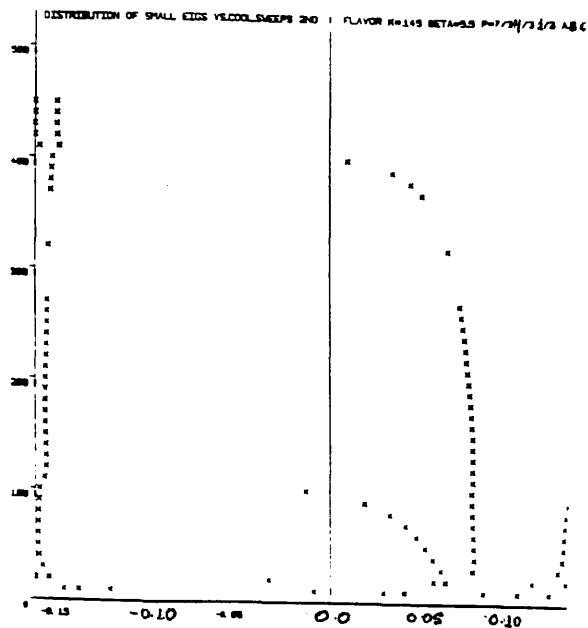


Fig. 4.3.6e

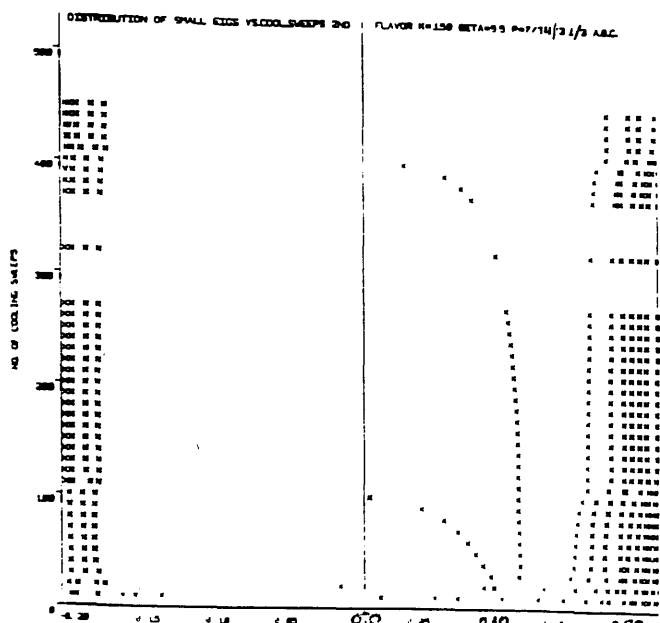


Fig. 4.3.6f

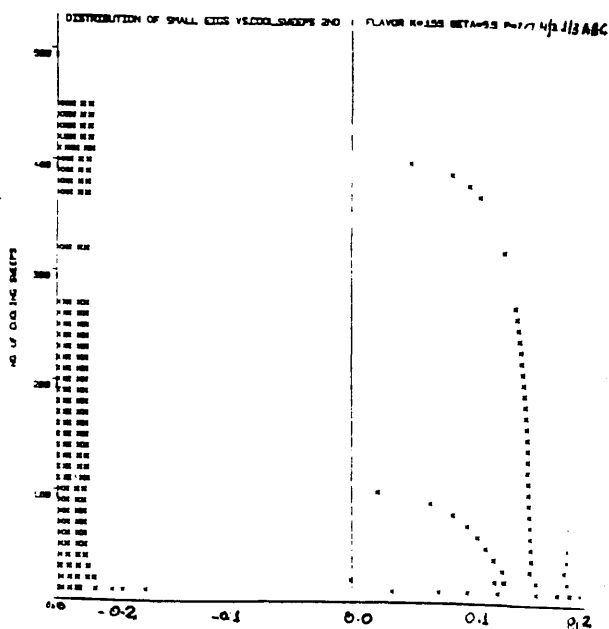


Fig. 4.3.6g

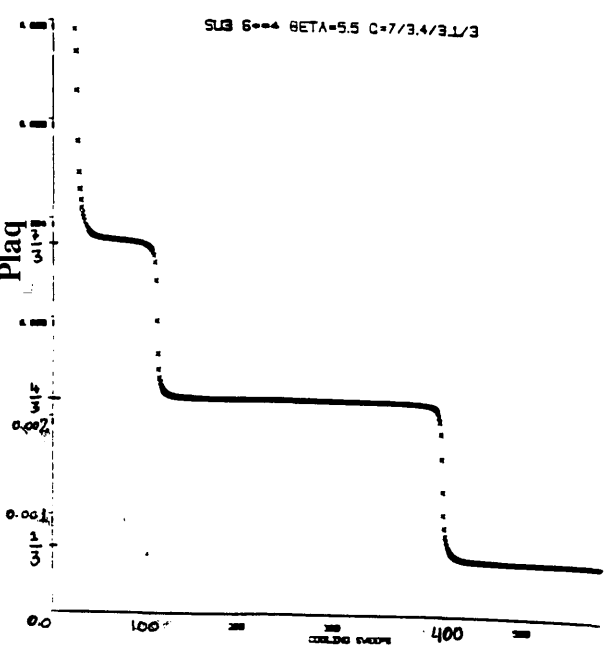
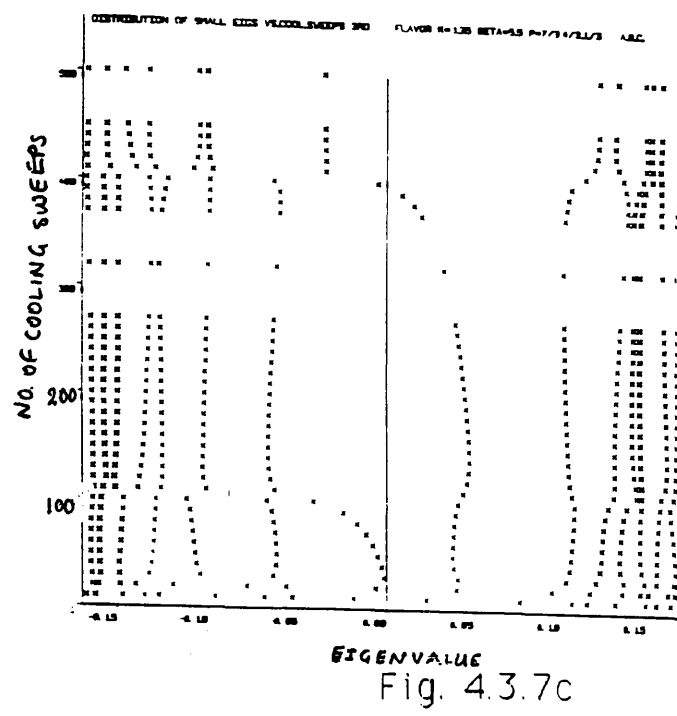
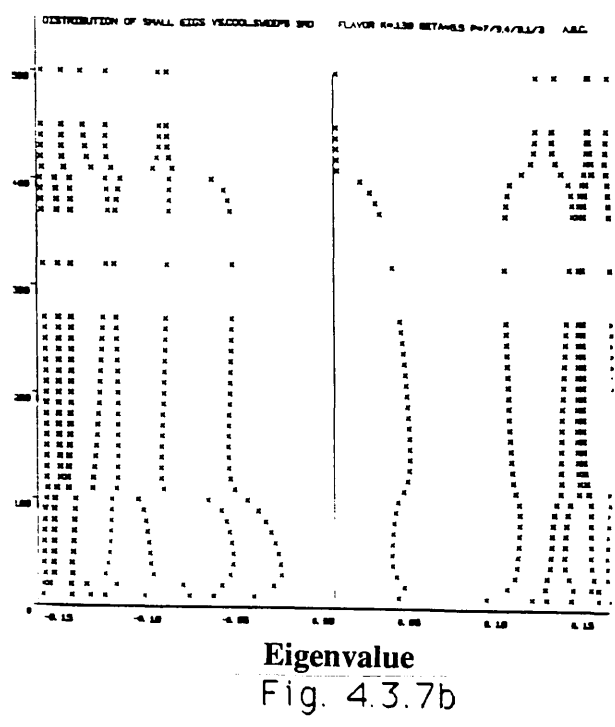
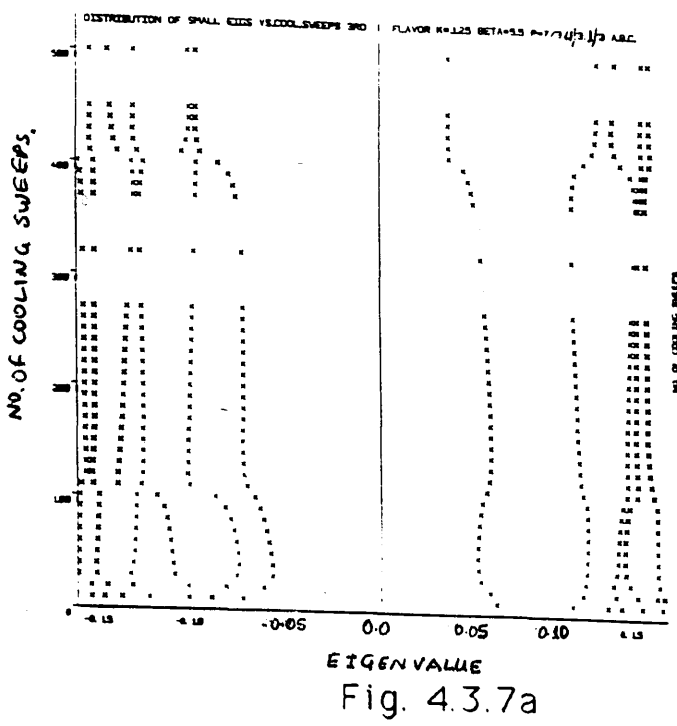
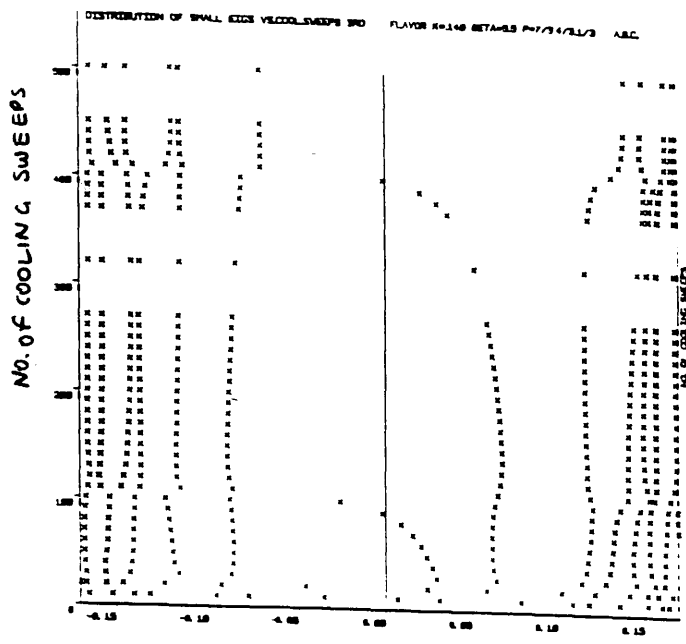
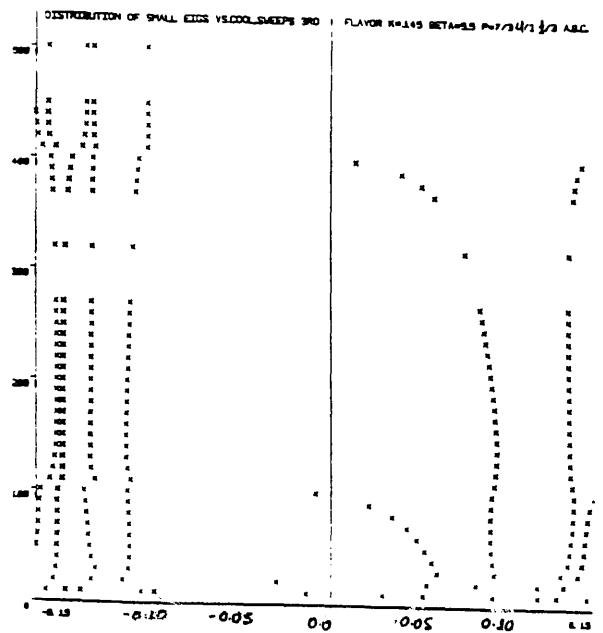


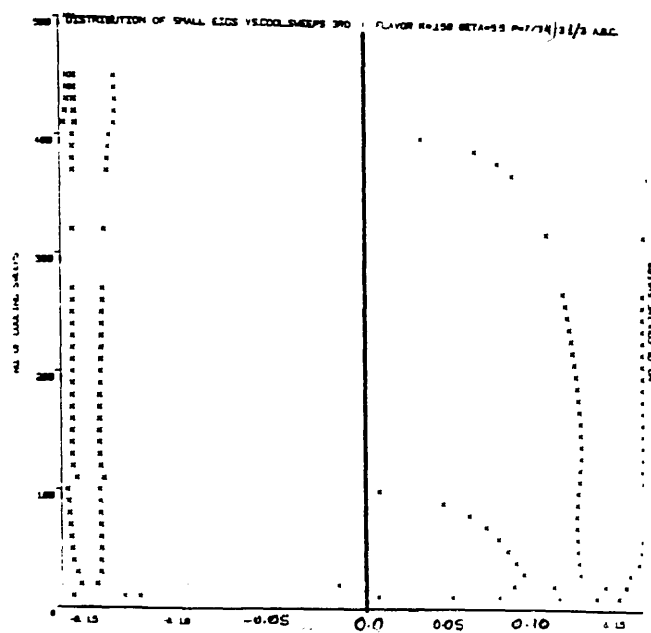
Fig. II



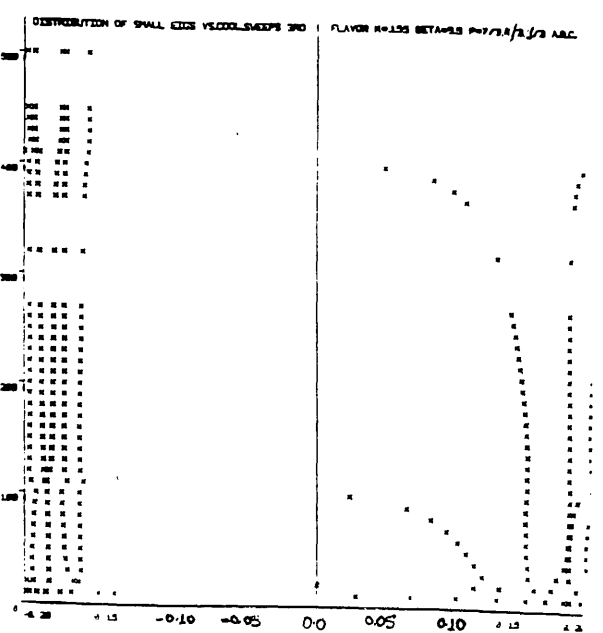
EIGENVALUE  
Fig. 4.3.7d



EIGENVALUE  
Fig. 4.3.7e



EIGENVALUE  
Fig. 4.3.7f



EIGENVALUE  
Fig. 4.3.7g



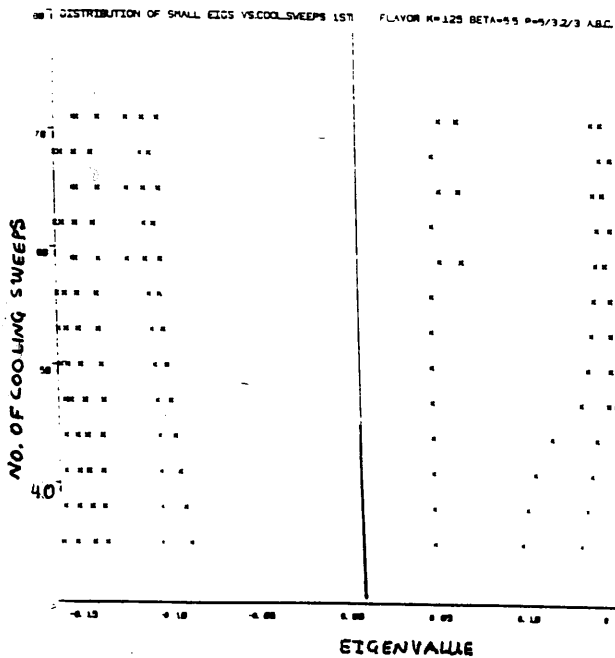


Fig. 4.3.8a

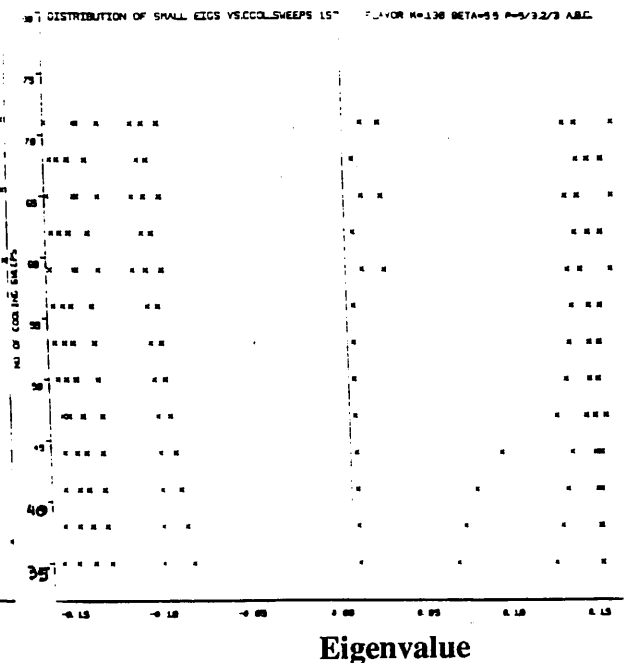


Fig. 4.3.8b

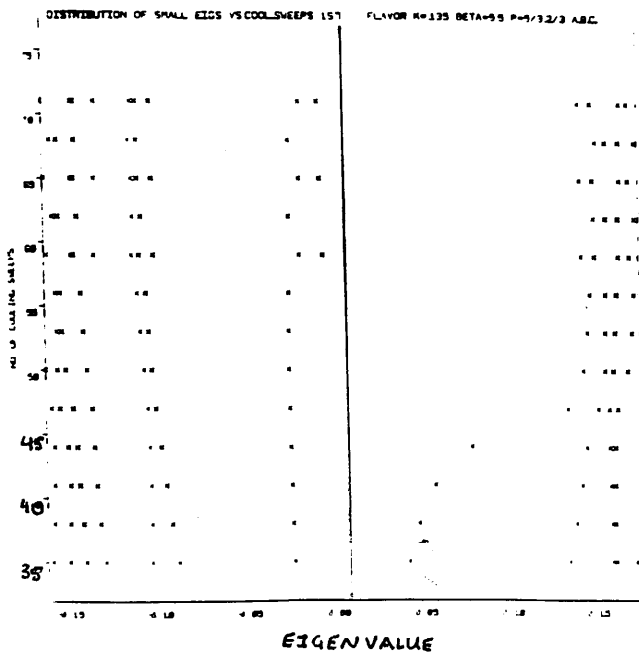


Fig. 4.3.8c

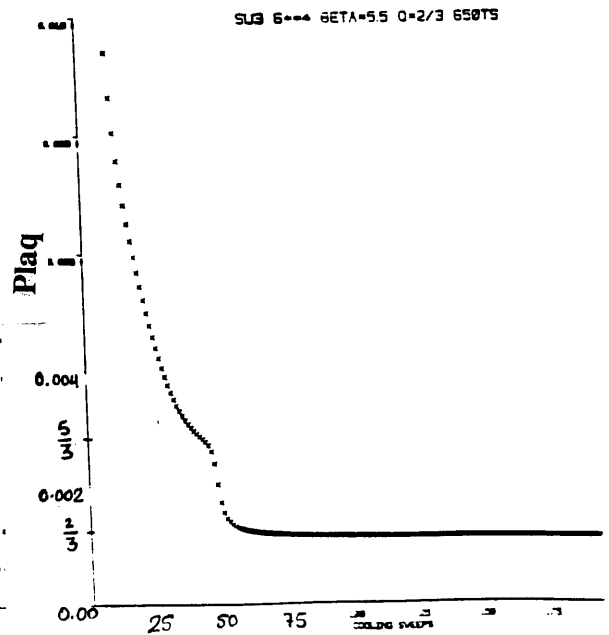
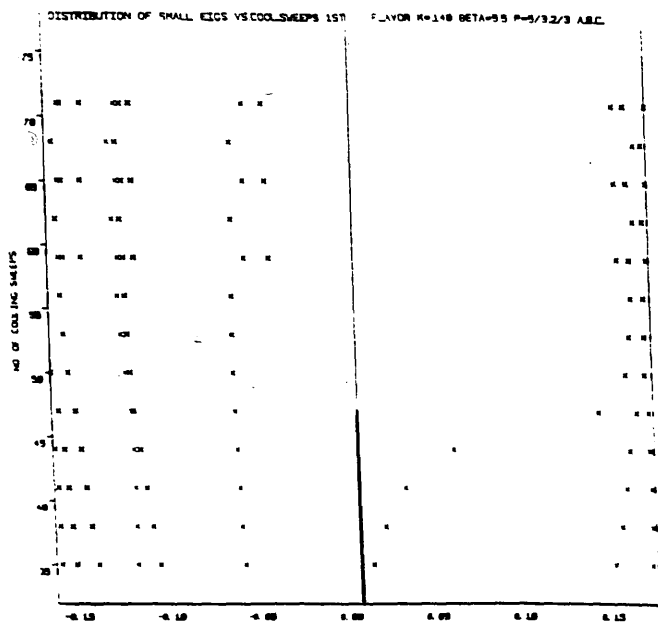
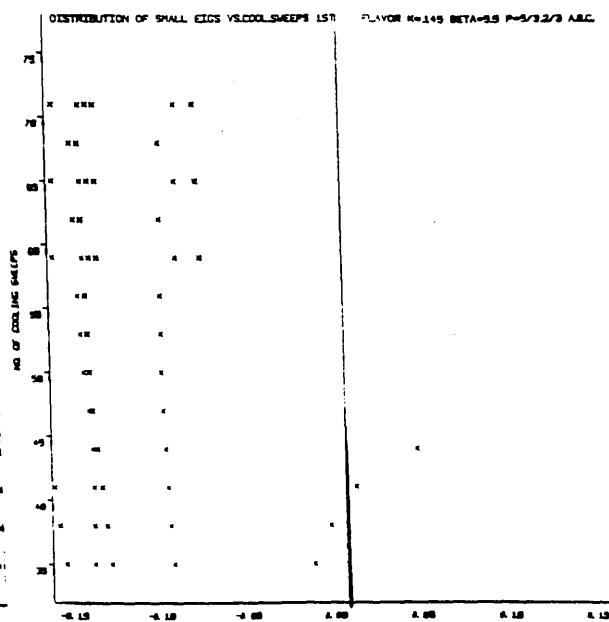


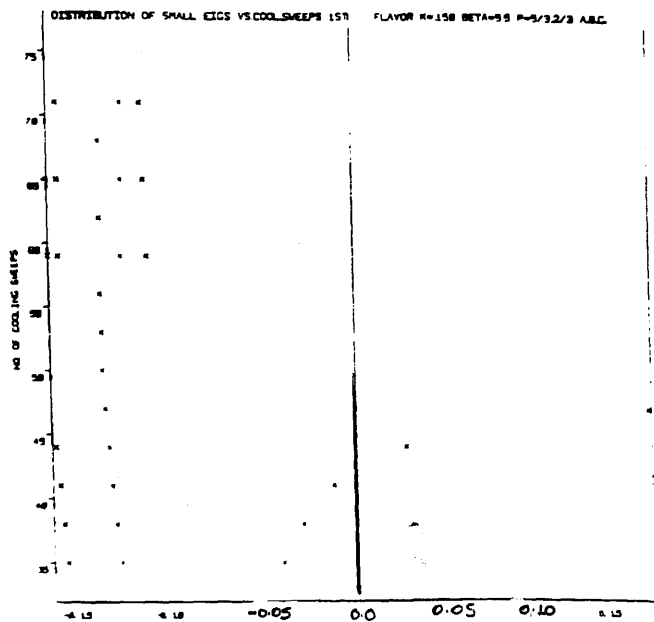
Fig. H1



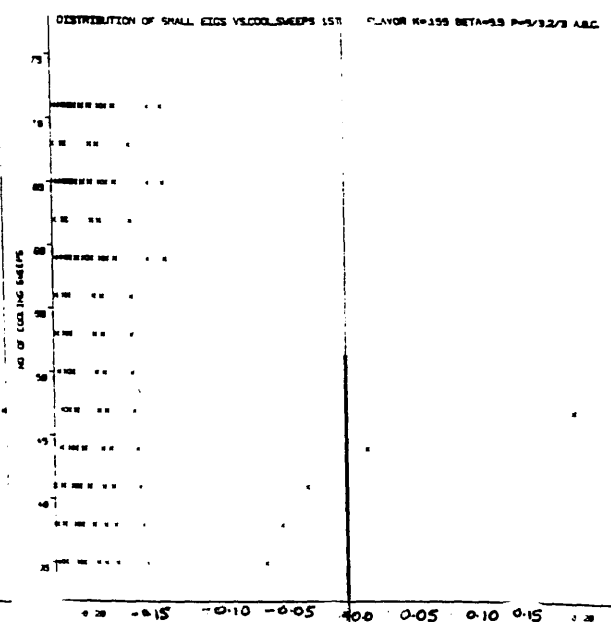
EIGENVALUE  
Fig. 4.3.8d



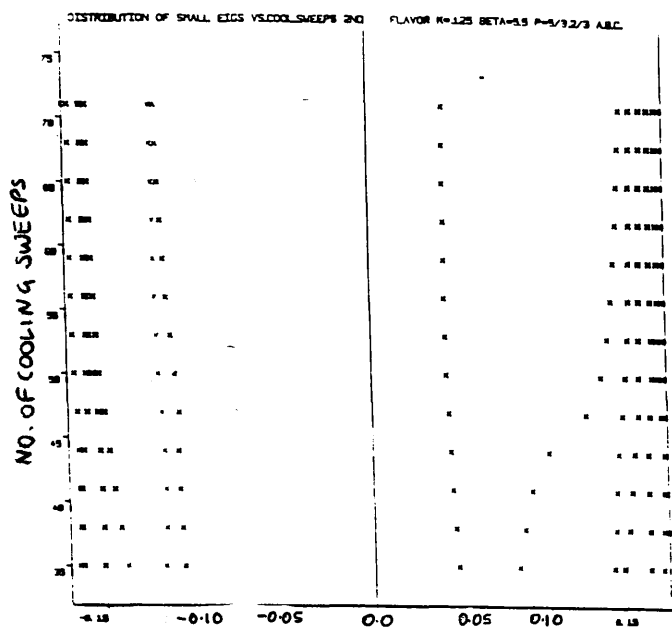
EIGENVALUE  
Fig. 4.3.8e



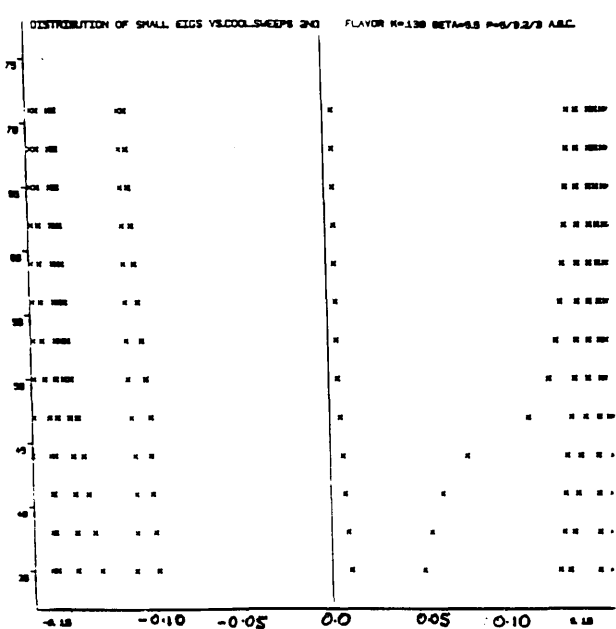
EIGENVALUE  
Fig. 4.3.8f



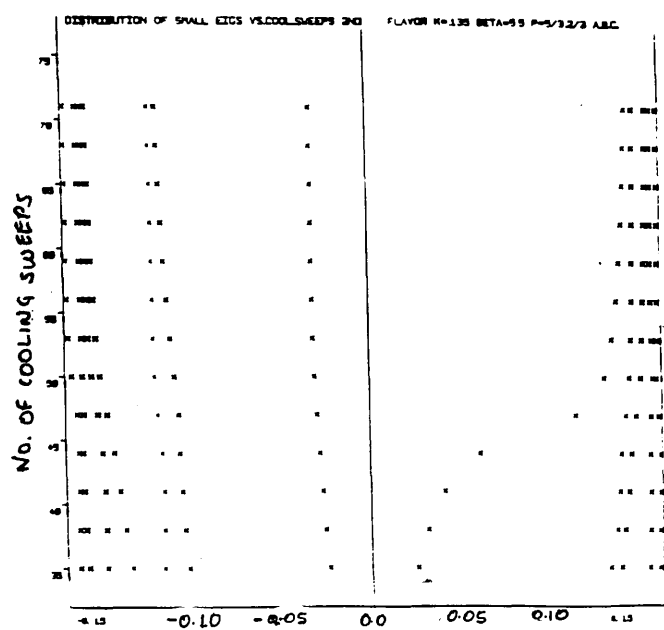
EIGENVALUE  
Fig. 4.3.8g



Eigenvalue  
Fig. 4.3.9a



Eigenvalue  
Fig. 4.3.9b



Eigenvalue  
Fig. 4.3.9c

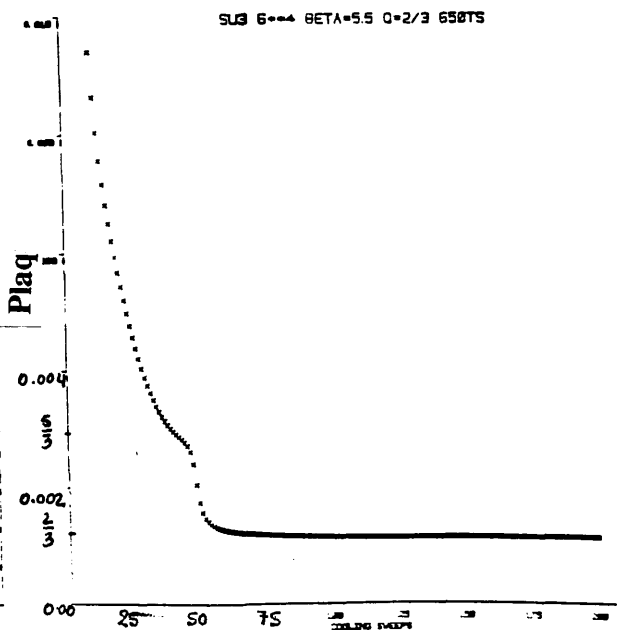


Fig. H1

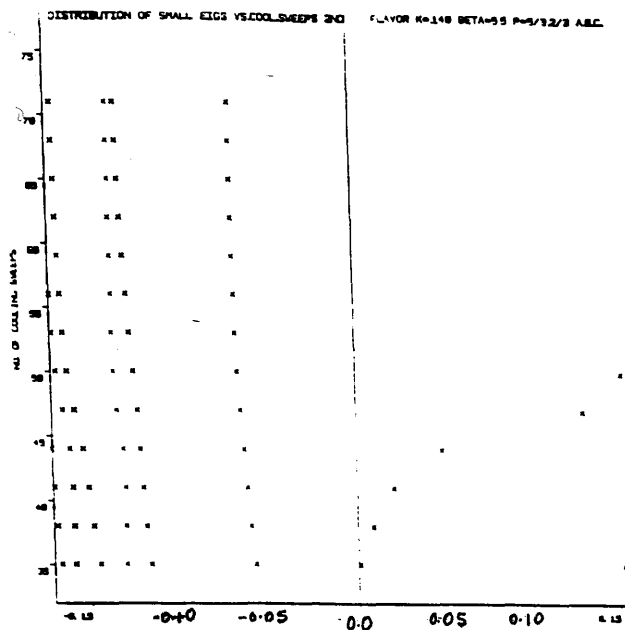


Fig. 4.3.9d

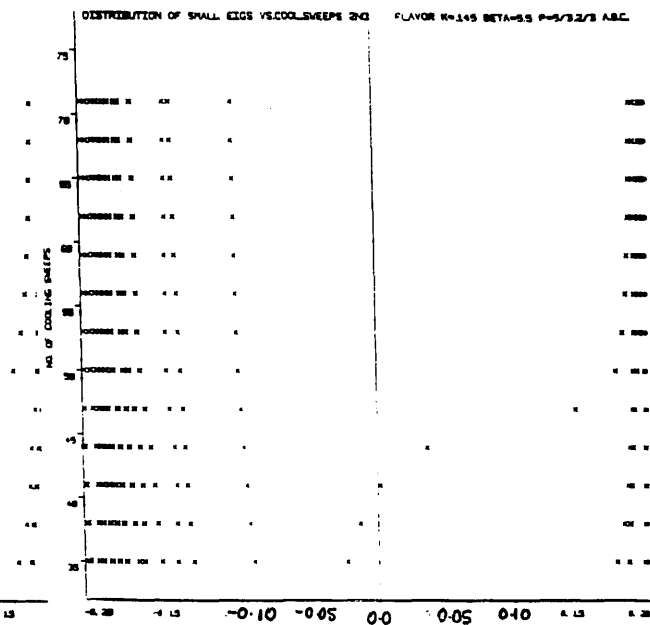


Fig. 4.3.9e

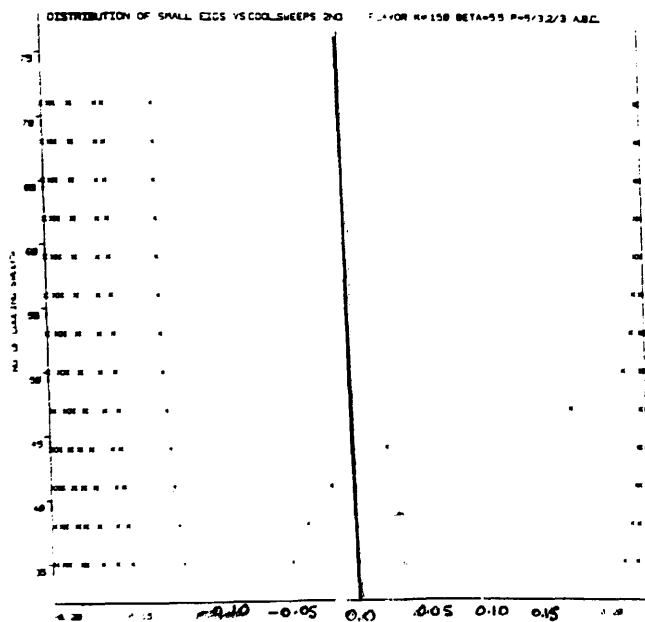


Fig. 4.3.9f

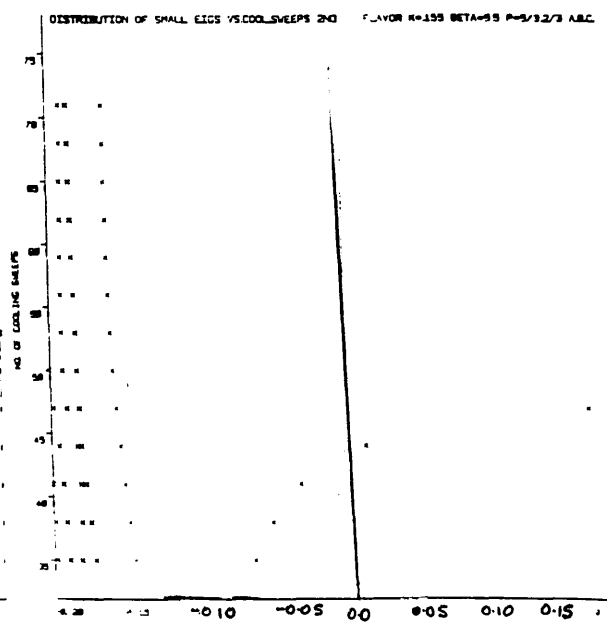
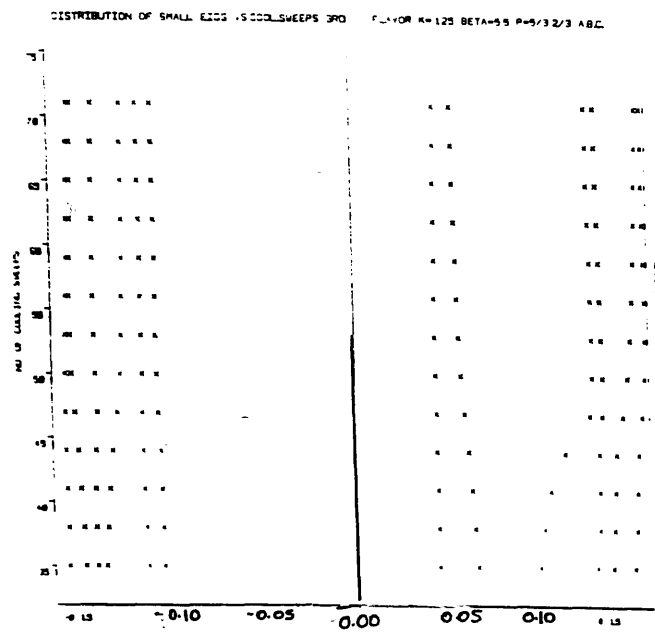
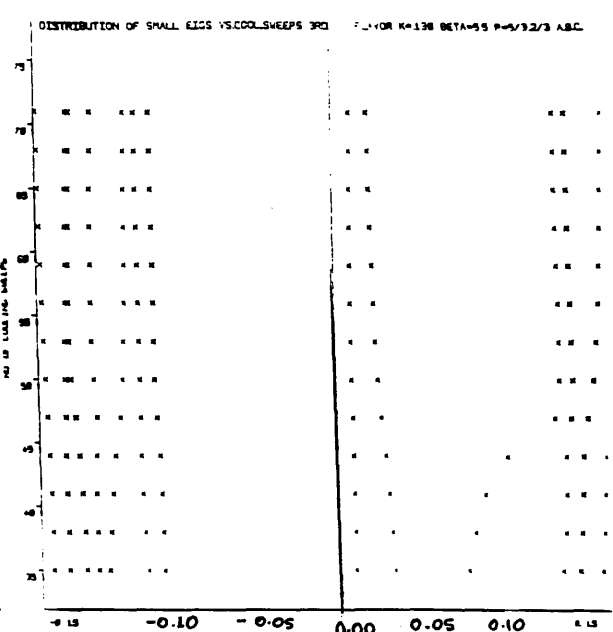


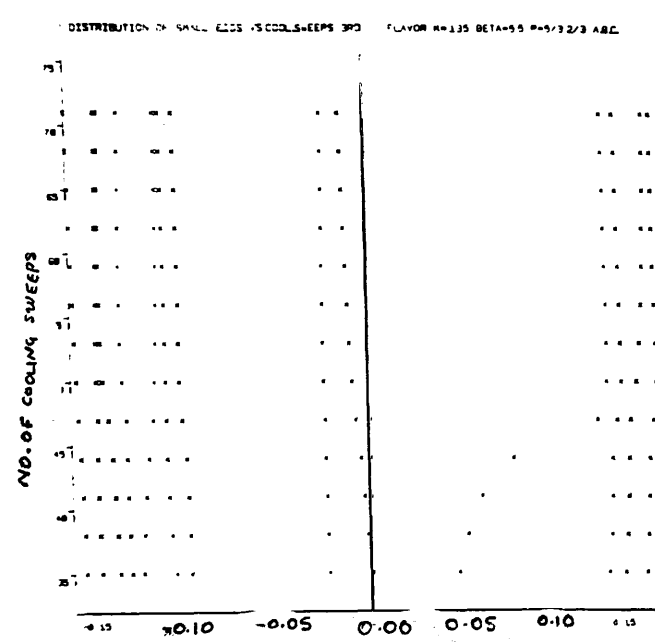
Fig. 4.3.9g



Eigenvalue  
Fig. 4.3.10a



EIGENVALUE  
Fig. 4.3.10b



EIGENVALUE  
Fig. 4.3.10c

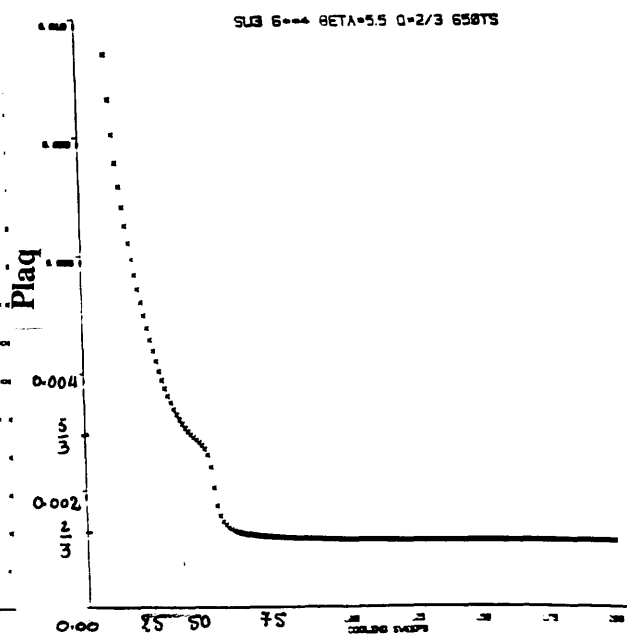


Fig. H1

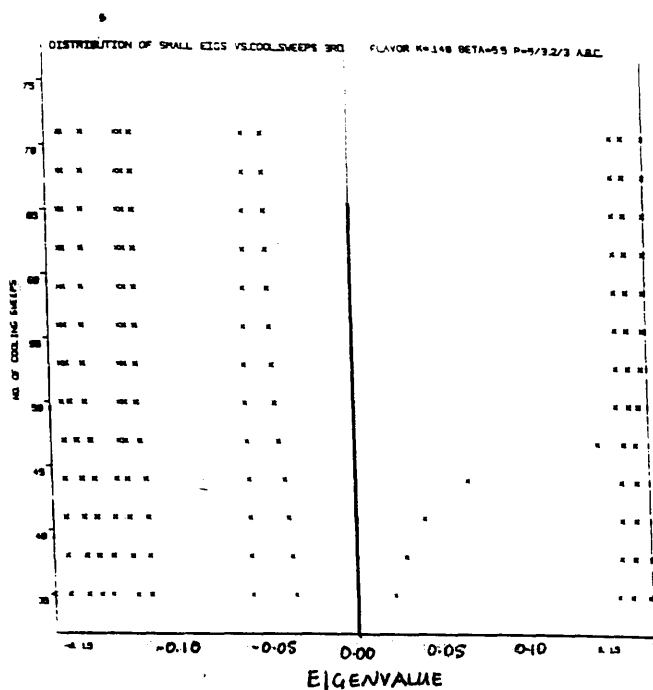


Fig. 4.3.10d

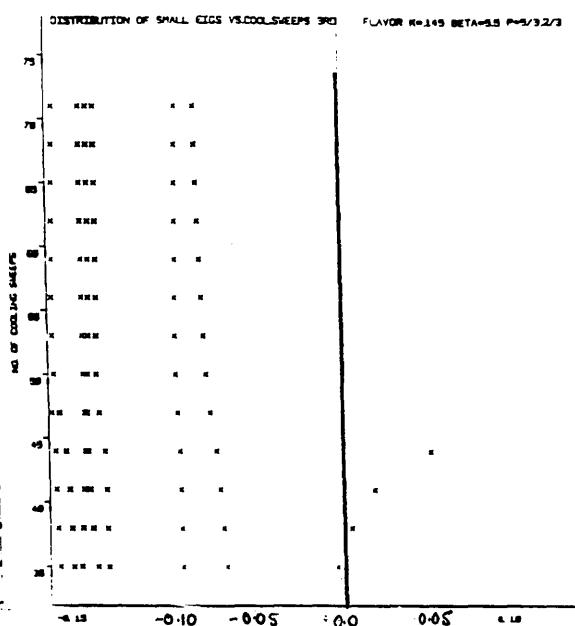


Fig. 4.3.10e

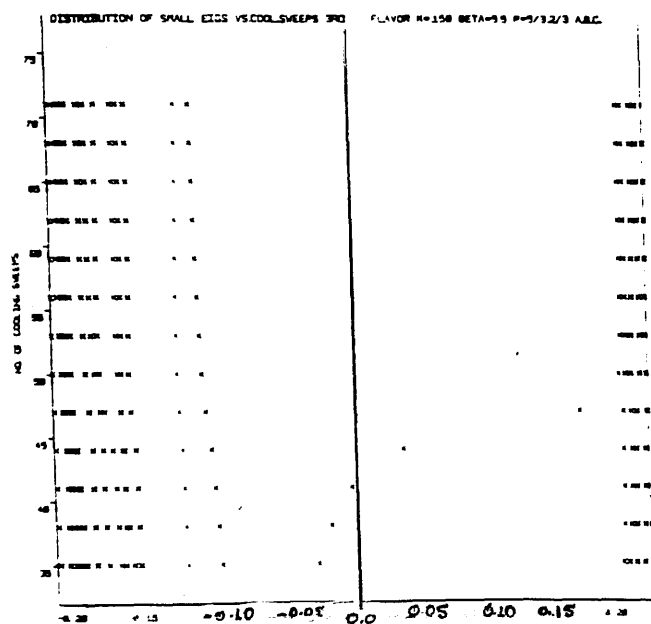


Fig. 4.3.10f

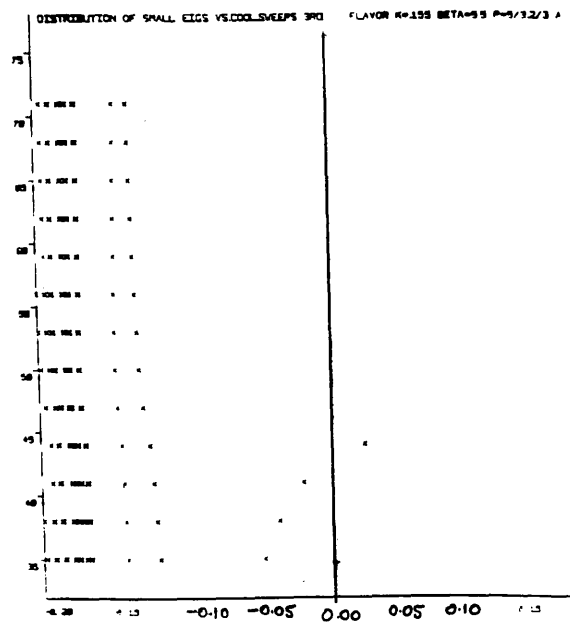
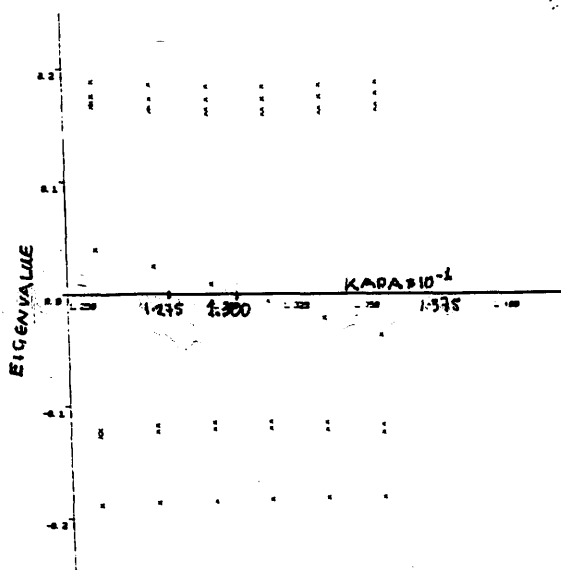
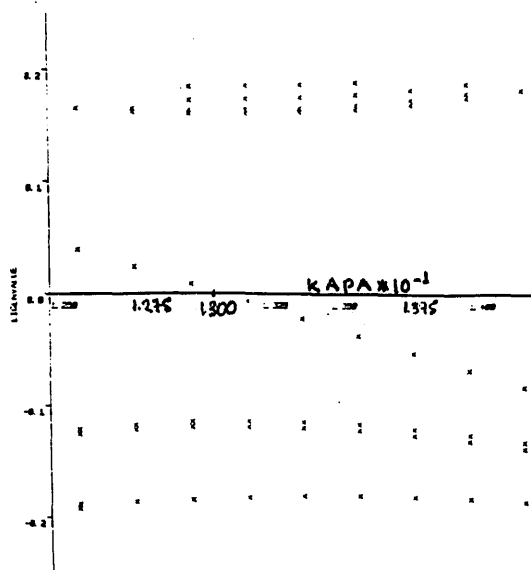


Fig. 4.3.10g



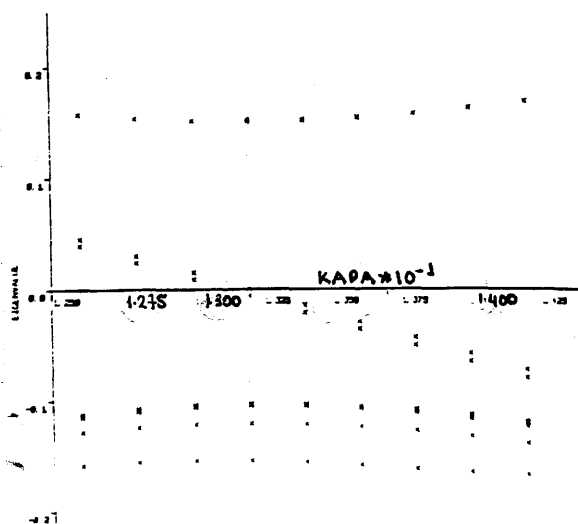
EXPLICIT CONF FOR P=2/3 1ST FLAVOR ABC

Fig. 4.3.11a



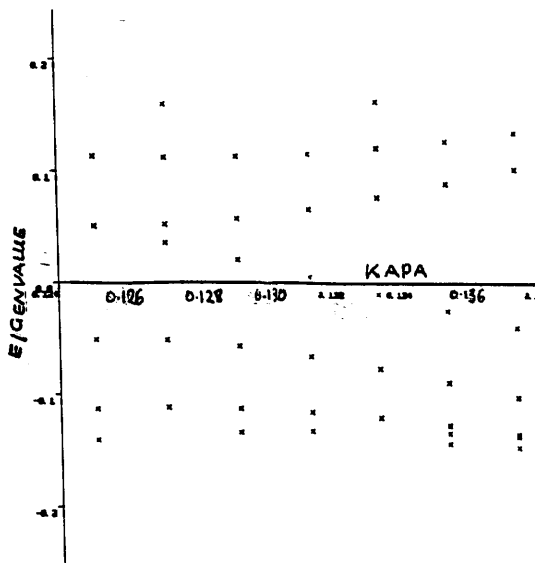
EXPLICIT CONF FOR P=2/3 2ND FLAVOR ABC

Fig. 4.3.11b



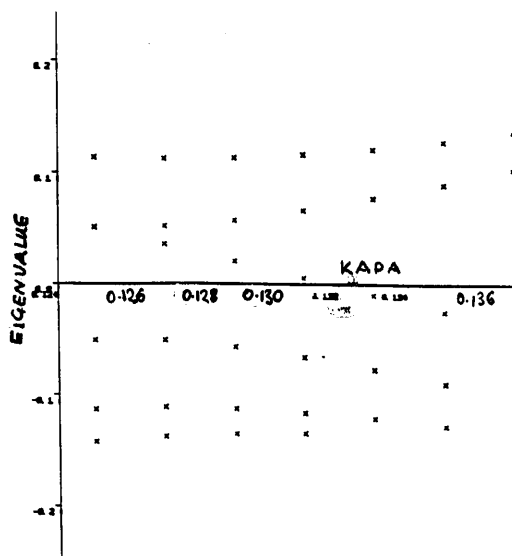
EXPLICIT CONF FOR P=2/3 3RD FLAVOR ABC

Fig. 4.3.11c



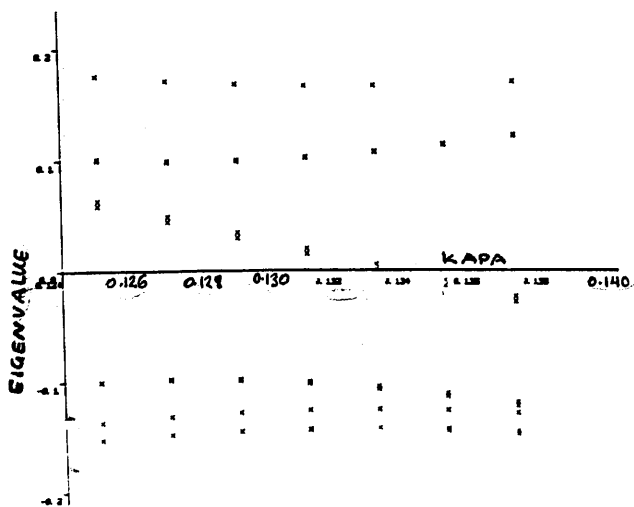
EXPLICIT CONF FOR P=2/3 1ST FLAVOR PBC

Fig. 4.3.12a



EXPLICIT CONF FOR P=2/3 2ND FLAVOR PBC

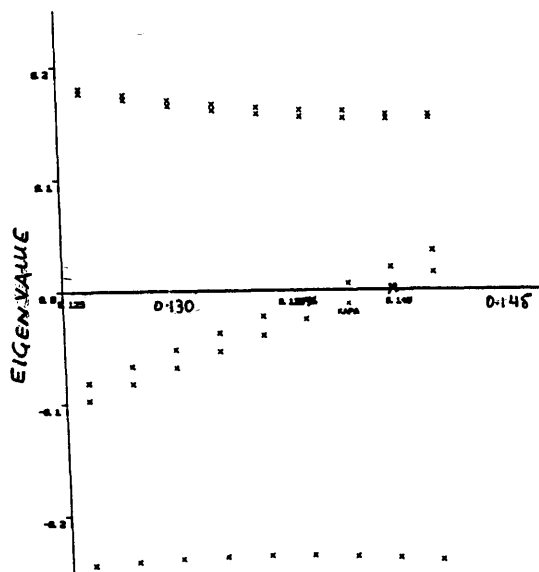
Fig. 4.3.12b



EXPLICIT CONF FOR P=2/3 3RD FLAVOR PBC

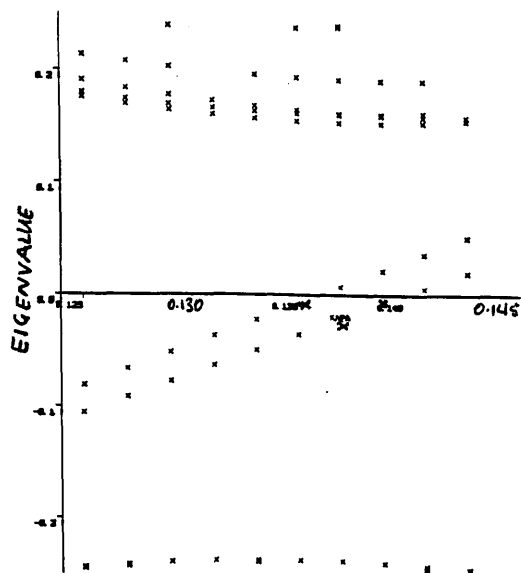
Fig. 4.3.12c





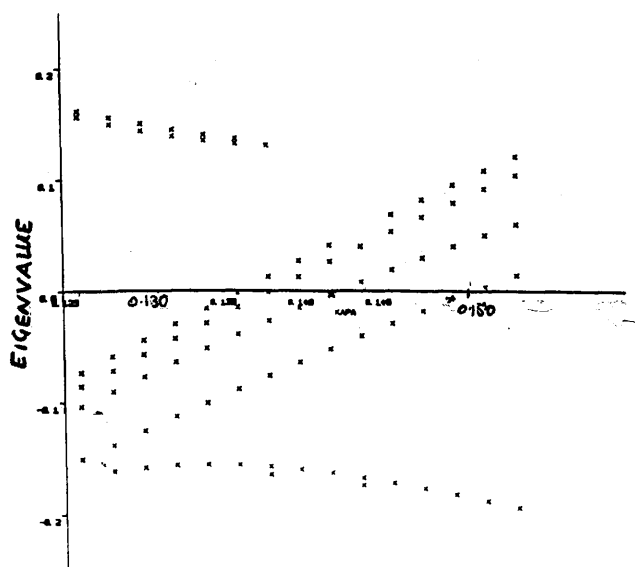
EXPLICIT CONF FOR  $P=4/3$  1ST FLAVOR A.B.C

Fig. 4.3.13a



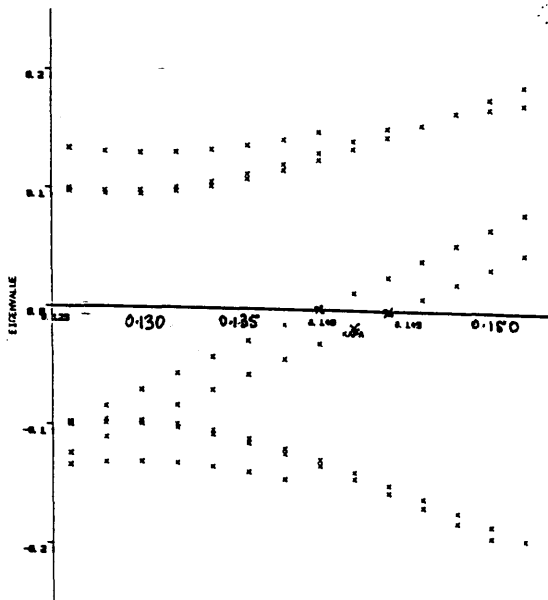
EXPLICIT CONF FOR  $P=4/3$  2ND FLAVOR A.B.C

Fig. 4.3.13b



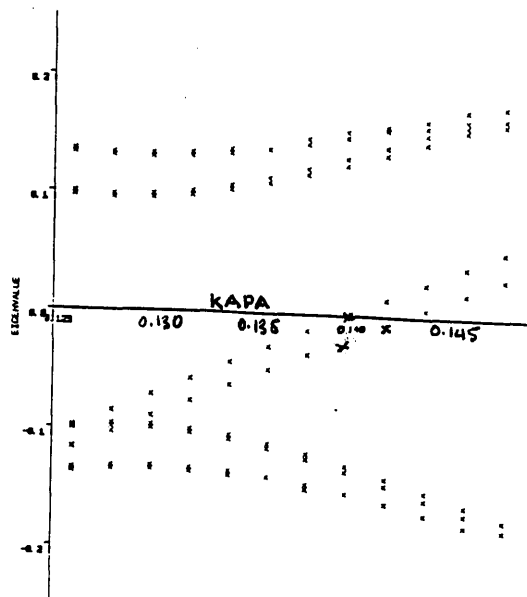
EXPLICIT CONF FOR  $P=4/3$  3RD FLAVOR A.B.C

Fig. 4.3.13c



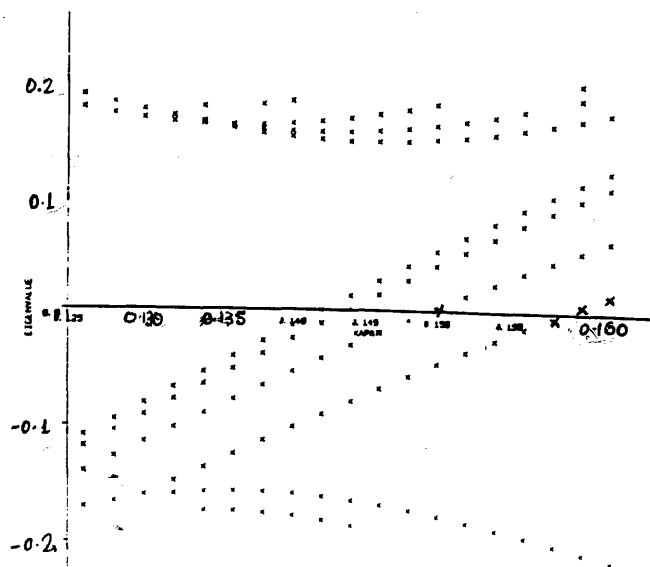
EXPLICIT CONF FOR P=4/3 1ST FLAVOR PBC

Fig. 4.3.14a



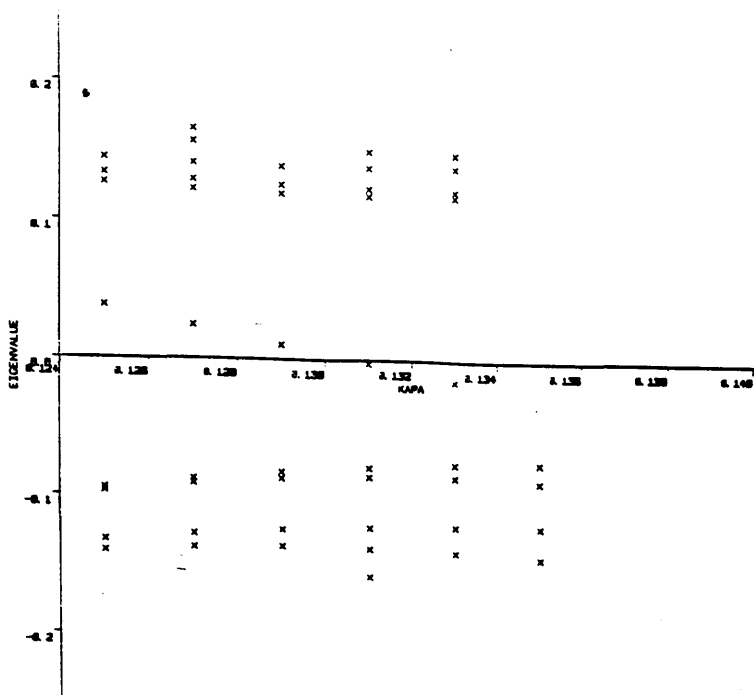
EXPLICIT CONF FOR P=4/3 2ND FLAVOR PBC

Fig. 4.3.14b



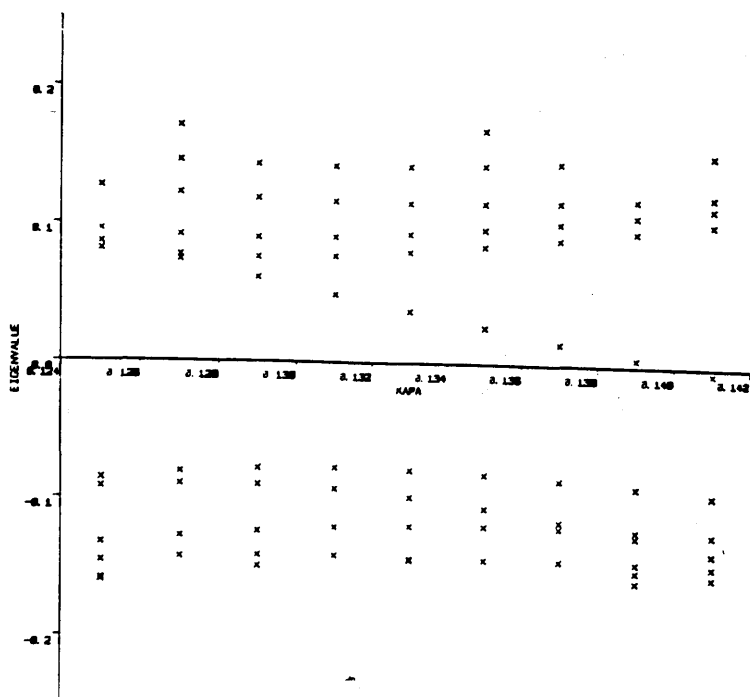
EXPLICIT CONF FOR P=4/3 3RD FLAVOR PBC

Fig. 4.3.14c



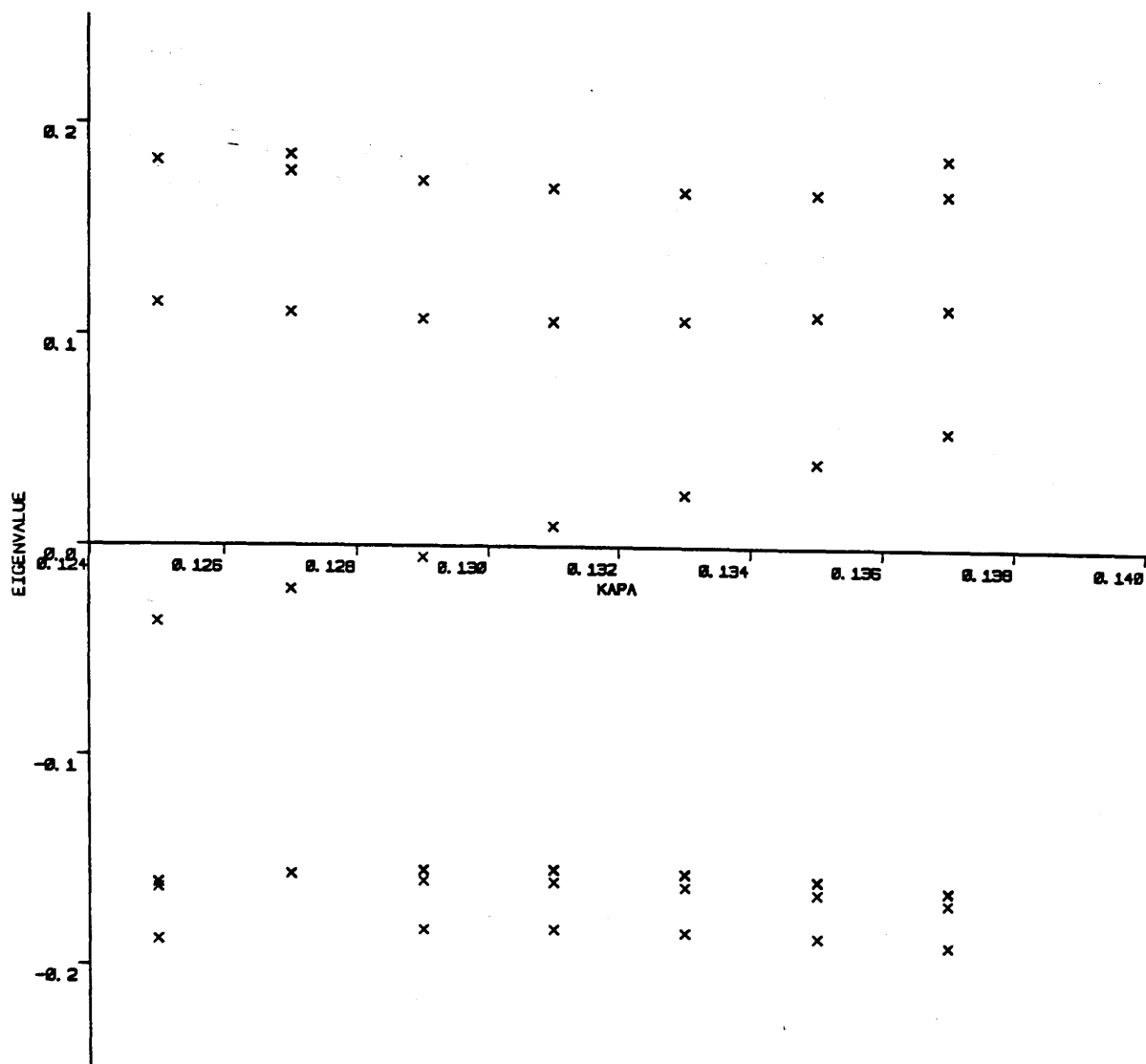
EXPLICIT CONF FOR P=2/3 COLOR TWIST A.B.C

Fig. 4.3.15a



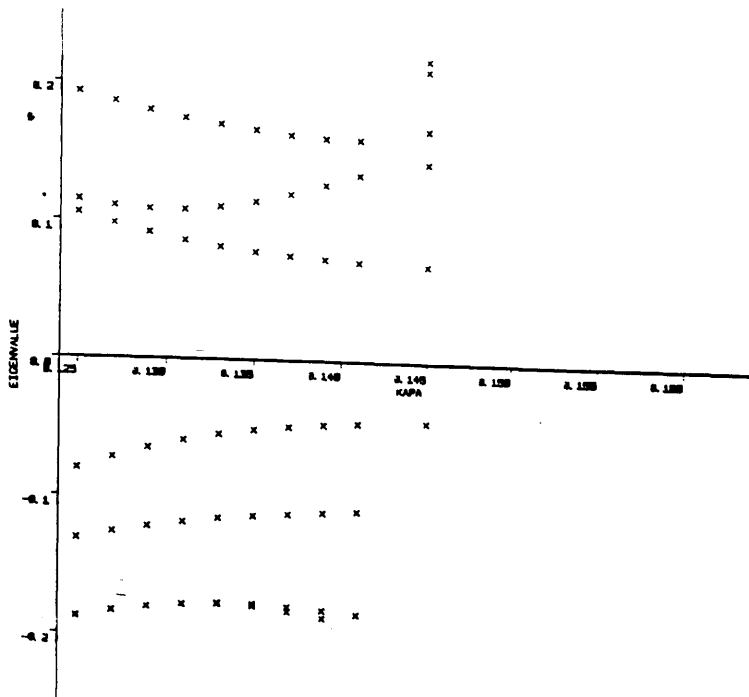
EXPLICIT CONF FOR P=2/3 COLOR TWIST P.B.C

Fig. 4.3.15b



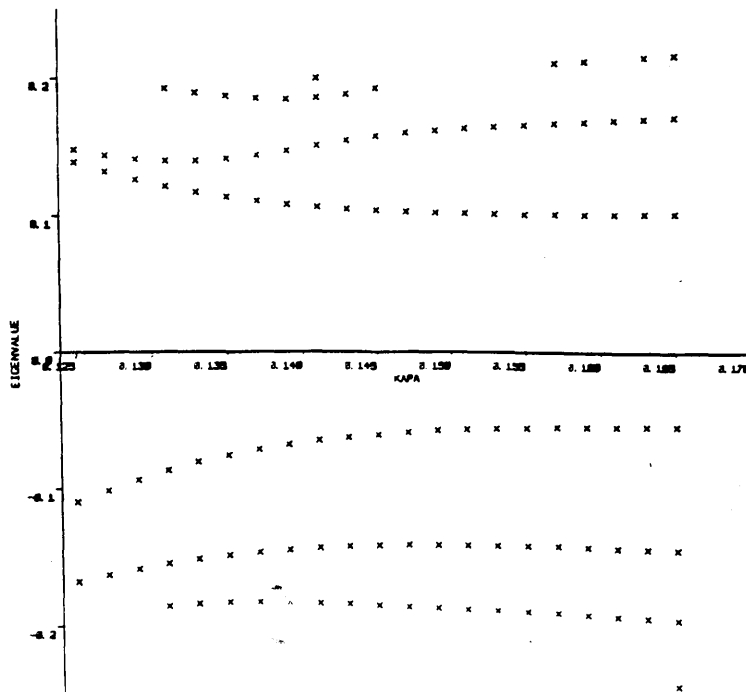
EXPLICIT CONF FOR P=1/2 1ST FLAVOR A.B.C

Fig. 4.3.16



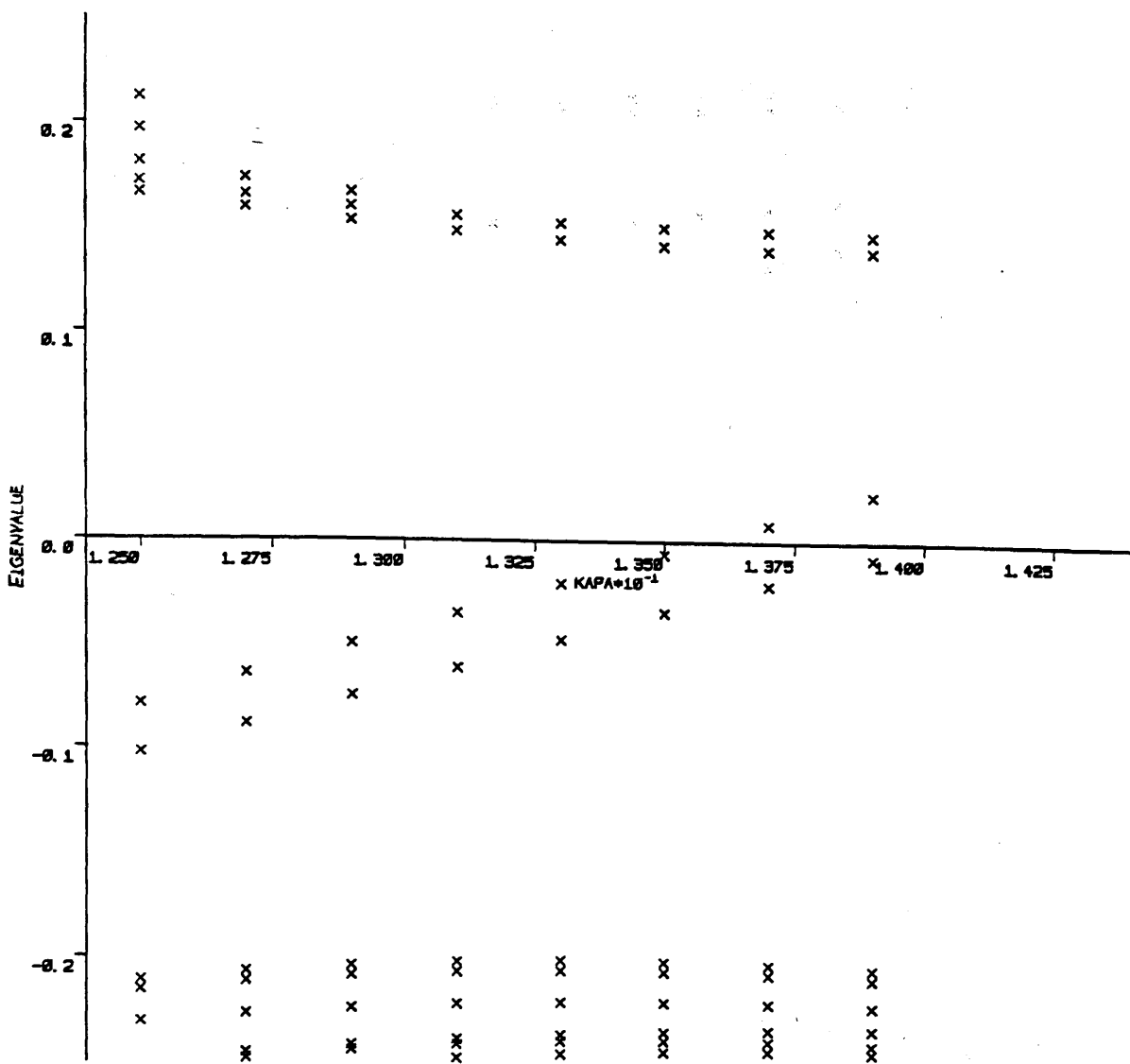
EXPLICIT CONF FOR P=1/2 COLOR TWIST A.B.C

Fig. 4.3.17a



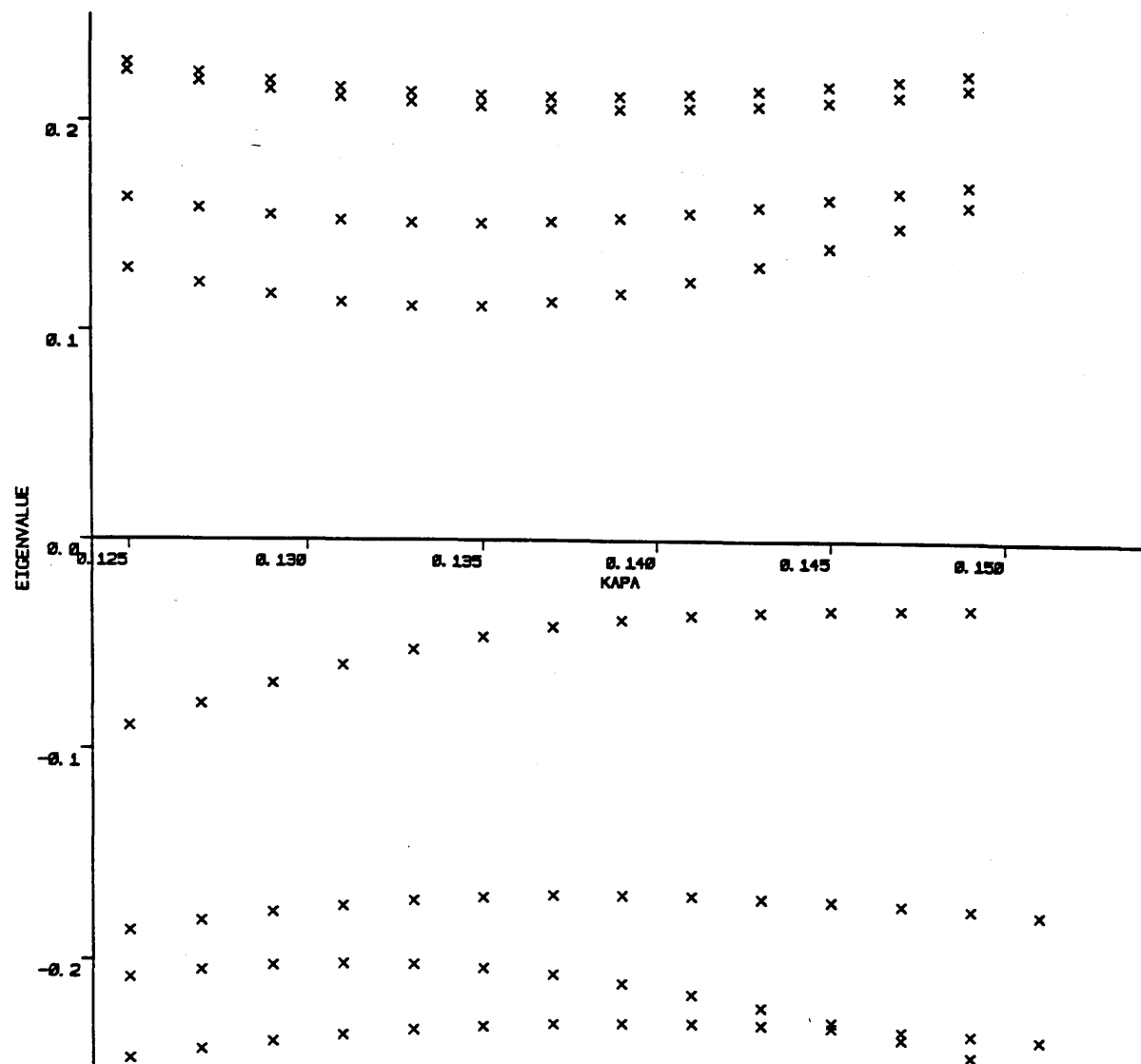
EXPLICIT CONF FOR P=1/2 COLOR TWIST P.B.C

Fig. 4.3.17b



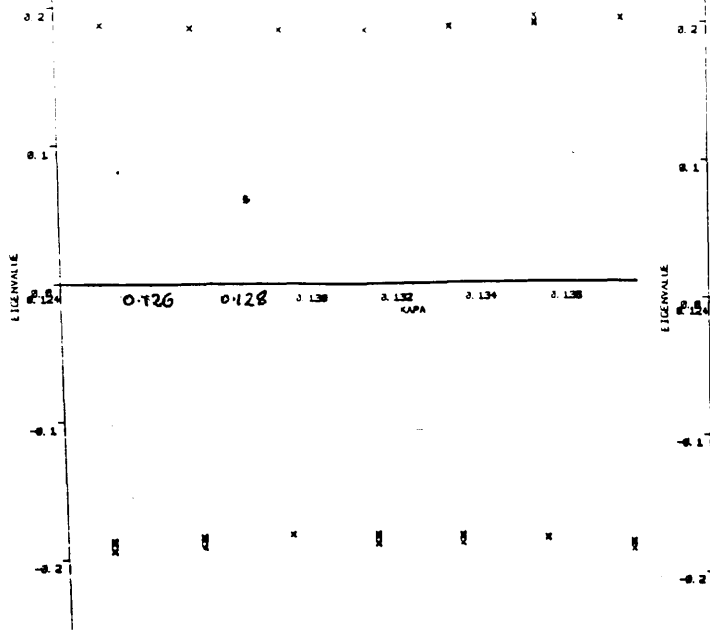
EXPLICIT CONF FOR P=1 1ST FLAVOR A.B.C

Fig. 4.3.18



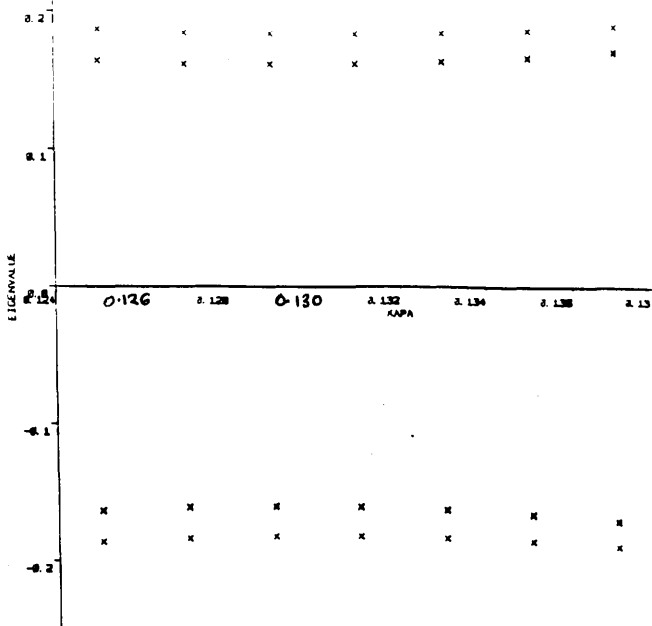
EXPLICIT CONF FOR P=1 COLOR TWIST A.B.C

Fig. 4.3.19



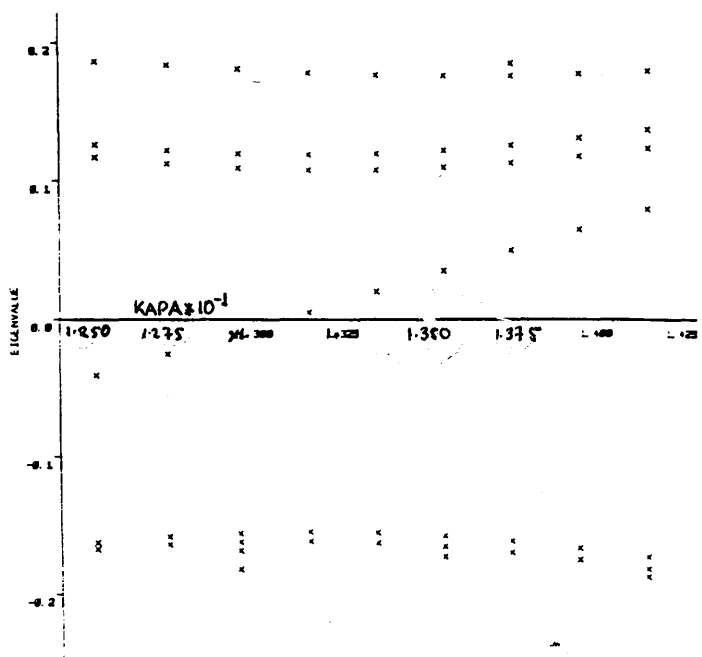
EXPLICIT CONF FOR P=1/2 SU(2)XSU(4) 1ST FLAVOR A.B.C.

Fig. 4.3.20a



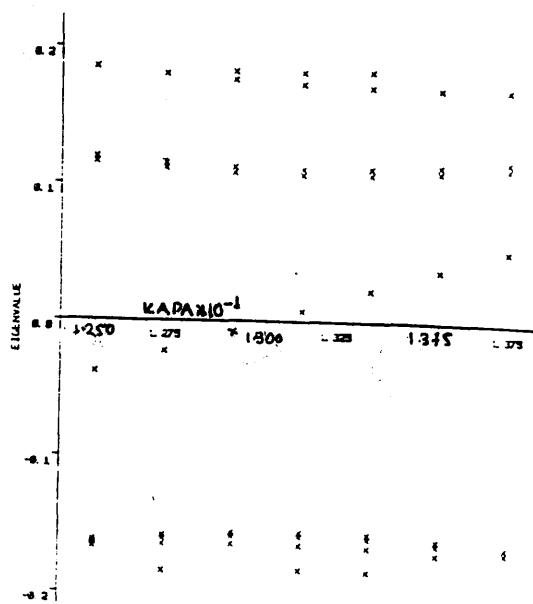
EXPLICIT CONF FOR P=1/2 SU(2)XSU(4) 2ND FLAVOR A.B.C.

Fig. 4.3.20b



EXPLICIT CONF FOR P=1/2 SU(2)XSU(4) 3RD FLAVOR A.B.C.

Fig. 4.3.20c



EXPLICIT CONF FOR P=1/2 SU(2)XSU(4) 4TH FLAVOR A.B.C.

Fig. 4.3.20d



## Appendix A

### Spin Diagonalisation

Here we will present an explicit construction of the flavor quark fields in terms of the  $x$  fields.

#### (a) Free Case

We start with the naive Euclidean action on a  $D$ -dimensional hypercubic lattice:

$$S = (1/2)a^{d-1} \sum_{n,\mu} [\bar{\Psi}(n)\Gamma^\mu\Psi(n+\mu) - \Psi(n+\mu)\Gamma^\mu\Psi(n)] \quad (A1)$$

where  $n = (n_1, n_2, n_3, \dots, n_D)$  is a lattice site.

For every lattice site  $(\Psi, \bar{\Psi})$  have  $2^{(D/2)}$  components,  $D$  an even integer. We choose representation of the  $\Gamma$  matrices

$$\{\Gamma_\mu, \Gamma_\nu\} = -2\delta_{\mu\nu}, \Gamma_{+\mu} = -\Gamma_\mu, \Gamma_\mu^+ \Gamma_\mu = 1$$

At every site, we perform a unitary transformation:

$$\Psi(n) = T(n)X(n), \quad (A2)$$

$$\bar{\Psi}(n) = X(n)T^+(n) \quad (A3)$$

where

$$T^+(n)\Gamma^\mu T(n+\mu) = \Delta^\mu(n) \quad (A4)$$

$$T^+(n)T(n) = T(n)T^+(n) = 1 \quad (A5)$$

and  $\Delta^\mu(n) \in U(1)^{\otimes C}$  is a diagonal unitary matrix ( $C=(D/2)$ ). After this transformation the action becomes:

$$S=(1/2)a^{D-1}\sum_{n,\mu}[\bar{X}(n)\Delta^\mu X(n+\mu)+\bar{X}(n+\mu)\Delta^\mu X(n)]. \quad (A6)$$

One possible choice for  $T(n)$  is

$$T^0(n) = \Gamma_1^{\eta_1} \Gamma_2^{\eta_2} \Gamma_3^{\eta_3} \Gamma_4^{\eta_4} \quad (A7)$$

which gives

$$\Delta_\mu^{(0)}(n) = -(-1)^{\eta_1+\eta_2+\dots+\eta_{\mu-1}} \quad (A8)$$

From the above equations we observe that  $\Delta_\mu(n)$  obeys the constraint:

$$\Delta_P = -1, \quad (A9)$$

i.e., its parallel transport around a plaquette is -1.

Conversely , if we have  $\Delta_\mu(n)$  matrices which obey (A9) we can recover the form of the action (A1) from the action in terms of the  $X$  fields. So all the different choices for  $T(n)$  are equivalent.

We now present the construction of the different quark flavors fields in terms of the  $X$  fields[38].

We write

$$q^{fa} = (1/8)\sum_n \Gamma_n^{fa} X_n(y) \quad (A10)$$

( $f$  = flavor index,  $a$  = spinor index) and we work explicitly in four dimensions with

$$\Gamma_n = \Gamma_1^{\eta_1} \Gamma_2^{\eta_2} \Gamma_3^{\eta_3} \Gamma_4^{\eta_4}.$$

Labelling the sites of the hypercube as follows:

( $\eta$  labels the 16 corners of the hypercube)

$n$		$(-1)^n$
(0, 0, 0, 0)	1	+ 1
(1, 1, 1, 1)	2	+ 1
(1, 1, 0, 0)	3	+ 1
(0, 0, 1, 1)	4	+ 1
(0, 1, 1, 0)	5	+ 1
(1, 0, 0, 1)	6	+ 1
(1, 0, 1, 0)	7	+ 1
(0, 1, 0, 1)	8	+ 1
(1, 0, 0, 0)	9	- 1
(0, 1, 1, 1)	10	- 1
(0, 1, 0, 0)	11	- 1
(1, 0, 1, 1)	12	- 1
(0, 0, 1, 0)	13	- 1
(1, 1, 0, 1)	14	- 1
(1, 1, 1, 0)	15	- 1
(0, 0, 0, 1)	16	-1

and choosing as  $\Gamma$  matrices representation

$$\Gamma_1 = \begin{bmatrix} 0 & 0 & 0 & -1 \\ 0 & 0 & -1 & 0 \\ 0 & 1 & 0 & 0 \\ 1 & 0 & 0 & 0 \end{bmatrix}, \quad \Gamma_2 = \begin{bmatrix} 0 & 0 & 0 & i \\ 0 & 0 & -i & 0 \\ 0 & -i & 0 & 0 \\ i & 0 & 0 & 0 \end{bmatrix},$$

$$\Gamma_3 = \begin{bmatrix} 0 & 0 & -1 & 0 \\ 0 & 0 & 0 & 1 \\ 1 & 0 & 0 & 0 \\ 0 & -1 & 0 & 0 \end{bmatrix}, \quad \Gamma_4 = \begin{bmatrix} 0 & 0 & i & 0 \\ 0 & 0 & 0 & i \\ i & 0 & 0 & 0 \\ 0 & i & 0 & 0 \end{bmatrix}.$$

we get

$$\Psi^1 = 1/8 \begin{bmatrix} -ix_3 & -ix_4 & -x_2 & +x_1 \\ x_7 & -ix_5 & -ix_6 & -x_8 \\ ix_{15} & +x_{14} & +ix_{16} & -x_{13} \\ -x_9 & +ix_{11} & +x_{10} & +ix_{12} \end{bmatrix}$$

$$\Psi^2 = 1/8 \begin{bmatrix} -x_7 & -ix_5 & -ix_6 & +x_8 \\ x_1 & +ix_3 & +ix_4 & -x_2 \\ -ix_{12} & +x_{10} & -ix_9 & -ix_{11} \\ x_{13} & +ix_{15} & -x_{14} & -ix_{16} \end{bmatrix}$$

$$\Psi^3 = 1/8 \begin{bmatrix} x_{13} & -ix_{15} & +x_{14} & +ix_{16} \\ x_9 & -ix_{11} & +x_{10} & +ix_{12} \\ x_1 & -ix_3 & +ix_4 & +x_2 \\ x_7 & -ix_5 & -ix_6 & +x_8 \end{bmatrix}$$

$$\Psi^4 = 1/8 \begin{bmatrix} x_9 & -ix_{11} & +x_{10} & -ix_{12} \\ -x_{13} & -ix_{15} & -x_{14} & +ix_{16} \\ -x_7 & -ix_5 & +ix_6 & -x_8 \\ x_1 & +ix_3 & -ix_4 & +x_2 \end{bmatrix}$$

where the indices 1, 2, 3, 4 for the  $\Psi$  refer to the 4 groups of the 4 degenerate flavors.

## Interacting Case

Here, we have:

$$q^{fa} = (1/8) \sum_n \Gamma_n^{fa} U_n(y) X_n(y) \quad (A11)$$

where

$$U_n(y) = [U_1(2y)]^{n_1} [U_2(2y+n_1)]^{n_2} U_3[2y+n_2]^{n_3} \\ U_4[2y+n_1+n_2+n_3]^{n_4} .$$

For example,  $U(0,0,0,0) = 1$ ,

$U(1,1,1,1) = U(1,1) U(9,2) U(3,3) U(15,4)$  etc. and the construction of the different quark flavors follows the same pattern as in the free field case.

## Appendix B

### The Lanczos Algorithm

To find the eigenvalues of the fermion matrix on the lattice we use the Lanczos Algorithm<sup>[39]</sup>, which we discuss without giving details.

We require a similarity transformation to produce a tridiagonal symmetric (real) matrix  $T$  from a general Hermitian matrix  $H$ , i.e.,  $X^{-1}HX = T$  with

$$T = \begin{bmatrix} a_1 & \beta_1 & 0 & 0 & . \\ \beta_1 & a_2 & \beta_2 & 0 & . \\ 0 & \beta_2 & a_3 & \beta_3 & . \\ . & . & . & . & . \end{bmatrix}$$

Write  $X$  as a series of orthonormal column vectors:

$$X = (x_1, x_2, x_3, \dots),$$

the Lanczos equations are given by:

$$HX_1 = a_1 X_1 + \beta_1 X_2 \quad (B1a)$$

$$Hx_i = \beta_{i-1} x_{i-1} + a_i x_i + \beta_i x_{i+1} \quad (B1b)$$

Using the Lanczos equations recursively, we calculate all the  $a$ 's,  $b$ 's and  $x$ 's starting by choosing the  $x_1$  to be a unit vector.

## Appendix C

### The eigenvalue problem for specific configurations

Here we deal with the calculation of the eigenvalues of the Dirac operator, using, as background gauge field, an explicit configuration with  $P=1/2$  ( $P$  denotes the topological charge) . Instead of using the configuration (for  $P=1/2$ ) of (4.2.1) ,we construct a gauge equivalent configuration which is different from zero at only two directions.

It is easy to show that the gauge field

$$A_\mu = (0, A_2, 0, A_4) \text{ where } A_2 = 2\pi x_1/a_1 a_2, \quad A_4 = 2\pi x_3/a_1 a_2 \quad (C1)$$

satisfies (2.2.1) .

In this gauge, the transition functions are :

$$\Omega_1(x) = e^{i\pi x_2/a_2}, \quad \Omega_2(x) = 1, \quad \Omega_3(x) = e^{i\pi x_4/a_2}, \quad \Omega_4 = 1 \quad (C2)$$

We now proceed to find the eigenvalues of  $iD$ .

Since

$$\not{D}^2 = D^2 + (1/4)[\Gamma_\mu, \Gamma_\nu][D_\mu, D_\nu] = D^2 + (1/4)(-2i\sigma^{\mu\nu})[D_\mu, D_\nu] = D^2 - (i/2)\sigma^{\mu\nu}F_{\mu\nu} = D^2 - (2i\sigma_{12}F^{12}), \quad \sigma_{12} = 2i\sigma_3 \quad (C3)$$

the eigenvalue equation becomes

$$\not{D}^2\Psi = -\lambda^2\Psi \Rightarrow [(\partial_1 + iA_1)^2 + (\partial_2 + iA_2)^2 + (\partial_3 + iA_3)^2 + (\partial_4 + iA_4)^2 + 4\sigma_3 F_{12}]\Psi = -\lambda^2\Psi, \quad (C4)$$

where  $\Psi = \Psi(x_1, x_2, x_3, x_4)$ .

Using the gauge field in (C1) we notice that (C4) has no explicit dependence on  $x_2, x_4$  and therefore we write

$$\Psi(x_1, x_2, x_3, x_4) = e^{i(px_2 + kx_4)} \Phi(x_1, x_3) \quad (C5)$$

This reduces (C4) to

$$[(\partial^2 \Phi / \partial x_1^2) + (\partial^2 \Phi / \partial x_3^2) + (-p^2 - k^2 - 2A_2 p - 2A_4 k - A^2) \Phi - A^2_4 + 4\sigma_3 F_{12} + \lambda^2] \Phi(x_1, x_3) = 0 \quad (C6)$$

Since the choice of  $P=1/2$  corresponds to  $\eta_{12} = 1, \eta_{34} = 1$ , we choose the boundary conditions for the  $\Psi$  field to correspond to a global color twist, i.e.,

$$\Psi(x_1, x_2 + a_2, x_3, x_4) = e^{i\pi} \Psi(x_1, x_2, x_3, x_4), \quad (C7)$$

$$\Psi(x_1, x_2, x_3, x_4 + a_4) = e^{i\pi} \Psi(x_1, x_2, x_3, x_4) \quad (C8)$$

$$\Rightarrow pa_2 = (2n+1)\pi, \quad ka_4 = (2m+1)\pi, \quad m, n \in \mathbb{Z}. \quad (C9)$$

If  $A = (2\pi/a_1 a_2)$ ,  $\Rightarrow$

$$(\partial^2 \Phi / \partial x_1^2) + (\partial^2 \Phi / \partial x_3^2) + (-p^2 - k^2 - 2Ax_1 p - 2Ax_3 k - A^2 x_1^2 - A^2 x_3^2 + 4\sigma_3 A + \lambda^2) \Phi(x_1, x_3) = 0 \Rightarrow \quad (C10)$$

$$\begin{aligned} \Rightarrow & (\partial^2 \Phi / \partial x_1^2) + [-A^2(x_1^2 + (p/A)^2 + 2x_1 p/A) + 4\sigma_3 A + \lambda^2] \Phi \\ & = -(\partial^2 \Phi / \partial x_3^2) + [A^2(x_3^2 + (k/A)^2 + 2x_3 k/A)] \Phi \end{aligned} \quad (C11)$$

If  $\Phi(x_1, x_3) = X(x_1)Z(x_3)$ , then we get:

$$(X''/X) + \{-A^2(x_1 + p/A)^2 + 4\sigma_3 A + \lambda^2\} = -(Z''/Z + A^2(x_3 + k/A)^2) \equiv -\mu^2.$$

The above equations are the equations for a shifted harmonic oscillator with frequency  $\omega = A = k$  and energy:



$$(\lambda^2 + \mu^2 + 4\sigma_3 A) = (n' + 1/2)k \quad (C12a)$$

$$-\mu^2 = (m' + 1/2)k \quad (C12b)$$

$$\Rightarrow \lambda^2 = (n' + 1/2)k + (m' + 1/2)k \mp 4A, \quad (C13)$$

$$n', m' \in \mathbb{Z}$$

The formal part of the calculation of the eigenvalues of  $D$  is now finished and it is time to compare (C13) with our numerical results. In the calculation we used boundary conditions for the  $\Psi$ -field which did not correspond to a local twist. This renders the fermion field multi-valued and comparing our numerical results, using the boundary conditions (C7), (C8), with the ones for color-flavor or only a color twist, we notice that in the latter cases the small eigenvalues are smaller than the first small eigenvalues of the first case.

Also the numerical result for the case we set only a global color twist on the  $\Psi$ -field does not agree with what we expect from (C13).

Now we present the same problem in 2 dimensions.  
Using the configuration:

$$A_1 = (\pi/2)(x_2/a_1 a_2), \quad A_2 = -(\pi/2)(x_1/a_1 a_2), \quad (C14)$$

i.e., twist  $\eta_{12} = 1$  at the 1-2 level, and the eigenvalue equation is read:

$$[(\partial_1^2 + \partial_2^2) - A^2(x_1^2 + x_2^2) + 2A + \lambda^2]\Psi(x_1, x_2) = 0, \quad (C15)$$

$$A = \frac{\pi}{2a_1 a_2}$$

Using polar coordinates,

$$\nabla^2 = (d^2/dr^2) + (1/r)(d/dr) \Rightarrow$$

$$(d^2R/dr^2) + (1/r)(dR/dr) - A^2r^2 + \lambda^2 + 2A)R(r) = 0. \quad (C16)$$

After trial we use:

$$R(r) = \xi^\mu e^{\beta \xi} u(\xi) \Rightarrow \xi u'' + (1 - \xi)u' + \{-1/2 + (\lambda^2 + 2A)/4A\}u(\xi) = 0 \quad (C17)$$

This is a confluent hypergeometric equation and for the series solution to terminate we require:

$$\begin{aligned} (-1/2) + (\lambda^2 + 2A)/4A &\in \mathbb{Z} \Rightarrow \\ (\lambda^2/4A) = n &\Rightarrow \lambda^2 = (2n\pi/a_1 a_2), \quad n \in \mathbb{Z} \end{aligned} \quad (C18)$$

If we define the topological charge in D=2 as:

$$Q = (1/2\pi) \int d^2x F_{12} \quad \text{then}$$

$$Q = (1/2\pi) a_1 a_2 \pi / a_1 a_2 = 1/2. \quad (C19)$$

In [40] transition functions for  $Q = 1$  were used (and periodicity of the lattice was preserved i.e.  $Q = 1$ ) ,and it was found that for the eigenvalues of the Dirac operator  $\lambda^2 = 4n\pi/a_1 a_2$ .

## Conclusions

As in the cases of periodic boundary conditions and the investigation for instantons on the lattice, there are strong indications that we should be able to find topological objects of non-integer topological charge on the lattice. In Chapter 3 it was shown that numerical results provide strong evidence for the existence of objects with non-integer charge and their lifetime is remarkably longer than that of the instantons. Cooling from a cold start we were able to have exact "twist" objects and for thermalized configurations there was always at least one instanton around.

In all the cases we thermalized a "twisted" configuration, the time needed to reach the equilibrium was bigger than that for a periodic configuration. This is justified due to the fact that, under TBC, we actually simulate a bigger lattice from the lattice we had originally. C Michael [41] had also made this observation.

In chapter 4 we see that despite the fact that continuity is lost on the lattice, there are remnants of the index theorem on the lattice. Of course, the difficulties of putting the fermions on the lattice (the spread of the flavors around the corners of the hypercube for the K-S fermions and the 15 "unwanted" flavors for the Wilson case) obscure the full evidence for the index theorem on the lattice. The Wilson fermion action violates the chiral symmetry, hence zero modes of the eigenvalue equation  $M\Psi = \lambda\Psi$ ,  $M$  is the fermion matrix, are not eigenvectors of chirality, but approximate eigenvectors, i.e.  $\Gamma_5\Psi \approx \pm\Psi$ .

Another notable point regards our lattice. Since our lattice is not a torus since we do not identify the gauge field at sites  $x, x + Nx$  ( $Nx$  = lattice size in the  $x$ -direction), we should actually find from a pure mathematical point of view the values of the constants which appear in 4.1.4 (in 4.1.4 there is no the Euler-Poincare number which generally, for an arbitrary manifold, is different from zero and equals to 2 for a topological sphere). This is also another possible explanation for the discrepancy between the formula (4.3.1) and our numerical results.

In this thesis we dealt with the application of the TBC regarding

only the 'pure mathematical part' of the 'twist'. We believe that we can extend this work to the physical applications of the TBC.

There are some papers which have dealt with this, for example, in [42] the analysis considers the elimination of the finite size effects on the lattice using the TBC.

It could be interesting to examine the dependence of the various thermodynamical quantities (free energy etc.) on the TBC.

Generalising the solutions of [20] to non-abelian ones, it should provide a way to calculate the energy of the magnetic fluxes. Using then duality arguments [13], we, in principle, could be able to compute the energy of an electric flux tube.

Also, since from (1.10.1) we see that the chiral symmetry is connected to the density of the zero modes, we consider that this could give a way to study the connection between topology and chiral symmetry breaking [43].

## References

- 1) K.G. Wilson, Phys .Rev. D10, 2445 (1974)
- 2) R.P. Feynmann, A.R. Hibbs, *Quantum Mechanics and Path Integrals* (McGraw-Hill, New York,1965).
- 3) P.H. Frampton, Gauge Field Theories, *Frontiers in Physics*,1986.
- 4) I.G. Halliday, Rep. Prog. Phys. 47, 987 (1984).
- 5) N. Metropolis, A.W. Rosenbulth, M.N. Rosenbulth, A.H. Teller, E. Teller, J. Chem. Phys., 21, 1087,1953;  
M. Creutz, L. Jacobs, C. Rebbi, Physics Reports 95, 4  
201 (1983).  
I.M.Sobol, *The Monte Carlo Theory*, MIR, Publisher Moscow
- 6) H.B. Nielsen, M. Ninomiya, Nucl. Phys. B193 173 (1981).
- 7) G. Schierholz, Lattice QCD, in SUSSP,1984.
- 8) I.M. Barbour, J.P. Gilchrist, G. Schierholz , H. Schneider, M. Teper M., Phys. Lett. 127B, 433 (1983).
- 9) C. Nash, S. Siddhartha, *Topology and Geometry for Physicists* (Academic Press,1983).
- 10) G. Parisi, F. Rapuano, CERN-Th. 4044/84 .
- 11) A.A. Belavin, A.M. Polyakov, A.S. Schwarz, Yu S. Tyupkin, Phys. Lett., 59B 85 (1975) .
- 12) A.S. Kronfeld et.al., Nucl. Phys. B192 330 (1987)..
- 13) G. 't-Hooft, Nucl. Phys. B153 141 (1979).
- 14) J. Ambjorn, P. Olesen, Nucl. Phys. B170 265 (1980).

- 15) P. Van Baal, J. Koller, *Annals of Physics*, Vol.174, No.2, March 1987.
- 16) J. Ambjorn et.al., Nucl. Phys. B175 349 (1980).
- 17) J. Ambjorn, H. Flyvbjerg, Phys.Lett. 97B 240 (1980).
- 18) E. Cohen, C. Gomez, Nucl. Phys. B 223 183 (1983).
- 19) P. Van Baal, Commun. Mathematical Physics., 85, 529 (1982).
- 20) G. 't-Hooft, Commun. Mathematical Physics., 81, 267 (1981).
- 21) K. Ishikawa, G. Schierholz, H. Schneider, M. Teper, Phys. Lett. 128B 309 (1983) .
- 22) A.S. Kronfeld, *Topological Aspects of Lattice Gauge Theories* DESY 87-152, ISSN 0418-9833.
- 23) I.A. Fox, J.P. Gilchrist, M.L. Laursen, G. Schierholz, Phys. Rev. Lett. 54 749 (1985) .
- 24) J. Hoek, M. Teper, J. Waterhouse, *Topological Fluctuations and Susceptibility in SU(3) Lattice Gauge Theory*, Ral-86-103.
- 25) T. Yoneya, Nucl. Phys. B144 195 (1978).
- 26) J. Groeneveld, J. Jurkiewicz, C.P. Korthals Altes, Physica Scripta 23,1002 (1981).
- 27) A.G. Arroyo, C.P. Korthals Altes, FSU-SCRI-87-77.
- 28) B. Soderberg, LUND-TP 87-2.
- 29) R. Jackiw, C. Rebbi, 16,4, 1052 (1977).
- 30) K. Fujikawa, Phys. Rev. D21, 2848 (1980).  
K. Fujikawa, Phys. Rev. Lett. 42 1195 (1979).

- 31) G. 't'Hooft, Phys. Rev. D14, 3431 (1976)
- 32) C.W. Bernard, N.H. Christ, A.M. Guth, E.J. Weinberg ,  
Phys.Rev. D16, 2967 (1977).
- 33) A.S. Schwarz, Phys. Lett. 67B 172 (1977).
- 34) A.S. Schwarz, Commun. Mathematical Physics,  
64, 529 (1982).
- 35) M. Atiyah, R. Bott and V.K. Patodi, Invent. Math. 19 279 (1973).
- 36) J.P. Bourguignon, H.B. Lawson, Commun. Mathematical  
Physics, 79, 189 1984.
- 37) R. Setoodeh, C .Davies, I.M. Barbour, *Wilson fermions on the  
lattice - A study of the eigenvalue spectrum*, GUTPA/88/6-1
- 38) H. Kluberg-Stern, A. Morel, O. Napoly, B. Petersson,  
Nucl. Phys.B 220, 447 (1983).
- 39) I.M. Barbour, N.E. Behilil, P.E. Gibbs, G. Scierholtz,M. Teper,  
in *The Recursion Method and its Application* (Spring Series  
in Solid State Sciences), Eds. D.G. Pettifor, D.L. Weire,  
(Springer, Berlin), p 149 (1985).
- 40) J. Smit, J.C. Vink, ITFA-86-I4.
- 41) C.Michael, LTH -147-1986.
- 42) A. Coste, A. Gonzalez-Arroyo, C.P. Korthals Altes,  
B. Soderberg, A. Tarancon, Nucl. Phys. B 287, 569 (1987).
- 43) I.M. Barbour, M. Teper, Phys. Lett. 175B 445 (1986) .

